

- Animal care and holding procedures should be described.
2. Controls should be comparable with test animals in all respects except the treatment variable ("negative").
    - Concurrent controls must minimally include an "air-only" exposure group; if a vehicle is used, it is desirable that there be a "vehicle-only" group.
    - Historical control data can be useful in the evaluation of results, particularly where the differences between control and treated animals are small and are within anticipated incidences based on examination of historical control data.
  3. Endpoints should address the specific hypothesis being tested in the study, and the observed effects should be sufficient in number or degree (severity) to establish a dose-response relationship that can be used in estimating the hazard to the target species.
    - The outcome of the reported experiment should be dependent on the test conditions and not influenced by competing toxicities.
  4. The test performed must be valid and relevant to human extrapolation. The validity of using the test to mimic human responses must always be assessed. Issues to consider include the following:
    - Does the test measure an established endpoint of toxicity or does it measure a marker purported to indicate an eventual change (i.e., severity of the lesion)?
    - Does the test indicate causality or merely suggest a chance correlation?
    - Was an unproven or unvalidated procedure used?
    - Is the test considered more or less reliable than other tests for that endpoint?
    - Is the species a relevant or reliable human surrogate? If this test conflicts with data in other species, can a reason for the discrepancy be discerned?
    - How reliable is high exposure (animal) data for extrapolation to low exposure (human scenario)?

5. Conclusions from the experiment should be justified by the data included in the report and consistent with the current scientific understanding of the test, the endpoint of toxicology being tested, and the suspected mechanism of toxic action.
6. Due consideration in both the design and the interpretation of studies must be given for appropriate statistical analysis of the data.
  - Statistical tests for significance should be performed only on those experimental units that have been randomized (some exceptions include weight-matching) among the dosed and concurrent control groups.
  - Some frequent violations of statistical assumptions in toxicity testing include:
    - Lack of independence of observations.
    - Assuming a higher level of measurement than available (e.g., interval rather than ordinal).
    - Inappropriate type of distribution assumed.
    - Faulty specification of model (i.e., linear rather than nonlinear).
    - Heterogeneity of variance or covariance.
    - Large Type II error.
7. Subjective elements in scoring should be minimized. Quantitative grading of an effect should be used whenever possible.
8. Peer review of scientific papers and of reports is extremely desirable and increases confidence in the adequacy of the work.
9. When the data are not published in the peer-reviewed literature, evidence of adherence to good laboratory practices is highly recommended, with rare exceptions.
10. Reported results have increased credibility if they are reproduced (confirmed) by other researchers and supported by findings in other investigations.

11. Similarity of results to those of tests conducted on structurally related compounds should be considered.

The reader is also referred to Part 798, the Health Effects Testing Guidelines, of the U.S. Toxic Substances Control Act Test Guidelines delineated in 40 Code of Federal Regulations (1991d). The chronic testing guidelines for all administration routes are provided in Subpart D, Section 798.3260. Subpart C, Section 798.2450, and Subpart B, Section 798.1150, describe the guidelines for subchronic and acute inhalation testing, respectively. Guidelines for inhalation developmental toxicity testing are discussed in Subpart E, Section 798.4350.

These guidelines provide recommendations on laboratory animal selection (e.g., species, number, sex, age, and condition); on number of test concentrations and the objectives of each; on physical parameters of exposure that should be monitored and recorded and with what frequency (e.g., chamber air changes, oxygen content, air flow rate, humidity, and temperature); on what testing conditions should be reported and how (e.g., mean and variance of both nominal and breathing zone exposure concentration, particle size, and geometric standard deviation); and on what gross pathology and histopathology, clinical, biochemical, hematological, ophthalmological, and urinary excretion tests to perform, intervals at which to perform them, which exposure levels to process these data for, and how to report their results.

The recommendations on what diagnostic tests to perform and how to report the data are particularly useful for evaluating a given study. Although the mechanism of action should dictate the repertoire of tests performed, Table F-1 provides a general list of recommended clinical biochemistry examinations; and Table F-2 provides a list of organs and tissues recommended for histological examination. If specific mechanisms of action are hypothesized, specific assays or functional tests for those would be added. It is also important to establish that appropriate removal and tissue processing was performed.

Results should be reported in tabular form, showing the number of animals at test start, number with lesions, the types of lesions, and the percentage of animals with each type. Group animal data should be reported to show number of animals dying, number showing signs of toxicity, and number exposed. Individual animal data should include time of death;

**TABLE F-1. GENERAL CLINICAL BIOCHEMISTRY EXAMINATIONS**

---



---

Calcium
Phosphorus
Chloride
Sodium
Potassium
Fasting glucose
Serum glutamic-pyruvic transaminase (serum alanine aminotransferase)
Serum glutamic-oxaloacetic transaminase (serum aspartate aminotransferase)
Ornithine decarboxylase
Gamma glutamyl transpeptidase
Urea nitrogen
Albumin
Blood creatinine
Creatinine phosphokinase <sup>a</sup>
Total cholesterol <sup>a</sup>
Total bilirubin
Total serum protein
Lipids <sup>b</sup>
Hormones <sup>b</sup>
Acid/base balance <sup>b</sup>
Methemoglobin <sup>b</sup>
Cholinesterase activity <sup>b</sup>

---



---

<sup>a</sup>Suggested for chronic inhalation toxicity test.

<sup>b</sup>May be required for a complete toxicological evaluation.

Source: Shoaf (1993).

time of observed toxicity; body weight; food consumption; and results of hematological tests, clinical biochemistry tests, necropsy, histopathology, and statistical analyses.

**TABLE F-2. ORGANS AND TISSUES PRESERVED FOR  
HISTOLOGICAL EXAMINATION**

All gross lesions	Aorta
Nasopharyngeal tissues	Gall bladder
Lungs <sup>a</sup>	Esophagus
Trachea	Stomach
Pituitary	Duodenum
Thyroid/parathyroid	Jejunum
Thymus	Ileum
Brain and sections <sup>b</sup>	Cecum
Heart	Colon
Sternum with bone marrow	Rectum
Salivary glands	Urinary bladder
Liver	Representative lymph node
Spleen	Peripheral nerve
Kidney	Thigh muscle <sup>c</sup>
Adrenals	Mammary gland <sup>c</sup>
Pancreas	Eyes <sup>c</sup>
Gonads	Skin <sup>c</sup>
Uterus	Spinal cord <sup>c,d</sup>
Accessory genital organs <sup>c,e</sup>	Exorbital lachrymal glands <sup>c</sup>

<sup>a</sup>Removed intact, weighed, and treated with fixative (e.g., perfusion) to ensure maintenance of lung structure.

<sup>b</sup>Medulla/pons, cerebellar cortex, and cerebral cortex.

<sup>c</sup>If indicated by signs of toxicity or as a target organ.

<sup>d</sup>Cervical, midthoracic, and lumbar.

<sup>e</sup>Epididymis, prostate, seminal vesicles.

Source: Shoaf (1993).

## APPENDIX G

# THE PARTICLE DEPOSITION DOSIMETRY MODEL

In this appendix, the revised empirical model used to estimate fractional regional deposition efficiency for calculation of RDDR (Equation 4-5) to be used as a dosimetric adjustment factor is described (Ménache et al., submitted). This revised model represents refinement of previously published models used to calculate the RDDR in the 1990 interim RfC methods (Jarabek et al., 1989, 1990; Miller et al., 1988). For example, rather than linear interpolation between the published (Raabe et al., 1988) means for deposition measured at discrete particle diameters, as previously done for the laboratory animal deposition modeling, equations have now been fit to the raw data as described herein.

The equations to perform calculations for monodisperse particles are provided; how the calculated efficiencies may be transformed to fractional depositions is indicated; how to use the model to predict deposition fractions for polydisperse particles is explained; and the effects of the mass median aerodynamic diameter (MMAD) and the geometric standard deviation ( $\sigma_g$ ) on the regional deposited dose ratio (RDDR<sub>r</sub>) calculations are illustrated. Because  $\dot{V}_E$  must be calculated from the default body weights (Table 4-5) using allometric scaling (Equation 4-4) for use as input to the empirical model, the example of hand calculation of monodisperse deposition includes a  $\dot{V}_E$  calculation.

Fractional deposition of particles in the airways of the respiratory tract may be estimated using theoretical or empirical models or some combination of the two. Progress is being made in answering the data needs of theoretical models (e.g., exact airflow patterns, complete measurements of the branching structure of the respiratory tract, pulmonary region mechanics), however, many uncertainties remain. Empirical models are systems of equations that are fit to experimentally determined deposition in vivo. These models do not require the detailed information needed for theoretical models, however, they can not provide estimates of dose to localized specific sites (e.g., respiratory versus olfactory nasal epithelium terminal bronchioles, carinal ridges). Measurement techniques are such that only general regions can

be defined (Stahlhofen et al., 1980; Lippmann and Albert, 1969; Raabe et al., 1977) which limits the regions that can be defined for a dosimetry model. Despite this level of generality, regional information is available now for humans and a number of commonly used laboratory animals. Empirical models of regional fractional deposition have been presented for humans (Yu et al., 1981; Miller et al., 1988; Stahlhofen et al., 1989). The empirical model described in this appendix was fit for five species of commonly used laboratory rodents using experimental data received from Dr. Otto Raabe (Raabe et al., 1988). At the same time, Dr. Morton Lippmann (Lippmann and Albert, 1969; Lippmann, 1970, 1977; Chan and Lippmann, 1980; Miller et al., 1988) and Dr. Wilhelm Stahlhofen and colleagues (Stahlhofen et al., 1980, 1983, 1989; Heyder and Rudolf, 1977; Heyder et al., 1986) provided the individual experimental measurements from their published studies. Using these data, the human model published in Miller et al. (1988) was extended by refitting the extrathoracic (ET) (oral breathing) and tracheobronchial (TB) deposition efficiencies with the original raw data as well as by fitting a pulmonary (PU) deposition efficiency equation (Ménache et al., submitted).

## **G.1 EMPIRICAL MODEL FOR REGIONAL FRACTIONAL DEPOSITION EFFICIENCIES**

The equations describing fractional deposition were fit using data on particle deposition in CF<sub>1</sub> mice, Syrian golden hamsters, Fischer 344 rats, Hartley guinea pigs, and New Zealand rabbits. A description of the complete study including details of the exposure may be found elsewhere (Raabe et al., 1988). Briefly, the animals were exposed to radiolabelled ytterbium (<sup>169</sup>Yb) fused aluminosilicate spheres in a nose-only exposure apparatus. Twenty unanesthetized rodents or eight rabbits were exposed simultaneously to particles of aerodynamic diameters ( $d_{ae}$ ) about 1, 3, 5, or 10  $\mu\text{m}$ . Half the animals were sacrificed immediately post exposure; the remaining half were held 20 h post exposure. One-half of the animals at each time point were male and the other half were female. The animals were dissected into 15 tissue compartments, and radioactivity was counted in each compartment. The compartments included the head, larynx, GI tract, trachea, and the five lung lobes. This information was used directly in the calculation of the deposition fractions. Radioactivity was

also measured in other tissues including heart, liver, kidneys, and carcass; and additionally in the urine and feces of a group of animals held 20 hours. In the animals sacrificed immediately post exposure, these data were used to ensure that there was no contamination of other tissue while the data from the animals held 20 hours were used in the calculation of a fraction used to partition thoracic deposition between the TB and PU regions. This partition is discussed below briefly and described in detail elsewhere (Raabe et al., 1977). Finally, radioactivity was measured in the pelt, paws, tail, and headskin as a control on the exposure.

Although there are some other studies of particle deposition in laboratory animals (see review by Schlesinger, 1985), no other data have the level of detail or the experimental design (i.e., freely breathing, unanesthetized, nose-only exposure) required to provide deposition equations representative of the animal exposures used in many inhalation toxicology studies. However, many inhalation toxicology studies are not nose-only exposures. While this is a necessary exposure condition to determine fractional particle deposition, adjustments for particle inhalability and ingestion can be made to estimate deposition fractions under whole-body exposure conditions.

The advantages of using the data of Raabe et al. (1988) to develop the deposition equations include:

- the detailed measurements were made in all tissues in the animal, providing mass balance information and indicating that there was no contamination of nonrespiratory tract tissue with radioactivity immediately post exposure,
- the use of five species of laboratory animals under the same exposure conditions,
- the use of unanesthetized, freely breathing animals, and
- the use of an exposure protocol that makes it virtually impossible for the animals to ingest any particles as a result of preening.

Regional fractional deposition,  $F_r$ , was calculated as activity counted in a region normalized by total inhaled activity (Table G-1). The proportionality factor,  $f_L$ , in Equations G-2 and G-3 is used to partition thoracic deposition between the TB and PU regions. It was calculated using the 0 and 20-h data and is described in detail by Raabe and co-workers (1977).

**TABLE G-1. REGIONAL FRACTIONAL DEPOSITION**

$F_r = \frac{\text{Activity Counted in a Region}}{\text{Total Inhaled Activity}}$	
Extrathoracic (ET): $F_{ET} = \frac{[\text{head} + \text{GI tract} + \text{larynx}]_{0\text{ h}}}{\text{Total Inhaled Activity}}$	(G-1)
Tracheobronchial (TB): $F_{TB} = \frac{\text{trachea}_{0\text{ h}} + f_L \times \sum_{i=1}^5 \text{lobe}_{i,0\text{ h}}}{\text{Total Inhaled Activity}}$	(G-2)
Pulmonary (PU): $F_{PU} = \frac{(1 - f_L) \times \sum_{i=1}^5 \text{lobe}_{i,0\text{ h}}}{\text{Total Inhaled Activity}}$	(G-3)

These regional deposition fractions,  $F_r$ , however, are affected not only by the minute volume ( $\dot{V}_E$ ), MMAD and  $\sigma_g$ , but also by deposition in regions through which the particles have already passed. Deposition efficiency,  $\eta_r$ , on the other hand, is affected only by  $\dot{V}_E$ , MMAD, and  $\sigma_g$ . The differences between deposition fraction and efficiency, calculated as described below, are described in more detail later in this appendix. In the aerodynamic domain, that is for particles with diameters  $>0.5\ \mu\text{m}$  (see Appendix H for further discussion of particle dimension issues), efficiencies increase monotonically and are bounded below by 0 and above by 1. The logistic function (Equation G-4) has mathematical properties that are consistent with the shape of the efficiency function (Miller et al., 1988):

$$E(\eta_r) = \frac{1}{1 + e^{\alpha + \beta \log_{10} x}}, \quad (\text{G-4})$$

where  $E(\eta_r)$  is the expected value of deposition efficiency ( $\eta_r$ ) for region  $r$ , and  $x$  is expressed as an impaction parameter,  $d_{ae}^2 Q$ , for extrathoracic deposition efficiency and as aerodynamic particle size,  $d_{ae}$ , for TB and PU deposition efficiencies. The flow rate,  $Q$ , in the impaction parameter may be approximated by  $\dot{V}_E/30$ . The parameters  $\alpha$  and  $\beta$  are estimated using nonlinear regression techniques.

To fit this model, efficiencies must be derived from the deposition fractions that were calculated as described in Table G-1. Efficiency may be defined as activity counted in a region divided by activity entering that region. Then, considering the region as a sequence of filters in steady state, efficiencies may be calculated as follows:

$$\eta_{ET} = F_{ET} \quad (G-5)$$

$$\eta_{TB} = \frac{\text{trachea}_{0h} + f_L \times \sum_{i=1}^5 \text{lobe}_{i,0h}}{(1 - \eta_{ET})} \quad (G-6)$$

$$\eta_{PU} = \frac{(1 - f_L) \times \sum_{i=1}^5 \text{lobe}_{i,0h}}{(1 - \eta_{ET})(1 - \eta_{TB})} \quad (G-7)$$

Using these calculated regional efficiencies in the individual animals, the logistic function (Equation G-4) was fit for the ET, TB, and PU regions for the five animal species and humans. The parameter estimates from these fits are listed in Table G-2. Curves produced by these equations have been compared where applicable to the data reported in Schlesinger (1985), and the results are not inconsistent. As discussed by Schlesinger (1985), there are many sources of variability that could explain differences in predicted deposition using this model and the observed deposition data in the studies reported by Schlesinger (1985).

## G.2 TRANSFORMING FITTED EFFICIENCIES TO PREDICTED REGIONAL FRACTIONAL DEPOSITION

The fitted equations are then used to generate predicted efficiencies ( $\eta$ ) as a function of impaction in the ET region and of aerodynamic particle size in the TB and PU regions. Finally, the predicted efficiencies are multiplied together and adjusted for inhalability,  $I$ , as shown in Equations G-8 through G-10 to produce predicted deposition fractions ( $F_p$ ) for monodisperse and near monodisperse ( $\sigma_g < 1.3$ ) particles.

**TABLE G-2. DEPOSITION EFFICIENCY EQUATION  
ESTIMATED PARAMETERS**

Species	ET (Nasal)		TB		PU	
	$\alpha$	$\beta$	$\alpha$	$\beta$	$\alpha$	$\beta$
Human	7.129 <sup>a</sup>	-1.957 <sup>a</sup>	3.298	-4.588	0.523	-1.389
Rat	6.559	-5.524	1.873	-2.085	2.240	-9.464
Mouse	0.666	-2.171	1.632	-2.928	1.122	-3.196
Hamster	1.969	-3.503	1.870	-2.864	1.147	-7.223
Guinea Pig	2.253	-1.282	2.522	-0.865	0.754	0.556
Rabbit	4.305	-1.628	2.819	-2.281	2.575	-1.988

\*Source: Miller et al., 1988.

$$\hat{F}_{ET} = I \times \hat{\eta}_{ET} \quad (G-8)$$

$$\hat{F}_{TB} = I \times (1 - \hat{\eta}_{ET}) \times \hat{\eta}_{TB} \quad (G-9)$$

$$\hat{F}_{PU} = I \times (1 - \hat{\eta}_{ET}) \times (1 - \hat{\eta}_{TB}) \times \hat{\eta}_{PU} \quad (G-10)$$

Inhalability,  $I$ , is an adjustment for the particles in an ambient exposure concentration that are not inhaled at all. For humans, an equation has been fit using the logistic function (Ménache et al., 1995). Using the experimental data of Breysse and Swift (1990):

$$I = 1 - \frac{1}{1 + e^{10.32 - 7.17 \log_{10} d_{ae}}} \quad (G-11)$$

The logistic function was also fit to the data of Raabe et al. (1988) for laboratory animals (Ménache et al., 1995):

$$I = 1 - \frac{1}{1 + e^{2.57 - 2.81 \log_{10} d_{ae}}} \quad (G-12)$$

For example, calculation of  $\hat{F}_{PU}$  for a female Syrian golden hamster exposed to a nearly monodisperse particle ( $\sigma_g < 1.3$ ) with an MMAD of 1.8 in a subchronic study would proceed as follows.

1. Calculate the default  $\dot{V}_E$ . (If the study for which the  $RDDR_{PU}$  is being calculated has information on experimentally measured  $\dot{V}_E$ , that information may be substituted for the default value; however, this could necessitate changes to surface areas and body weight (if extrapulmonary tract effects are being examined). If there is inadequate information to change *all* of these values, then the default values should be used.)
  - a. The default body weight for a female Syrian hamster in a subchronic study from Table 4-4 is 0.095 kg.
  - b. Calculation of  $\dot{V}_E$  expressed in natural logarithms using hamster coefficients from Table 4-5:
 
$$\begin{aligned}\log(\dot{V}_E) &= -1.054 + 0.902 \times \log(0.095) \\ &= -3.177\end{aligned}$$
  - c. Convert from natural logs to arithmetic units
 
$$\exp(-3.177) = 0.0417$$
  - d. Convert from L to mL by multiplying by 1,000
 
$$\dot{V}_E = 41.7$$
2. Calculate the impaction parameter as  $MMAD^2 \times \dot{V}_E/30$  for the ET region
 
$$\begin{aligned}&= (1.8)^2 \times (41.7/30) \\ &= 4.504 \\ &\text{and take the } \log_{10} \\ &= 0.654\end{aligned}$$
3. Calculate  $\hat{\eta}_{ET}$  using the parameters from Table G-2
 
$$\begin{aligned}&= 1/(1 + \exp(1.969 - 3.503 \times 0.654)) \\ &= 0.580\end{aligned}$$

4. Calculate  $\log_{10}$  (MMAD) for the TB and PU regions

$$\begin{aligned} &= \log_{10}(1.8) \\ &= 0.255 \end{aligned}$$

5. Calculate  $\hat{\eta}_{TB}$  using the parameters from Table G-2

$$\begin{aligned} &= 1/(1 + \exp(1.870 - 2.864 \times 0.255)) \\ &= 0.242 \end{aligned}$$

6. Calculate  $\hat{\eta}_{PU}$

$$\begin{aligned} &= 1/(1 + \exp(1.147 - 7.223 \times 0.255)) \\ &= 0.667 \end{aligned}$$

7. Calculate the inhalability fraction, I

$$\begin{aligned} &= 1 - (1/(1 + \exp(2.57 - 2.81 \times 0.255))) \\ &= 0.865 \end{aligned}$$

8. Calculate  $\hat{F}_{ET}$  (if desired)

$$\begin{aligned} &= 0.865 \times 0.580 \\ &= 0.502 \end{aligned}$$

9. Calculate  $\hat{F}_{TB}$  (if desired)

$$\begin{aligned} &= 0.865 \times (1 - 0.580) \times 0.242 \\ &= 0.088 \end{aligned}$$

10. Calculate  $\hat{F}_{PU}$

$$\begin{aligned} &= 0.865 \times (1 - 0.580) \times (1 - 0.242) \times 0.667 \\ &= 0.184 \end{aligned}$$

These hand-calculated fractional depositions for monodisperse particles might differ slightly from the fractions generated by the computer program due to rounding errors. In particular, the parameter estimates in Table G-2 are only reported to three decimal places but are used with nine decimal places in the program. Because all of these digits are not significant, however, **the deposition fractions should never be reported to more than two digits.**

The human deposition fractions may be calculated using the same strategy. The only default  $\dot{V}_E$ , however, is 13.8 L/min. As described in step 1.d, this value should be

converted to mL by multiplying by 1,000. The information provided in Table G-2 allows for estimation of deposition in humans for nasal breathing only. When exercising ( $\dot{V}_E$  greater than 35 L/min), a portion of the inhaled air will enter through the mouth. The ET deposition efficiencies for oral breathing are different from those for nasal breathing and are not recorded in Table G-2. They are, however, included in the computer program as well as proportionality factors defining flow splits between the nose and mouth at higher  $\dot{V}_E$ . The additional complexities engendered in the calculation of the ET deposition fraction when both oral and nasal breathing are involved are such that those calculations should not be performed by hand.

Figure G-1 illustrates the relationship between the predicted efficiencies and predicted depositions using this model for the mice. A qualitatively similar set of curves could be produced for any of the other four species. The calculations were made according to the ten steps listed above. The particles were assumed to be monodisperse and the default body weight (BW) for the mice, taken from Table 4-4, was 0.0261 kg. This is the default BW of male BAF1 mice for chronic exposure study durations. Regional deposition efficiencies and fractions were calculated for particles with  $d_{ae}$  ranging from 0.5 to 10  $\mu\text{m}$ . These calculated points were connected to produce the smooth curves shown in Figure G-1. The three panels on the left of Figure G-1 are plots of the predicted regional deposition efficiencies; the three panels on the right show the predicted regional deposition fractions derived from the estimated efficiencies and adjusted for inhalability. The vertical axis for the predicted deposition efficiency panels range from 0 to 1. Although the deposition fraction is also bounded by 0 and 1, the vertical axes in the figure are less than 1 in the TB and PU regions. The top two panels of Figure G-1 are the predicted deposition efficiency and fraction, respectively, for the ET region. These two curves are plotted as a function of the impaction parameter described for Equation G-4. The middle two and lower two panels show the predicted deposition efficiencies and fractions for the TB and PU regions, respectively. These four curves are plotted as a function of  $d_{ae}$ . When a particle is from a monodisperse size distribution, the  $d_{ae}$  and the MMAD are the same. If, however, the particle is from a polydisperse size distribution, the particle can not be described by a single  $d_{ae}$ ; the average value of the distribution, the MMAD, must be used. (See Appendix H for further discussion of particle sizing, units, and averaging methods). In the aerodynamic particle size range, the

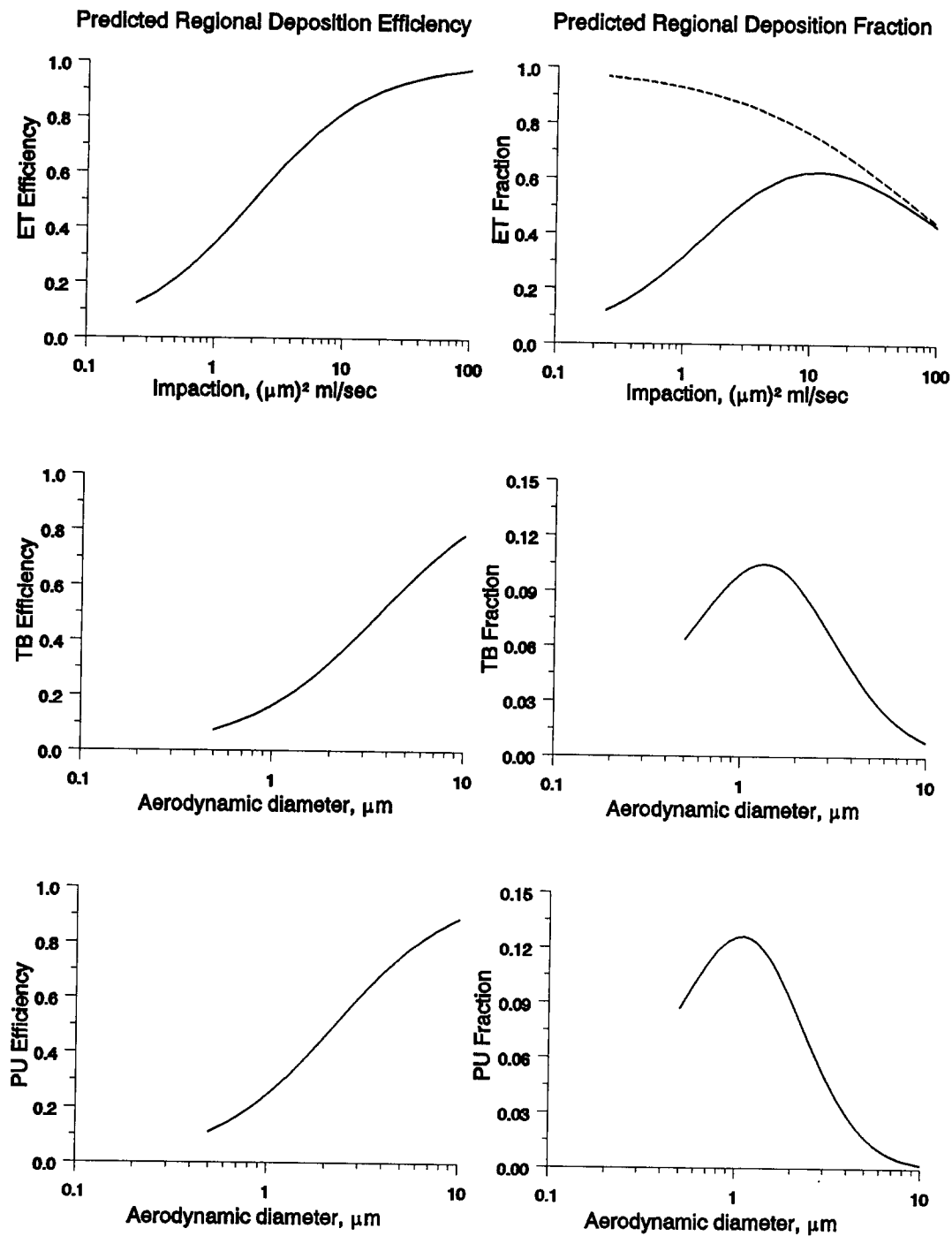


**Figure G-1. Comparison of regional deposition efficiencies and fractions for the mouse. A default body weight of 0.0261 kg (from Table 4-4) was used in these calculations. The fractional deposition (solid line) and inhalability (dashed line) are shown in the upper right panel.**

deposition efficiency curves all increase monotonically as a function of the independent variable (i.e., either the impaction parameter or  $d_{ae}$ ) and have both lower and upper asymptotes. The curves describing the deposition fractions, however, have different shapes that are dependent on the respiratory tract region. Deposition fractions in all three regions are nonmonotonic—initially increasing as a function of particle size but decreasing as particle sizes become larger. This is because particles that have been deposited in proximal regions are no longer available for deposition in distal regions. As an extreme example, if all particles are deposited in the ET region, no particles are available for deposition in either the TB or PU regions. In the ET region, the nonmonotonic shape for fractional deposition is due to the fact that not all particles in an ambient concentration are inhalable.

### G.3 POLYDISPERSE PARTICLES

As discussed in Appendix H, particles in an experimental or ambient exposure are rarely all a single size but rather have some distribution in size around an average value. As this distribution becomes greater, the particle is said to be polydisperse. Panel A of Figure G-2 illustrates the range of particle sizes from a distribution that is approximately monodisperse ( $\sigma_g = 1.1$ ) and particles that come from a lognormal highly polydisperse distribution ( $\sigma_g = 3.0$ ), although both distributions have the same MMAD of  $4.0 \mu\text{m}$ . Also drawn in Panel A of Figure G-2 is a vertical line through the MMAD that represents the extreme case of  $\sigma_g = 1.0$ , that is, an exact monodisperse particle distribution in which all particles are a single size, which is also the MMAD.

The empirical model described in this appendix was developed from exposures using essentially monodisperse particles (which are treated as though they are exactly monodisperse). It is therefore possible to multiply the particle size distribution function (which is customarily considered to be the lognormal distribution) by the predicted depositions (calculated as described in Equations G-8 through G-10) and integrate over the entire particle size range (0 to  $\infty$ ). Mathematically, this calculation is performed as described by Equation G-3, and is illustrated for the mouse and human ET regions in panels B and C respectively, of Figure G-2.

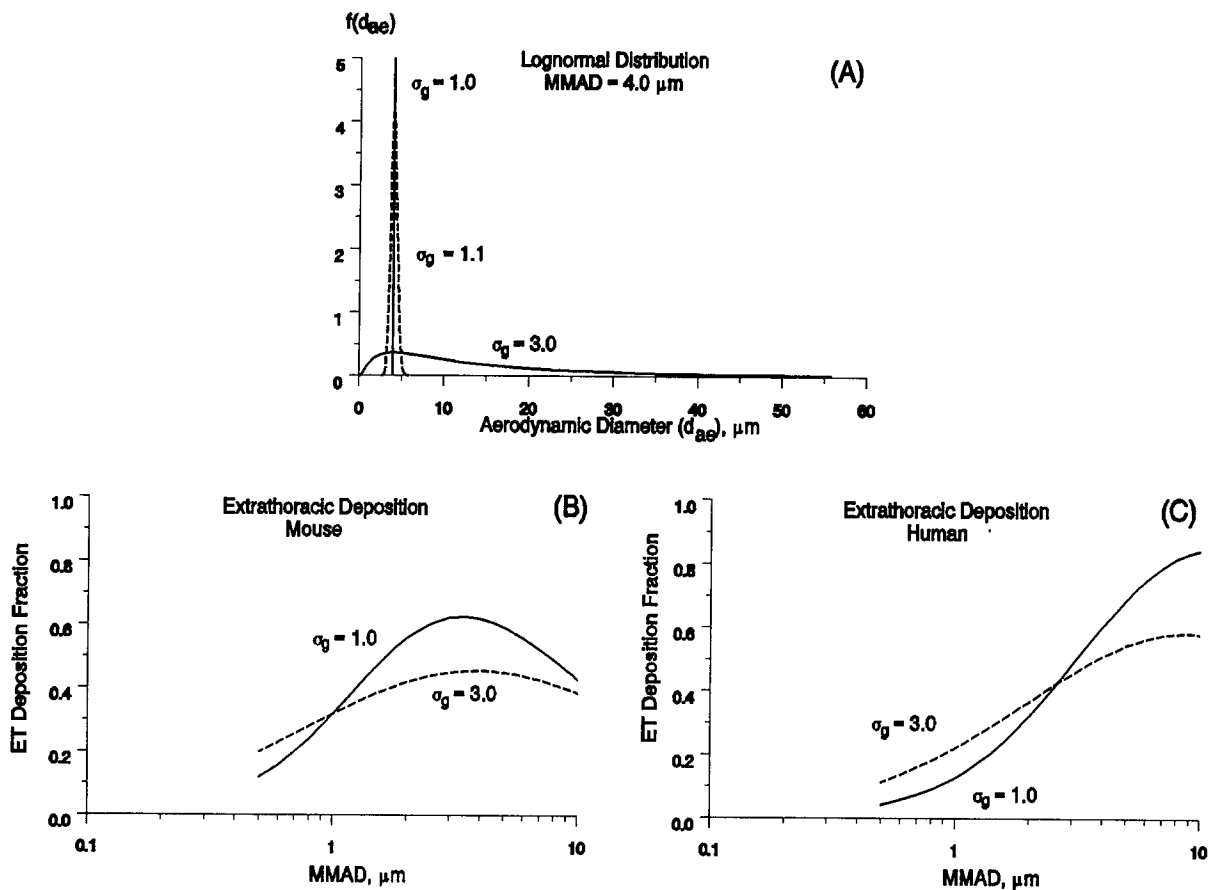


**Figure G-2.** Range of particles for lognormal distributions with same MMAD but differing geometric standard deviations (A). Effect of polydisperse particles on predicted extrathoracic deposition fractions in mice (B) and humans (C).

$$[\hat{F}_r]_p = \int_0^{\infty} [\hat{F}_r]_m \times \frac{1}{d_{ae}(\log \sigma_g) \sqrt{2\pi}} \times \exp \left[ -1/2 \frac{(\log d_{ae} - \log \text{MMAD})^2}{\log \sigma_g} \right] dd_{ae} \quad (\text{G-13})$$

where  $\log$  refers to the natural logarithm,  $[\hat{F}_r]_p$  is the predicted polydisperse fractional deposition for a given MMAD, and  $[\hat{F}_r]_m$  is the predicted monodisperse fractional deposition for particles of size  $d_{ae}$ . The limits of integration are defined from 0 to  $\infty$  but actually include only four standard deviations (99.95% of the complete distribution). For each particle size in the integration,  $[\hat{F}_r]_m$  is calculated as described in the ten steps listed in this appendix, then

multiplied by the probability of observing a particle of that size in a particle size distribution with that MMAD and  $\sigma_g$ .

Panels B and C of Figure G-2 illustrate one of the principal effects of polydisperse particle size distributions on predicted deposition fractions in the ET region, which is to flatten the deposition curve as a function of MMAD. This same effect is observed also in the TB and PU regions. (Note that the curves in panels B and C are expressed as a function of MMAD. They were generated as a function of the impaction parameter but are expressed as a function of MMAD for ease of comparison between species. A  $\dot{V}_E$  of 37.5 mL/min was used for the mouse and of 13.8 L/min for the human.) Rudolf and colleagues (1988) have also investigated the effect of polydisperse particle size distributions on predicted regional uptake of aerosols in humans and present a more detailed discussion of these and related issues.

#### **G.4 REGIONAL DEPOSITED DOSE RATIO CALCULATIONS IN RATS AND HUMANS: AN EXAMPLE**

Three respiratory tract  $RDDR_r$  values were calculated as described by Equation 4-7 using (1) the default body weight for a female Fischer 344 rat in a subchronic study from Table 4-5 to estimate  $\dot{V}_E$  for the rat and (2) the regional respiratory tract surface areas as the normalizing factor for the rat and human from Table 4-4. In Figure G-3, the ET, TB, and PU  $RDDR_r$ , as a function of particle size, for particles in the aerodynamic size range are compared for monodisperse and a highly polydisperse particle size distribution ( $\sigma_g = 3.0$ ). When the  $RDDR_r$  is 1, both human and rodent would be predicted to have a comparable dose rate per unit surface area of the inhaled particles. Ratios with a value of less than 1 indicate that for an equivalent external exposure concentration, the dose rate per unit surface area in the human will be greater than in the rodent; while  $RDDR_r$  which are greater than 1 occur when the rodent receives a larger surface area adjusted dose rate than the human. Figure G-3 indicates that in the ET region, the human will be expected to have a higher dose rate per unit surface area than the rat over the aerodynamic particle size range for both monodisperse and polydisperse particle size distributions. For the highly polydisperse particle size distribution, the  $RDDR_r$  in the ET region is relatively constant as a function of aerodynamic

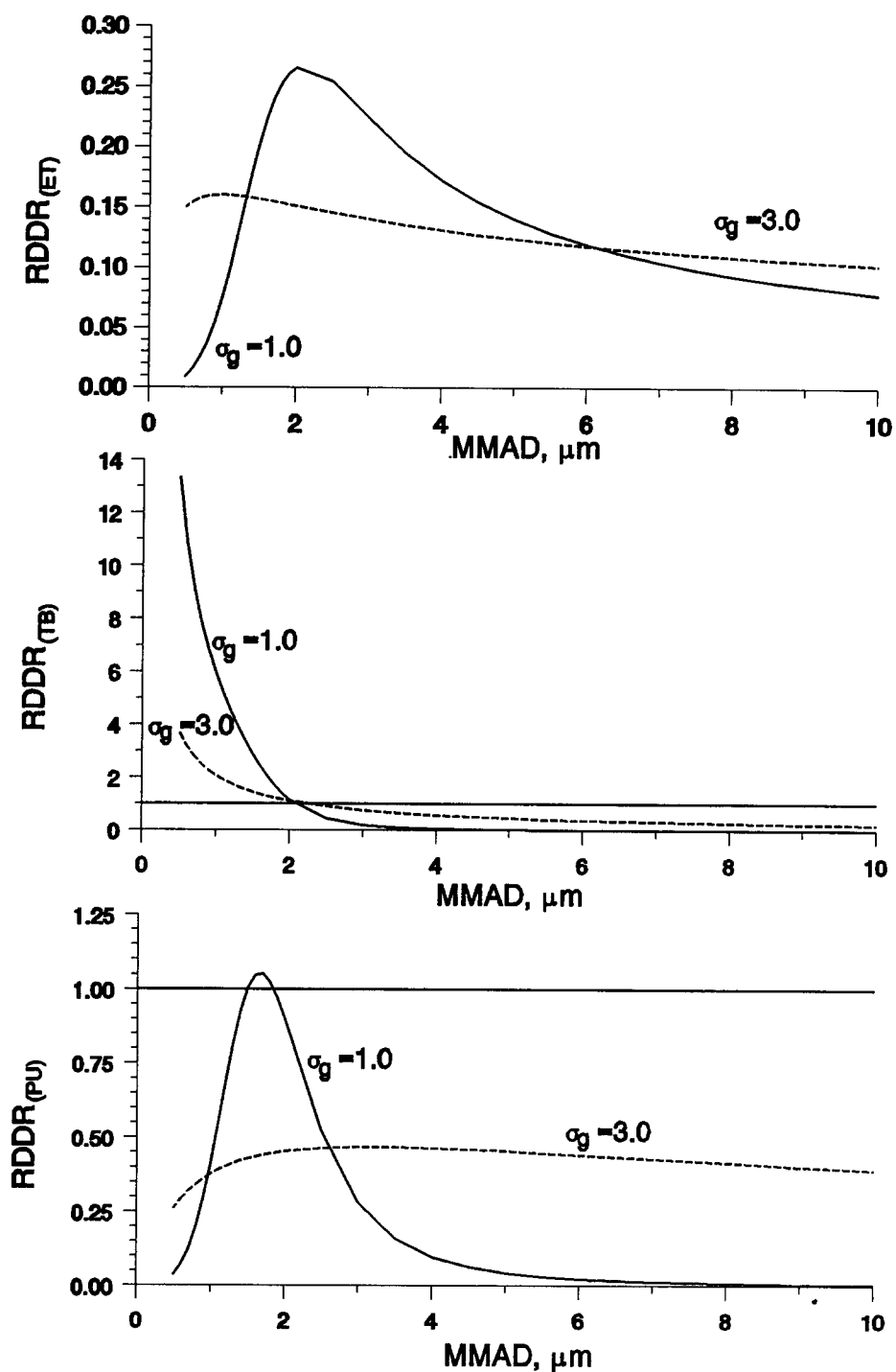


Figure G-3. Regional deposited dose ratios ( $\text{RDDR}_r$ ) for rat:human as a function of mass median aerodynamic diameter (MMAD) for monodisperse ( $\sigma_g = 1$ ) and polydisperse ( $\sigma_g = 3$ ) particle size distributions.

particle size. This may be interpreted to mean that for a highly polydisperse size distribution, the dose rate per unit surface area to the ET region of the human will be approximately 10 to 15 times that to the ET region of the rat regardless of the particle MMAD. In the TB region, the RDDR declines over the aerodynamic particle size range for both mono- and polydisperse particle size distributions. For particles smaller than about  $2 \mu\text{m}$  MMAD, the rat is predicted to have a higher dose rate than the human; for larger particles, the relationship is reversed. In the PU region, a relationship that is qualitatively similar in shape to the  $\text{RDDR}_{\text{ET}}$  is observed; however, the range of the  $\text{RDDR}_{\text{PU}}$  is much larger and there is a suggestion that the dose rate in the rat is greater than that in the human for particles of about  $2 \mu\text{m}$  MMAD since the  $\text{RDDR}_{\text{PU}} > 1.0$ .

This example illustrates the complexities in the relationships between dose rate per unit surface area in the three respiratory tract regions for rodents and humans. The regional differences as well as the differences due to MMAD and  $\sigma_g$  indicate the importance of replacing administered dose with dosimetric information whenever possible in making risk evaluations.

# APPENDIX H

## PARTICLE SIZING CONVENTIONS

Solid or liquid particles suspended in a gas are called an aerosol. In toxicological experiments and epidemiological studies, aerosol particles from a given exposure are commonly described by some measure of the average size of the particle and some measure of variability in that average size. Although the average size is usually expressed as a diameter, there are numerous methods for calculating diameter. In this appendix, some of the more common sizing conventions for spherical (or nearly spherical) particles are briefly discussed. Conversions from reported units to the units required to use the particle dosimetry model described in this document are provided. More detailed discussions of particle properties and behavior may be found elsewhere (Raabe, 1971, 1976; Hinds, 1982).

### H.1 GENERAL DEFINITIONS

Particles in an exposure are rarely all a single size but rather have some distribution in size around an average value. It is generally accepted (Raabe, 1971) that the lognormal distribution provides a reasonable approximation for most observed spherical particle distributions. For this reason, particle exposures are frequently characterized by median diameter and the geometric standard deviation ( $\sigma_g$ ). Statistically speaking, data from a lognormal distribution may be completely described by the median and geometric standard deviation. As  $\sigma_g$  approaches 1.0, the distribution of the particles approaches a single size and the particles are said to be monodisperse. As a matter of practicality, a distribution is considered to be near monodisperse when  $\sigma_g$  is less than 1.3. As  $\sigma_g$  approaches infinity, the distribution contains particles of many sizes and is said to be polydisperse. By definition,  $\sigma_g$  cannot be less than 1.0.

In toxicological experiments, researchers might use (or try to use) monodisperse spherical particles because deposition is a function of particle size. Real world exposures, however, are rarely to monodisperse particles. Accordingly, laboratory animal experiments

designed to mimic some real exposure will use polydisperse particle distributions. Studies of diesel exhaust and of Mt. St. Helens volcanic ash, for example, used highly polydisperse particles. In addition to being polydisperse, such particles also have irregular shapes. Although some irregular particles may be described by their aerodynamic diameter and so be considered to behave like spherical particles, other particles have such extreme differences in shape that they must be described by other parameters. Fibers are one extreme example of nonspherical particle shapes. Deposition fractions for these particles may not be calculated with the particle dosimetry model used in the methodology.

Particle diameters are most frequently reported as geometric diameter ( $d_g$ ) or aerodynamic diameter ( $d_{ae}$ ). Aerodynamic diameter is defined as the diameter of a unit density sphere having the same settling velocity as the geometric diameter of the particle in question. Geometric diameters may be converted to aerodynamic diameters according to the following equation:

$$d_{ae} = d_g \sqrt{\rho C(d_g)/C(d_{ae})} \approx d_g \sqrt{\rho}, \quad (\text{H-1})$$

where  $\rho$  is the particle density in  $\text{g/cm}^3$  and  $C(d)$  is the Cunningham slip correction factor.

The particle dosimetry model requires that the particle size be expressed in aerodynamic diameter so studies reporting particle sizes in these units will most likely not require any further conversion. There are, however, two commonly used definitions for  $d_{ae}$ ; the methodology uses the definition of the Task Group on Lung Dynamics (1966). Because of the complexities in calculating  $d_{ae}$  by the Task Group equation, other investigators have developed an alternate specification for aerodynamic diameter (Mercer et al., 1968; Raabe, 1976). This  $d_{ae}$  is called an aerodynamic resistance diameter,  $d_{ar}$ , and may be converted to  $d_{ae}$  according to the following equation:

$$d_{ae} = (d_{ar}^2 + 0.0067)^{0.5} - 0.082. \quad (\text{H-2})$$

Summary information from an exposure will most often be presented as count (CMD), mass (MMD), surface (SMD) or activity (AMD), median (geometric) diameter. The summary information might be reported in terms of median aerodynamic diameters instead (CMAD, MMAD, SMAD, AMAD).

Because the particle distributions are assumed to be lognormal, estimation of count, surface area, or mass distributions for any given sample of particles may be made once one of those distributions has been measured. Figure H-1 shows a typical log-normal distribution and the various indicated diameters encountered in inhalation toxicology literature.

Table H-1 provides the definitions of these diameters. A series of conversion equations originally derived by Hatch and Choate (1929) may be used to convert the reported units to MMAD, the units required by the particle dosimetry model. Figure H-2 shows the same aerosol as in Figure H-1 plotted on log-probability paper and illustrates the various size parameters that can be computed using the Hatch-Choate equations. The relevant conversion equations are summarized in Table H-2. It is a characteristic of any weighted distribution of a lognormal distribution (such as the conversions described in Table H-2) that the geometric standard deviation will be unchanged.

Conversion of activity median diameter (AMD) to MMAD depends on how the radiolabeling of the particle was done. If the label was generated in a liquid, then the label is distributed throughout the volume of the particle and the AMAD may be considered to be equivalent to the MMAD. If, however, the radioactivity was attached to the surface of the particle, then the activity median diameter may be considered to be proportional to the surface area median diameter. More information on the labelling procedure is required to provide an estimate of the proportionality factor. Further discussion of issues related to activity diameters may be found elsewhere (Hofmann and Koblinger, 1989).

The concept of activity diameter is also useful when considering the physical characteristics of particles that are responsible for the health effect or toxicity of concern. The activity diameter of a particle may be the most appropriate expression of size for this purpose. This expression takes into account the "activity" of the physical property of the particle. For example, if the toxicant is distributed only on the surface, then the activity median diameter is equal to the surface median diameter; and conversions to MMAD would

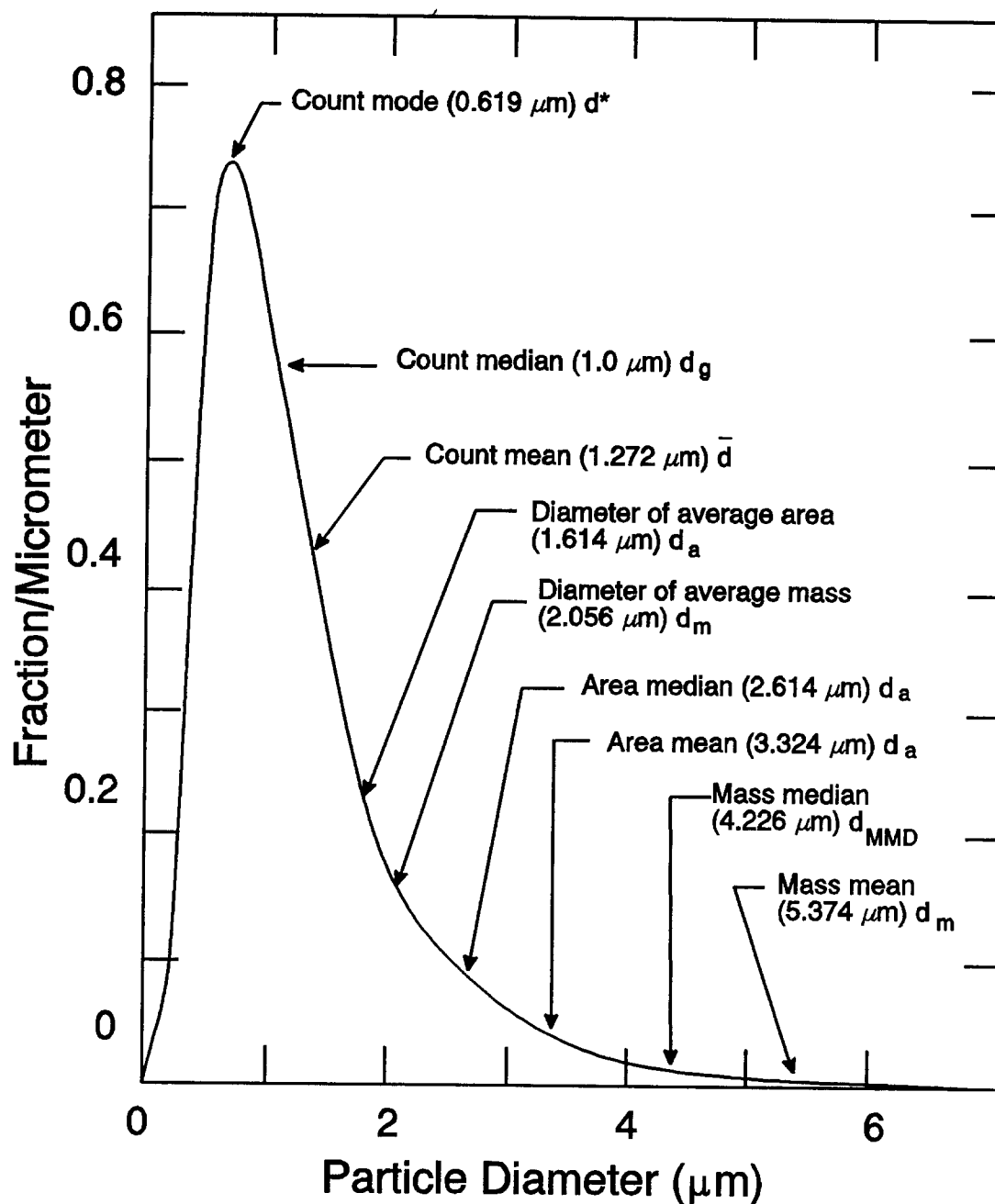


**Figure H-1.** An example of the log-normal distribution function of an aerosol. Definitions of diameters commonly used are provided in Table H-1. Note that if aerodynamic diameters were being measured, then count or other frequency distribution would be measured against that (e.g., count median aerodynamic diameter [CMAD]).

Source: Orr and Keng (1976).

**TABLE H-1. PARTICLE DIAMETER DEFINITIONS**

<b>Count mode diameter</b>	The most frequently characterized particle diameter. In Figure H-1, the frequency is normalized to frequency (or number) per micron. This type of graph is also used in analyzing cascade impactor data.
<b>Count median diameter</b>	This diameter is used to describe any log-normal distribution. It is the diameter of a particle that is both larger and smaller than half the particles sampled.
<b>Count mean diameter</b>	The average particle diameter. It is calculated by first multiplying each diameter measured by the number of particles having that diameter. Summing all of these products over the entire range of diameters measured and dividing by the total number of particles sampled gives the count mean diameter.
<b>Diameter of "average mass"</b>	Another average particle diameter related to the total mass of particles sampled. The mass of the particle of "average mass" multiplied by the total number of particles sampled, equals the total mass of particles sampled. The total mass of particles sampled is calculated by first multiplying the single-particle mass calculated for each diameter measured by the number of particles having that diameter and summing all of these products over the entire range of diameters measured. The average mass of each individual particle sampled is obtained by dividing this number by the total number of particles. The diameter is calculated by assuming a sphere and applying the density of the material to convert from mass to volume and then to diameter.
<b>Mass median diameter</b>	Diameter of the particle having a mass that is both larger and smaller than the mass of half the particles sampled.
<b>Mass mean diameter</b>	Average particle diameter, calculated by first multiplying each diameter measured by the cumulative mass of all particles having that diameter. Summing all of these products over the entire range of diameters measured and dividing by the total mass of the particles sampled gives the mass mean diameter.

Source: Moss and Cheng (1989).

be the same as described above for radiolabeled activity. If the toxicant is soluble, the surface area of the particle will influence the rate of dissolution because solubilization occurs at the surface. Such a situation needs to be understood more thoroughly, especially for complex particles.

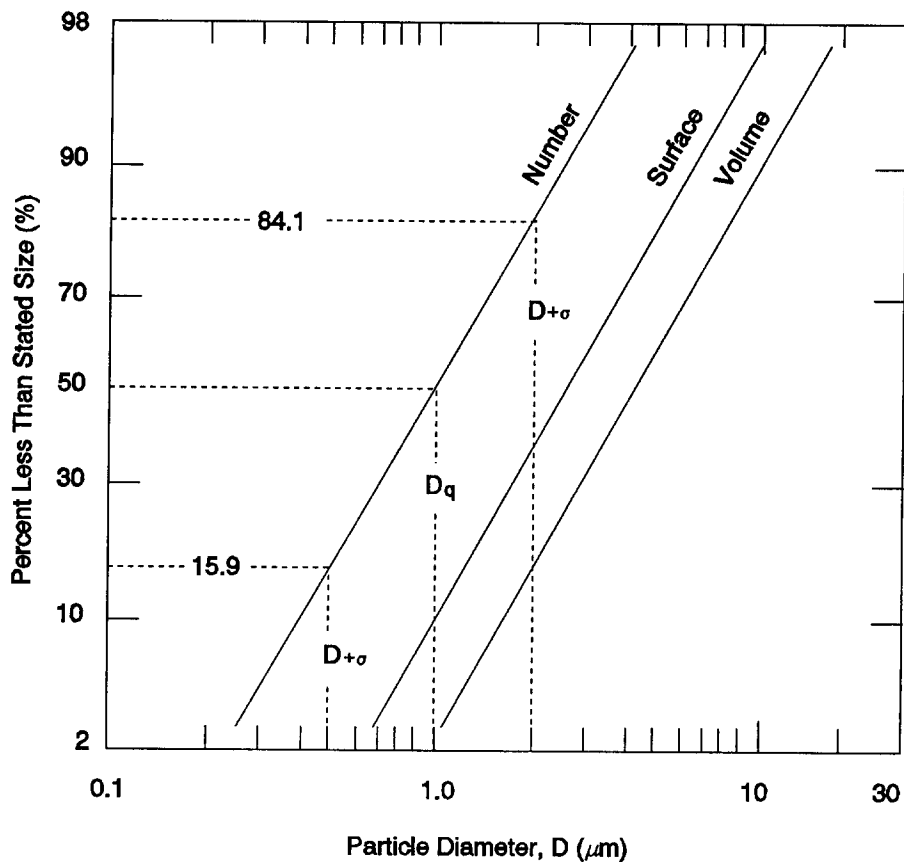


**Figure H-2.** Plot of same aerosol as in Figure H-1 on log-probability paper. The curves illustrate the various size parameters that can be computed using the Hatch-Choate equations.

Source: Marple and Rubow (1980).

## H.2 GENERATION SYSTEMS AND CHARACTERIZATION INSTRUMENTS

Aerosols may be generated by condensation of vapors, by dispersion of dry particles or liquids, or by dispersion of a suspension of solids in a liquid. Each of the currently available systems and applied techniques used to generate test atmospheres for inhalation toxicology testing have operating specifications that should be evaluated when attempting to determine whether the operating conditions and size range stated was appropriate to the technique and to ascertain the probable particle size range. The operating specifications (pressure, flow rate, output concentrations, particle diameters, and standard deviations) of various generation

**TABLE H-2. LOGNORMAL CONVERSION EQUATIONS FOR  
COMMON TYPES OF DIAMETERS**

---

**Count to Mass**

$$\text{MMAD} = \text{CMAD} \exp (3 [\log \sigma_g]^2)$$

$$\text{MMAD} = \rho^{0.5} \text{CMD} \exp (3 [\log \sigma_g]^2)$$

**Activity to Mass**

MMAD = AMAD if label may be assumed to be distributed throughout volume of particle

MMAD = pSMAD if label is attached to a proportion, p, of the surface of the particle

**Count to Surface**

$$\text{SMAD} = \text{CMAD} \exp (2 [\log \sigma_g]^2)$$

$$\text{SMAD} = \rho^{0.5} \text{CMD} \exp (2 [\log \sigma_g]^2)$$


---

**Note:** log = natural logarithm.

systems have been reviewed elsewhere and can serve as references (Moss and Cheng, 1989; American Conference of Governmental Industrial Hygienists, 1978; Willeke, 1980).

Characterizing test atmospheres includes defining the aerosol concentration, chemical composition, and particle size and shape. Aerosols for toxicology testing should be characterized to quantitate toxicant concentration, stability, and particle size distribution during exposure. Mass concentration of aerosols can be measured directly using filters, impingers, and impactors. Other methods of determining mass concentration include beta-attenuation, piezobalance, and photometers. The latter two instruments are real-time continuous samplers that enable monitoring and early detection of problems related to generation and delivery. Number concentrations are obtained by using nucleus counters, optical counters, electrical counting, and microscopy.

The shape and size of particles are determined by collecting particles on filters, on grids mounted on thermal or electrostatic precipitators or by microscopy. Dynamic size measurements made using inertial or mobility aerosol instruments are frequently used to determine the aerodynamic and mobility equivalent diameters. These diameters can be used in the conversions scenarios provided in the next section.

Inertial types of instruments are used to measure  $d_{ae}$  larger than about 0.5  $\mu\text{m}$ . For particles less than 0.5  $\mu\text{m}$  in diameter, most inertial instruments are not effective in

separating and measuring particle size. In these cases, the mobility type of aerosol instrument is used. The mobility equivalent diameter determines the collection efficiency in many processes that are controlled by the diffusion deposition mechanism. Two types of mobility instruments are the electrical aerosol analyzer (EAA) and the diffusion batteries. No single instrument can measure aerosol size distributions of particles with diameters from 0.005 to 10  $\mu\text{m}$ . Sometimes different exposure levels are generated or characterized with different instruments. Careful analysis of data is required, because the inertial instruments (e.g., cascade impactor) give mass distribution, and the EAA and screen diffusion battery give number distribution. Figure H-3 shows the measurement ranges of aerosol monitoring instruments. Knowledge of the measurement range of the instruments used to characterize the test atmosphere can be useful in determining the probable particle size range used in a given study.

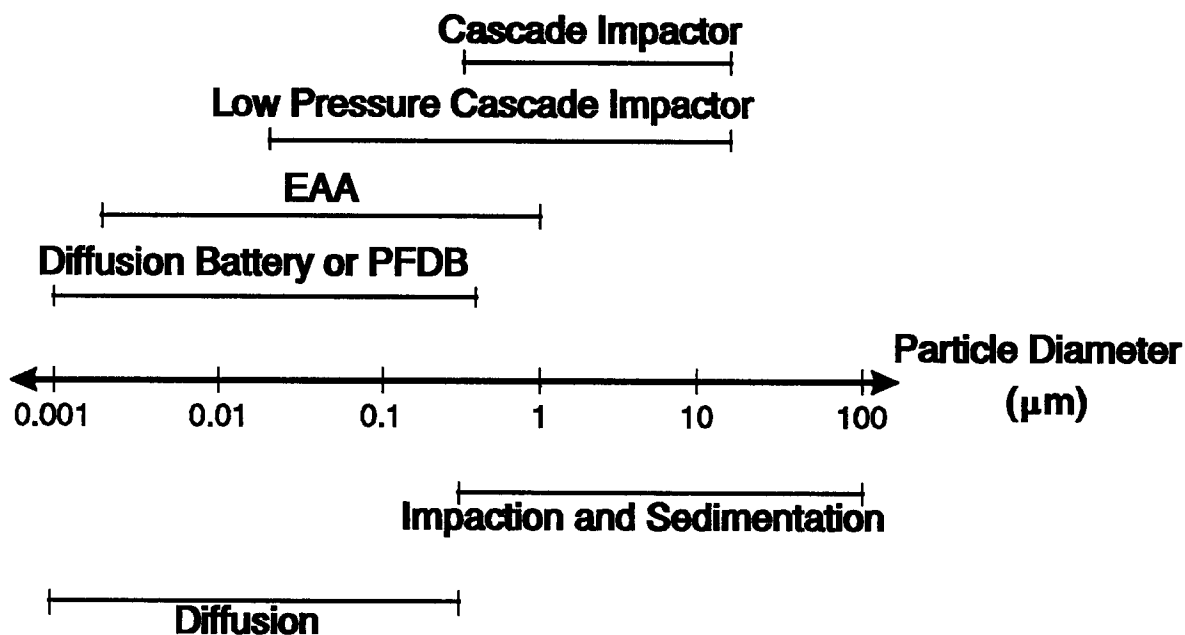


**Figure H-3. Measurement ranges of aerosol monitoring instruments.**

Source: Moss and Cheng (1989).

### H.3 CONVERSION SCENARIOS

Particle information reported in a study will most likely fall into one of the seven categories defined below. The remainder of this appendix describes these seven possibilities and outlines appropriate strategies to convert reported particle information to MMAD, required to run the particle dosimetry model.

**1. MMAD and  $\sigma_g$ .**

In this case the information in the study has been reported in the units required for analysis, and no conversions or changes are required to run the model.

**2. A median diameter and  $\sigma_g$ .**

Conversions from the most commonly used medians to MMAD are provided in Table H-2. No conversions are required for  $\sigma_g$ .

**3. A median diameter and a range of particle sizes.**

The variance,  $\sigma_g$ , may be estimated as

$$\begin{aligned}\sigma_g &= \exp \left[ \frac{\log(\text{median/lower bound})}{n} \right] \\ &= \exp \left[ \frac{\log(\text{upper bound/median})}{n} \right]\end{aligned}\tag{H-3}$$

where log is the natural logarithm, exp is the irrational number, e, raised to the power in the brackets, and the range falls between the reported upper and lower bounds. The range will include some percentage of the particles that is reflected in the parameter n, the number of standard deviations used in calculating  $\sigma_g$  (Table H-3). The median diameter may then be converted to MMAD according to the equations in Table H-2, if necessary.

**TABLE H-3. PERCENTAGE OF PARTICLES IN THE REPORTED RANGE ASSOCIATED WITH THE NUMBER OF STANDARD DEVIATIONS (n) USED TO CALCULATE THE GEOMETRIC STANDARD DEVIATION**

Percentage of Particles in the Reported Range	n
0.68	1
0.95	2
0.997	3
>0.999	4

**4. A median diameter only.**

An estimate of  $\sigma_g$  must be derived from outside sources. In order of preference, the following sources are recommended.

- a:** Other studies by the same group using the same compound for which the median and  $\sigma_g$  are reported.
- b:** A comparison of the variances reported by other studies for the same compound could be used to determine reasonable bounds on  $\sigma_g$ . Using the largest and smallest  $\sigma_g$  determined by this method, the dosimetry model can be run to determine the sensitivity of the dose ratio to  $\sigma_g$  for this particular particle size and rodent to human comparison.
- c:** The particle size range can be estimated from Figure H-4 and  $\sigma_g$  calculated according to Equation H-3 and Table H-3 (letting  $n = 4$ ). If necessary, the median can then be converted to MMAD according to Table H-2.

**5. A range of particle sizes is the only information provided.**

A median, in the same units as the reported particle size range, must be estimated from outside sources. In order of preference, the following sources are recommended.

- a:** Other studies by the same group using the same compound for which the median is reported.
- b:** A comparison of the medians reported by other studies for the same compound could be used to determine reasonable bounds on the median. If necessary, the dosimetry model could be run using the largest and smallest medians estimated by

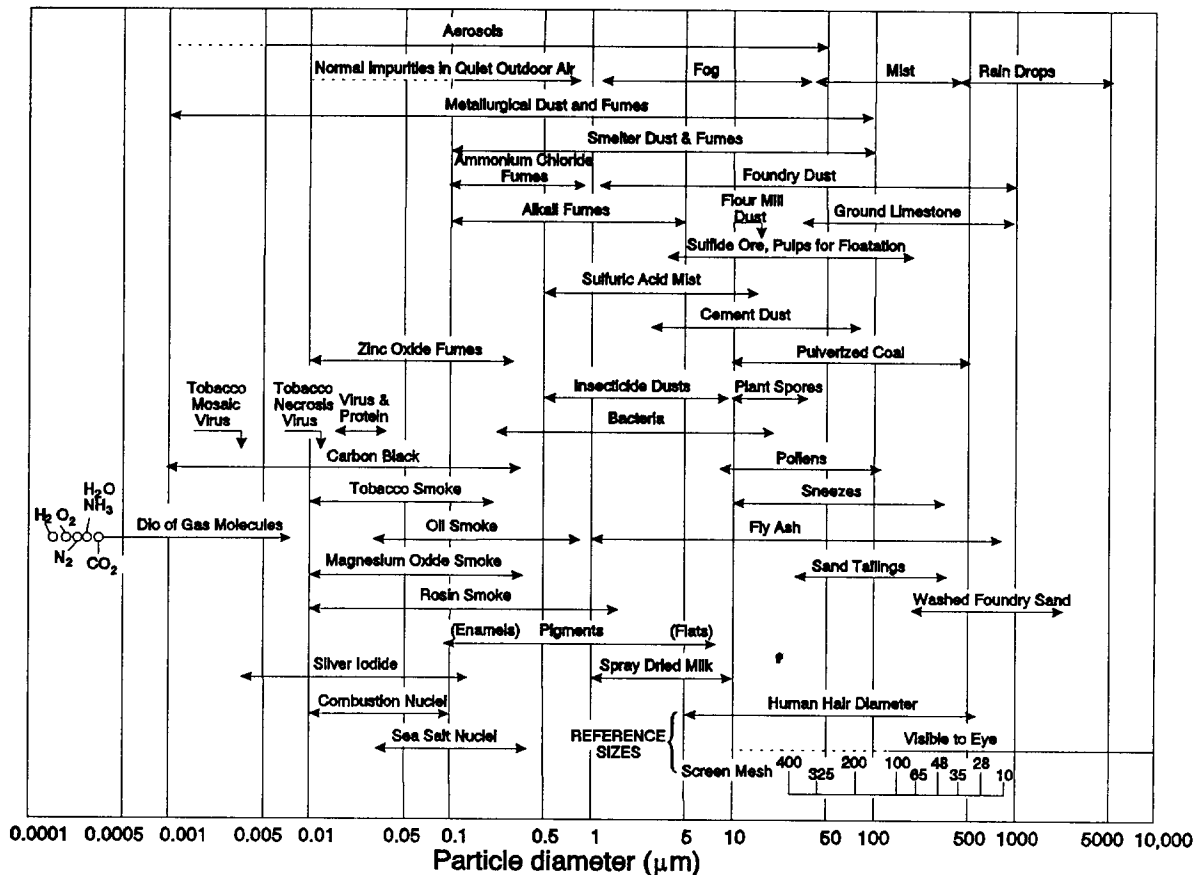


Figure H-4. Various airborne materials and their size ranges.

Source: Hatch and Gross (1964).

this method. Note that running the model with alternate estimates of the median will require alternate estimates of  $\sigma_g$ .

Using the estimated median and the range of particle sizes,  $\sigma_g$  may be estimated as described above in scenario 3. Finally, the median diameter may be converted to MMAD according to the equations in Table H-2, if necessary.

**6. Descriptive information on particle size is the only information provided.**

Some of the more commonly used expressions of particle characteristics and the generally accepted particle sizes associated with these characteristics are shown in Table H-4. Further information on ranges of sizes for some common classifications of

**TABLE H-4. GENERAL PARTICLE DESCRIPTIONS AND ASSOCIATED SIZES**

Particle Description	Size ( $\mu\text{m}$ )
Coarse	> 2.5
Fine	< 2.5
Fumes, Smoke	< 1
Fog, Mist	< 1 → 20

particles may be found in Figure H-4. Using this information, the median may be estimated as described in scenario 5, and  $\sigma_g$  estimated as described in scenario 4.

**7. No information on particle sizes provided.**

Studies that do not provide this information should be suspect for deficient quality. Some of the older toxicology literature may not provide this information, however, and a default value may need to be invoked. The first approach in this situation is to attempt an estimate of particle size and distribution based on the generation apparatus used. Operating specifications of various generation systems are available from the manufacturer or reviewed elsewhere (Moss and Cheng, 1989; American Conference of Governmental Industrial Hygienists, 1978; Willeke, 1980). In conjunction with this information, the knowledge that prior to the late 1970s, the generation technology was not sufficiently sophisticated to deliver consistent exposures of particle sizes above 3  $\mu\text{m}$  (MMAD) can be used to construct a default approach. The recommended default approach is to use the MMAD and  $\sigma_g$  characteristic for the given generation system that is  $\leq 3 \mu\text{m}$  and that yields the smallest (i.e., most conservative) RDDR values for the respiratory tract region of interest. Knowledge of the measurement range of the instrument used to characterize the test atmosphere can also be used to estimate a particle size. Figure H-3 provides the measurement ranges of some aerosol monitoring instruments.

The second approach is to use particle size information from other studies to estimate the particle characteristics for the exposure in question. If no such information is available, Figure H-4 provides the general size ranges for most common classifications of particles. Using this information, the median may be estimated as described in scenario 5, and  $\sigma_g$  estimated as described in scenario 4.

## APPENDIX I

# DERIVATION OF AN APPROACH TO DETERMINE HUMAN EQUIVALENT CONCENTRATIONS FOR EFFECTS OF EXPOSURES TO GASES IN CATEGORIES 1 AND 2

As discussed in Sections 3.2 and 4.3, the optimal approach to describe regional respiratory tract dose for extrapolation across species is to use a comprehensive dosimetry model. The limited number of sophisticated dosimetry models that currently exist are either chemical-specific or class-specific and require an extensive number of model parameters. As discussed in Section 3.2, the chemical-specific or class-specific nature of these models has been dictated by the physicochemical properties of the subject gases and therefore any single resultant model is not applicable to the broad range of physicochemical properties of gases (or vapors—herein referred to as gases) that this methodology is aimed at addressing. In addition, sufficient data from which to estimate model parameters for each gas are often unavailable.

A conceptual framework was thus developed to structure mathematical models that require limited gas-specific parameters and that may be further reduced by simplifying assumptions to forms requiring minimal information. The models in reduced form are the basis of the default adjustments used in Section 4.3 and are used to estimate the human equivalent concentrations (HECs) from no-observed-adverse-effect levels (NOAELs) of gases when the lack of data for the required parameters precludes more comprehensive modeling. This appendix provides the conceptual framework and background details of the default derivation for the adjustments used in Section 4.3.

Because adverse respiratory effects may be observed in the extrathoracic (ET), tracheobronchial (TB), or pulmonary region (PU), the conceptual framework is constructed to derive a regional description of dose, defined as the regional absorption rate. The regional absorption rate is used as a surrogate of regional dose and is assumed to represent the

effective dose for evaluation of the dose-response relationship. The physicochemical properties such as the water solubility and reactivity (e.g., ionic dissociation or tissue metabolism) of the gas in the respiratory system are major determinants of the regional absorption rate. For example, styrene is relatively insoluble in water and unreactive with the respiratory tract surface liquid and tissue. This gas is therefore absorbed primarily in the lung periphery, where it partitions across the blood-gas barrier. Formaldehyde, however, is both water soluble and reactive such that most of the gas is absorbed in the ET region. The concept of differentiating gases based on their stability, reactivity, or tissue metabolic activity has been proposed by Dahl (1990) who presented a methodology to assist in categorizing gases. As discussed in Section 3.2, delineation of the categories is accomplished by identifying dominant mechanistic determinants of absorption that are based on the physicochemical characteristics of the gases. The dominant mechanistic determinants are used to construct a conceptual framework that directs development of the dosimetry model structures.

The categorization scheme discussed in Section 3.2 and developed more fully herein is used to establish a dosimetry model structure for three categories of gases from which default equations are developed by imposing additional simplifying assumptions. Model structures for two of the three categories are developed in this Appendix. The structure for Category 3 gases is developed in Appendix J. Gases in Category 3 are relatively water insoluble and unreactive in the ET and TB surface liquid and tissue and thus exposures to these gases result in a relatively small dose to these regions. The uptake of these gases is predominantly in the PU region and is perfusion limited. The site of toxicity of these gases is generally remote to the principal site of absorption in the respiratory tract. Thus, the relatively limited dose to the ET and TB regions does not appear to result in any significant ET or TB respiratory toxicity. Toxicity may, however, be related to recirculation. An example of a Category 3 gas is styrene. Gases that fall in Category 3 are modeled using the structure and default equations presented in Appendix J.

The methodology developed in this appendix addresses the absorption of gases that are relatively water soluble and/or reactive in the respiratory tract (Categories 1 and 2 of the scheme described in Section 3.2). The focus here is on the description of dose for respiratory tract effects. This is not to suggest that the toxicity is limited to the respiratory

regions and in fact, for Category 2, the model structure may be used to define a dosimetric for remote toxicity because this category of gases has physicochemical characteristics that may result in some systemic circulation of toxicant. The assumption of this modeling approach is that the description of an effective dose to each of these regions for evaluation of respiratory effects must address the absorption or "scrubbing" of a relatively water soluble and/or reactive gas from the inspired airstream as it travels from the ET region to the PU region. That is, the dose to the distal regions (TB and PU) is affected by the dose to the region immediately proximal. The appropriateness of assessing proximal to distal dose representative of the scrubbing pattern is supported by the often observed proximal to distal progression pattern of dose-response for respiratory tract toxicity with increasing concentration. At low concentrations of relatively water soluble and/or reactive gases, observed effects are isolated to the ET region. At higher concentrations, more severe effects occur in the ET region and toxicity is also observed to progress to the distal regions. The intensity or severity of the distal toxicity also progresses with increased exposure concentrations.

In the following section, the conceptual framework that directs development of dosimetry models is discussed. The framework is constructed according to the categorization scheme of gases based on physicochemical characteristics. The physicochemical characteristics are used to define dominant mechanistic determinants of absorption and thereby determine the mathematical model structure to describe regional dosimetry. The model structures developed in the framework rely on models that are currently in use; a detailed review of potential structures is presented elsewhere (Ultman, 1988) and some are incorporated here. Description and derivation of the model structure for each category of gas follows with the exception of gases that are relatively insoluble in water (Category 3). The uptake of Category 3 gases is predominantly perfusion-limited and the dosimetry approach for these is discussed in Appendix J. Thus, the focus of this appendix is on those gases that are relatively water soluble and/or reactive in the respiratory tract. It should be noted that the definition of reactivity includes both the propensity for dissociation as well as the ability to serve as substrate for metabolism in the respiratory tract. The default equations are derived after the development of the modeling structure for gases in Categories 1 and 2. These equations result from the application of further simplifying assumptions necessary to reduce

the required parameters to perform the dosimetry adjustment when minimal data are available.

## **I.1 Conceptual Framework**

Extrapolation of the dose-response relationship from laboratory animals to humans is performed based on the absorption in the three respiratory tract regions as defined in Chapter 3: extrathoracic (ET), tracheobronchial (TB), and pulmonary (PU). Although toxic effects may sometimes be observed in a more local area within those regions (e.g., the olfactory epithelium of the ET region), the parameters required to further subdivide the description of dose within these regions are not available currently. Several active areas of investigation, such as the evaluation of regional mass transport within the nasal cavity to create maps of localized flows in rats and monkeys (Kimbell et al., 1993), of regional mass transport in the human (Lou, 1993), and of metabolic activity of localized tissues in rodents (Bogdanffy et al., 1986, 1987, 1991; Bogdanffy and Taylor, 1993; Kuykendall et al., 1993), are anticipated to provide the data required to estimate the necessary parameters on a species-specific basis.

The conceptual framework used to direct development of model structures for estimation of regional gas dose is based on the categorization scheme presented in Section 3.2.2. This categorization scheme is based on the physicochemical characteristics of water solubility and reactivity as shown in Figure I-1. These characteristics are used to define dominant mechanistic determinants of absorption and thereby direct development of model structures. As will be described, the modeling structure favored for this development has been used extensively to quantify gas exchange or absorption of pollutants. This structure is in no way promoted exclusively as the only one available; it is however used here to develop the approach for dosimetric adjustment. Its application to each category will be presented and the default equations for use with limited parameters will be derived.

### **I.1.1 Category Scheme for Gases with Respiratory Effects**

This appendix focuses on those gases that are relatively water soluble and/or reactive in the respiratory tract (i.e., those gases in Categories 1 and 2, initially defined in Section 3.2).

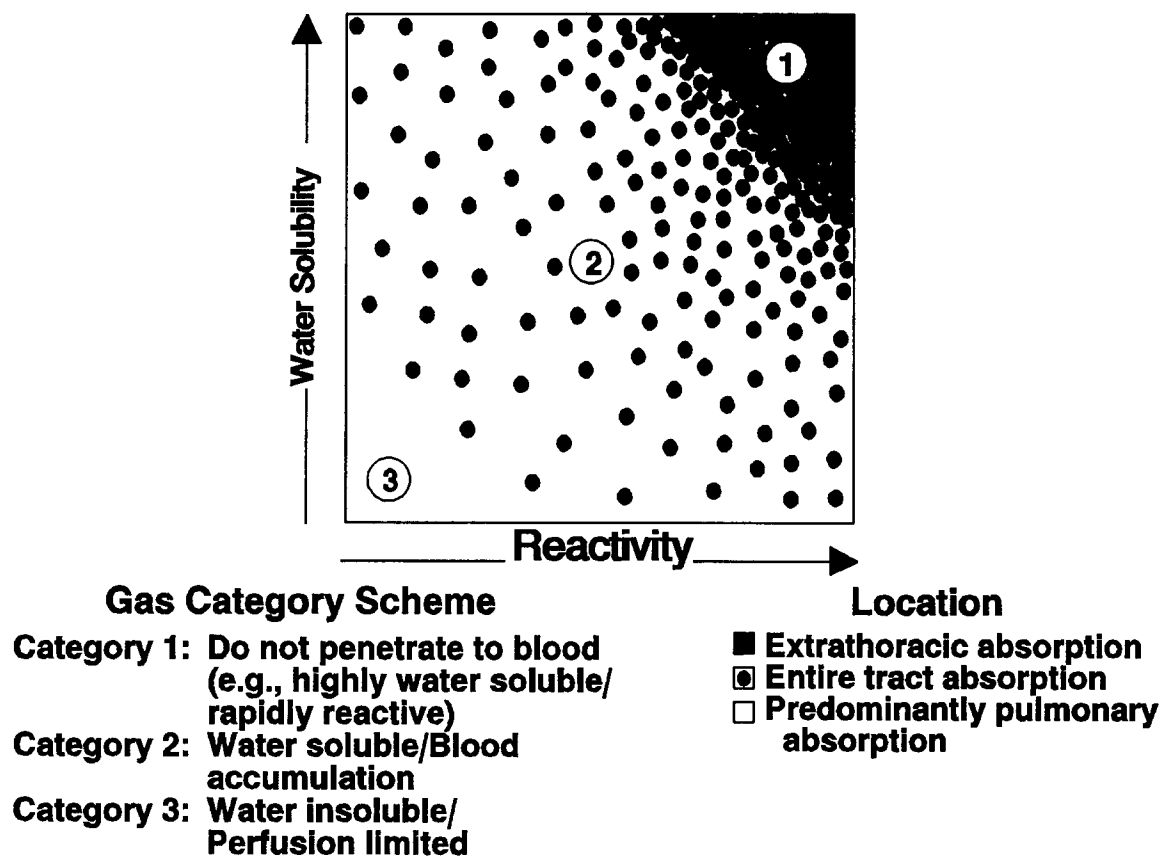


Figure I-1. Gas categorization scheme based on water solubility and reactivity as major determinants of gas uptake. Reactivity is defined to include both the propensity for dissociation as well as the ability to serve as substrate for metabolism in the respiratory tract. Definitive characteristic of each category and anticipated location (region) for respiratory tract uptake are shown.

Those gases which are relatively insoluble in water, principally absorbed in the PU region, and distributed remote to the respiratory tract (Category 3) are addressed in Appendix J. There are two points of departure between the treatments of Appendix I versus Appendix J: (1) uptake of Category 1 and 2 gases (Appendix I) is limited by absorption in the gas or surface-liquid/tissue phase, whereas uptake to the blood from the airspace for gases in Category 3 (Appendix J) is described by the blood-to-air partition coefficient only; and (2) Appendix I considers absorption in the regions proximal to the PU region.

Two categories of gases with potential respiratory effects at the uptake site have been identified for simplifying the methods for dose determination. The categories separate the gases on the basis of the physicochemical absorption parameters and the consequent dominant determinants of absorption. The two categories of gases with potential respiratory effects are (1) highly water soluble and/or rapidly irreversible reactive gases; and (2) water soluble gases and gases that may also be rapidly reversibly reactive or moderately to slowly irreversibly metabolized in respiratory tract tissue.

The gases in Category 1, highly water soluble and rapidly irreversibly reactive, are distinguished by the lack of a blood-phase component to the transport resistance (i.e., almost none of the gas reaches the bloodstream), which allows the overall transport to be described by the transport resistance through air and liquid/tissue phases only (i.e., the two-phase transport resistance model). Examples of gases in this category are hydrogen fluoride, chlorine, formaldehyde, and the volatile organic acids and esters.

Gases in Category 2 are distinguished from those in Category 1 by the potential for accumulation of a significant blood concentration that could reduce the concentration gradient driving the absorption process and thereby reduce the regional absorption rate. In addition, the accumulated blood or surface liquid/tissue concentration may impose a backpressure (i.e., a significant reverse in the concentration gradient) during exhalation which could result in desorption. Category 2 gases may be further subdivided by distinguishing between those that react reversibly with the surface liquid or underlying tissue from those that react irreversibly. A gas that is moderately to slowly irreversibly metabolized in the respiratory tract will effectively reduce tissue concentration and thereby increase the concentration gradient during absorption and decrease it during desorption. In contrast, reversible reactions will not affect the gradient dramatically. Consequently, in the case of irreversible reactions, the reaction rate may need to be included in the model. In the case of Category 2 gases undergoing a reversible reaction, the reaction may be incorporated into the model by the use of an enhanced solubility term. Examples of Category 2 gases are ozone, sulfur dioxide, xylene, propanol, and isoamyl alcohol.

General physicochemical properties of the gases have been used to delineate each of the categories. The boundaries between categories are not definitive. Some compounds may appear to be defined by either Category 1 or Category 2 because water solubility and

reactivity are a continuum. Thus, although sulfur dioxide is reversibly reactive, which would categorize it as a Category 2 gas, it is also highly soluble such as to be a Category 1 gas. Similarly, ozone is highly reactive yet only moderately water soluble. More explicit delineation of the categories will be made upon review of the empirical data and the predictability of the model structures for gases that may appear to fit more than one category. The modeling approach for the determination of dose for each of these categories of gases is discussed separately in the following sections, along with the determination of the default methods if sufficient detail from which to determine dose is not available for a specific gas.

### **I.1.2 General Model Structure**

Numerous model structures have been used to describe toxicant uptake in the respiratory tract. The structures range from compartmental models, such as physiologically based pharmacokinetic (PBPK) models in which spatial details are ignored, to distributed parameter models, such as the finite difference models of McJilton et al. (1972) and Miller et al. (1985). The finite difference models have been applied to specific gases, but a generalized structure was developed by Hanna et al. (1989) for water soluble gases. Several reviews of the various structures are available (Morgan and Frank, 1977; Ultman, 1988, 1994).

Methodologies to describe respiratory uptake of gases have been successfully applied by using two types of empirical compartmental models. These models are distinguished by the gases to which they have been applied. The ventilation-perfusion model first applied to the exchange of carbon dioxide/oxygen ( $\text{CO}_2/\text{O}_2$ ) in the lung periphery has been principally and most successfully employed to describe the stable and less soluble gases. The modeling of the respiratory tract using the ventilation-perfusion model has become a central component of PBPK models as described in Appendix J (Ramsey and Andersen, 1984; Andersen et al., 1987a; Overton, 1989; Andersen et al., 1991). In a ventilation-perfusion model (or Bohr model), the mass of inhaled chemical reaching the lung periphery, or PU region, is calculated as the product of the ambient concentration and the alveolar ventilation rate. The ventilation-perfusion model would overpredict the gas concentration that reaches the alveoli if the gas is absorbed or reacts with the ET and TB airway surface liquid and/or tissue.

The second type of model was developed to describe the fraction of an absorbing or reacting gas that penetrates the ET region. This model, which will be referred to as the

penetration fraction model, was first used by Aharonson et al. (1974) to demonstrate empirically the different upper airway absorption efficiencies for gases with differing physicochemical properties. This modeling concept has since been utilized by Kleinman (1984), Morgan and Frank (1977), Ultman (1988), Hanna et al. (1989), Gerde and Dahl (1991), and Morris and Blanchard (1992). A principal focus of these modeling efforts has been to predict the scrubbing efficiency of the ET airway based on the ventilation rate and the physicochemical properties of the gas. However, the general applicability of the penetration model has often been limited by the assumption that the gas blood concentration approaches zero, thereby requiring complete systemic elimination. Retaining the blood concentration in the model allows greater flexibility for inclusion of the reduction in the concentration gradient, which would reduce the absorption rate if the gas were to accumulate in blood.

In this conceptual framework, the methodology to adjust regional respiratory dose from laboratory animals to humans for evaluation of respiratory tract effects is achieved for the relatively water soluble and/or reactive gases (Categories 1 and 2) by integrating the above two types of empirical models. These models have been used extensively and are therefore favored due to their wide use and potential for empirical measurement of model parameters. The penetration fraction model provides estimation of the ET and TB doses. These are used to adjust the mass of inhaled gas reaching the PU region in the ventilation-perfusion model. Additional systemic compartments (e.g., liver and fat) may be required in the model to describe gases that accumulate significantly in the blood. The addition results in a model structure similar to PBPK models; however, it also incorporates the mass transport description of the scrubbing of the gas in the ET and TB regions.

The approach herein to determine the regional dose within the respiratory tract is developed by relying on the overall mass transport coefficient,  $K_g$ , to characterize the transport of gases between the airphase, the intervening surface liquid and tissue, and the blood. In the absence of empiric measurement,  $K_g$  may be estimated or scaled for a given gas based on its physicochemical properties and reactivity within the respiratory tract. In the following section, a derivation of  $K_g$  is provided and the influence of gas physicochemical characteristics on  $K_g$  is discussed. The definitions of parameter symbols used in the following sections are provided in Table I-1.

**TABLE I-1. DEFINITION OF PARAMETER SYMBOLS USED IN APPENDIX I**

$a$	Airway perimeter ( $\text{cm}^2$ )
$C_0$	Initial concentration ( $\text{mg}/\text{cm}^3$ )
$C_{av}$	Pulmonary region gas concentration ( $\text{mg}/\text{cm}^3$ )
$C_a(x)$	Gas concentration as a function of $x$ ( $\text{mg}/\text{cm}^3$ )
$C_b$	Blood concentration ( $\text{mg}/\text{cm}^3$ )
$C_{b/g}$	Gas concentration in equilibrium with blood concentration ( $\text{mg}/\text{cm}^3$ )
$C_{b/r}$	Concentration of gas in its chemically transformed (reacted) state ( $\text{mg}/\text{cm}^3$ )
$C_f$	Concentration in the fat compartment ( $\text{mg}/\text{cm}^3$ )
$C_g$	Gas phase concentration in airway lumen ( $\text{mg}/\text{cm}^3$ )
$C_{gi}$	Gas-phase concentration at the interface of the gas phase with the surface-liquid/tissue phase ( $\text{mg}/\text{cm}^3$ )
$C_i$	Inhaled concentration ( $\text{mg}/\text{cm}^3$ )
$C_l$	Surface-liquid/tissue phase concentration ( $\text{mg}/\text{cm}^3$ )
$C_{LG}$	Concentration in the lung compartment ( $\text{mg}/\text{cm}^3$ )
$C_{l/g}$	Surface-liquid/tissue concentration in equilibrium with the gas phase ( $\text{mg}/\text{m}^3$ )
$C_{li}$	Surface-liquid/tissue concentration at the interface of the gas phase and the surface-liquid/tissue phase ( $\text{mg}/\text{cm}^3$ )
$C_s$	Imposed concentration ( $\text{mg}/\text{cm}^3$ )
$C_{T/A}$	Concentration of reacted and unreacted gas in arterial blood ( $\text{mg}/\text{cm}^3$ )
$C_{T/V}$	Concentration of reacted and unreacted gas in venous blood ( $\text{mg}/\text{cm}^3$ )
$C_z$	Concentration in the surface-liquid/tissue phase ( $\text{mg}/\text{cm}^3$ )
CA	Arterial (unoxygenated) blood concentration ( $\text{mg}/\text{cm}^3$ )
$CL_{fat}$	Clearance from the fat compartment ( $\text{cm}^2/\text{min}$ )
$CL_{LV}$	Clearance from the liver compartment ( $\text{cm}^2/\text{min}$ )
$CL_{SYS}$	Clearance from the systemic compartment ( $\text{cm}^2/\text{min}$ )
CV	Concentration in venous (oxygenated) blood entering gas-exchange (PU) region ( $\text{mg}/\text{cm}^3$ )
$CX(\text{EXH})_{ET}$	Concentration exiting from extrathoracic region on exhalation ( $\text{mg}/\text{cm}^3$ )
$CX(\text{EXH})_{PU}$	Concentration exiting from pulmonary region upon exhalation ( $\text{mg}/\text{cm}^3$ )
$CX(\text{EXH})_{TB}$	Concentration exiting from tracheobronchial region upon exhalation ( $\text{mg}/\text{cm}^3$ )
$CX(\text{INH})_{ET}$	Concentration exiting from extrathoracic region upon inhalation ( $\text{mg}/\text{cm}^3$ )
$CX(\text{INH})_{TB}$	Concentration exiting from tracheobronchial region upon inhalation ( $\text{mg}/\text{cm}^3$ )
D	Deposited fraction of mass (unitless)
$D_l$	Liquid diffusivity ( $\text{cm}^2/\text{min}$ )
dx	Differential of axial distance into airway (cm)
dy	Differential of axial distance into capillary segment (cm)
dz	Differential of distance into the surface-liquid/tissue phase (cm)
$\dot{E}_{LG}$	Elimination rate in the lung compartment ( $\text{cm}^2/\text{min}$ )
$E_{MAX}$	Maximum extraction efficiency (unitless)

**TABLE I-1 (cont'd). DEFINITION OF PARAMETER SYMBOLS  
USED IN APPENDIX I**

$E_T$	Liver extraction efficiency (unitless)
$\text{erf}$	Error function (unitless)
ET	Extrathoracic respiratory region
F	Flux fraction (unitless)
fp	Fractional penetration (unitless)
$\text{fp}_{\text{ET}}$	Fractional penetration through the extrathoracic region (unitless)
$\text{fp}_{\text{PU}}$	Fractional penetration through the pulmonary region (unitless)
$\text{fp}_{\text{TB}}$	Fractional penetration through the tracheobronchial region (unitless)
Ha	Hatta number (unitless)
$H_{\text{b/g}}$	Blood:gas (air) partition coefficient (unitless)
$H_{\text{EFF}}$	Effective partition coefficient (unitless)
$H_{\text{Lb}}$	Tissue:blood partition coefficient (unitless)
$H_{\text{Lg}}$	Surface-liquid/tissue:gas (air) partition coefficient (unitless)
$K_g$	Overall mass transport coefficient (cm/min)
$K_{\text{ET}}$	Overall mass transport coefficient of the extrathoracic region (cm/min)
$K_{\text{PU}}$	Overall mass transport coefficient of the pulmonary region (cm/min)
$K_{\text{TB}}$	Overall mass transport coefficient of the tracheobronchial region (cm/min)
$k_g$	Transport coefficient in the gas phase (cm/min)
$k_1$	Transport coefficient in the surface-liquid/tissue phase (cm/min)
$k_{\text{LG}}$	Elimination rate from lung compartment ( $\text{min}^{-1}$ )
$k_m$	Alveolar membrane diffusion coefficient (cm/min)
$k_r$	Reaction rate constant in the blood or tissue ( $\text{min}^{-1}$ )
KM	Michaelis constant ( $\text{mg}/\text{cm}^3$ )
L	Airway length (cm)
$M_d$	Desorbed mass (mg)
$M_{\text{dET}}$	Desorbed mass from extrathoracic region (mg)
$M_{\text{dPU}}$	Desorbed mass from pulmonary region (mg)
$M_{\text{dTB}}$	Desorbed mass from tracheobronchial region (mg)
$\dot{M}_{\text{ET}}$	Mass flux from extrathoracic region to blood ( $\text{mg}/\text{cm}^2\text{-min}$ )
$\dot{M}_{\text{PU}}$	Mass flux from pulmonary region to blood ( $\text{mg}/\text{cm}^2\text{-min}$ )
$\dot{M}_{\text{TB}}$	Mass flux from tracheobronchial region to blood ( $\text{mg}/\text{cm}^2\text{-min}$ )
N	Overall transport or flux ( $\text{mg}/\text{cm}^2\text{-min}$ )
$N_g$	Flux through the air phase ( $\text{mg}/\text{cm}^2\text{-min}$ )
$N_1$	Flux through the surface liquid-tissue phase ( $\text{mg}/\text{cm}^2\text{-min}$ )
PU	Pulmonary respiratory tract region
$\dot{Q}_{\text{alv}}$	Alveolar ventilation rate ( $\text{cm}^3/\text{min}$ ) <sup>†</sup>

**TABLE I-1 (cont'd). DEFINITION OF PARAMETER SYMBOLS  
USED IN APPENDIX I**

$\dot{Q}_b$	Local blood flow rate ( $\text{cm}^3/\text{min}$ ) <sup>†</sup>
$\dot{Q}_r$	Cardiac output ( $\text{cm}^3/\text{min}$ ) <sup>†</sup>
RGD	Regional gas dose ( $\text{mg}/\text{cm}^2\text{-min}$ )
$\text{RGDR}_{\text{ET}}$	Regional gas dose ratio for the extrathoracic region (unitless)
$\text{RGDR}_{\text{PU}}$	Regional gas dose ratio for the pulmonary region (unitless)
$\text{RGDR}_{\text{TB}}$	Regional gas dose ratio for the tracheobronchial region (unitless)
SA	Surface area of unspecified respiratory region ( $\text{cm}^2$ )
$\text{SA}_{\text{ET}}$	Surface area of the extrathoracic region ( $\text{cm}^2$ )
$\text{SA}_{\text{TB}}$	Surface area of the tracheobronchial region ( $\text{cm}^2$ )
$\text{SA}_{\text{PU}}$	Surface area of the pulmonary region ( $\text{cm}^2$ )
$S_p$	Blood perfusion surface area ( $\text{cm}^2$ )
t	Time (min)
$t_{\text{EXH}}$	Time (duration) of exhalation (min)
TB	Tracheobronchial respiratory tract region
$\dot{V}$	Volumetric flow rate ( $\text{mg}/\text{min}$ )
$V_b$	Capillary blood volume ( $\text{cm}^3$ )
$V_{\text{LG}}$	Lung compartment volume ( $\text{cm}^3$ )
VMAX	Maximum velocity of saturable (Michaelis-Menton) metabolism path ( $\text{mg}/\text{cm}^2\text{-min}$ )
$\dot{V}_E$	Minute volume ( $\text{cm}^3/\text{min}$ ) <sup>†</sup>
x	Distance into the airway (cm)
$\Delta y$	Thickness of the surface liquid-tissue layer (cm)
z	Distance into the surface-liquid/tissue phase (cm)
$\Delta z$	Surface-liquid/tissue phase thickness (cm)

<sup>†</sup> 1 mL = 1 cm<sup>3</sup>, so cm<sup>3</sup>/min = mL/min.

Also note that concentrations are expressed as mg/cm<sup>3</sup> (1 mg/cm<sup>3</sup> = 10<sup>-6</sup> mg/m<sup>3</sup>).

### I.1.3 Overall Mass Transport Coefficient

The concept of the overall mass transport coefficient is based on a concentration gradient analysis similar to Fick's Law of Diffusion and is utilized to describe transport through several different phases such as air and liquid. The structure of the two-phase mass transport resistance model simplifies the description of mass transport to a minimal number of parameters that may be scaled to gases differing in their physicochemical properties as described later. The more definitive evaluation of transport is to describe absorption by a

simultaneous solution of the conservation of momentum and mass in the complex three-dimensional airway and tissue structure, which has yet to be performed in the respiratory tract. A finite difference solution of Fick's Law has been obtained in the TB and PU region by assuming no gas-phase component to mass transport, which eliminates the solution to the momentum equation (Miller et al., 1985). To include the gas-phase component,  $k_g$ , Hanna et al. (1989) and Lou (1993) used empirically determined  $k_g$  values in conjunction with conservation of mass in the liquid phase to solve for local absorption rates in a finite difference model.

Finite difference solutions are numerically intensive, however, and must be solved for each gas. Scaling of the transport coefficients based on the physicochemical properties of the gas thereby allows scaling of the absorption rate without labor intensive calculations. Furthermore, the transport coefficients may be determined empirically, reducing concern for the appropriateness of the modeling assumptions. Two-phase mass transport resistance models incorporating overall mass transport coefficients have been used in other applications, such as the evaluation of atmospheric absorption of gases by aerosols (Seinfeld, 1986), volatilization or absorption of gases by surface water bodies (Lyman et al., 1990), operation of air strippers (Perry and Chilton, 1973), and absorption in the respiratory tract (Miller et al., 1985; Hanna et al., 1989).

To simplify the respiratory tract into a two-phase resistance model for illustration of the overall mass transport approach, it must be assumed that the blood concentration is constant. For very reactive gases, such as ozone, it can further be assumed to be zero. Under these conditions, the transport of the gas would occur primarily through the air phase and surface-liquid/tissue phase. It is assumed that the surface-liquid and tissue phases are a single phase because of the limited data to identify differing transport parameters for these two phases. The two-phase transport is shown in Figure I-2. The overall transport or flux,  $N$ , through these two phases is expressed by

$$N = K_g(C_g - C_{1/g}) \quad (\text{I-1})$$

where  $C_g$  is the bulk gas phase (or air phase) concentration, and  $C_{1/g}$  is the gas phase concentration in equilibrium with the bulk surface-liquid/tissue phase concentration,  $C_1$

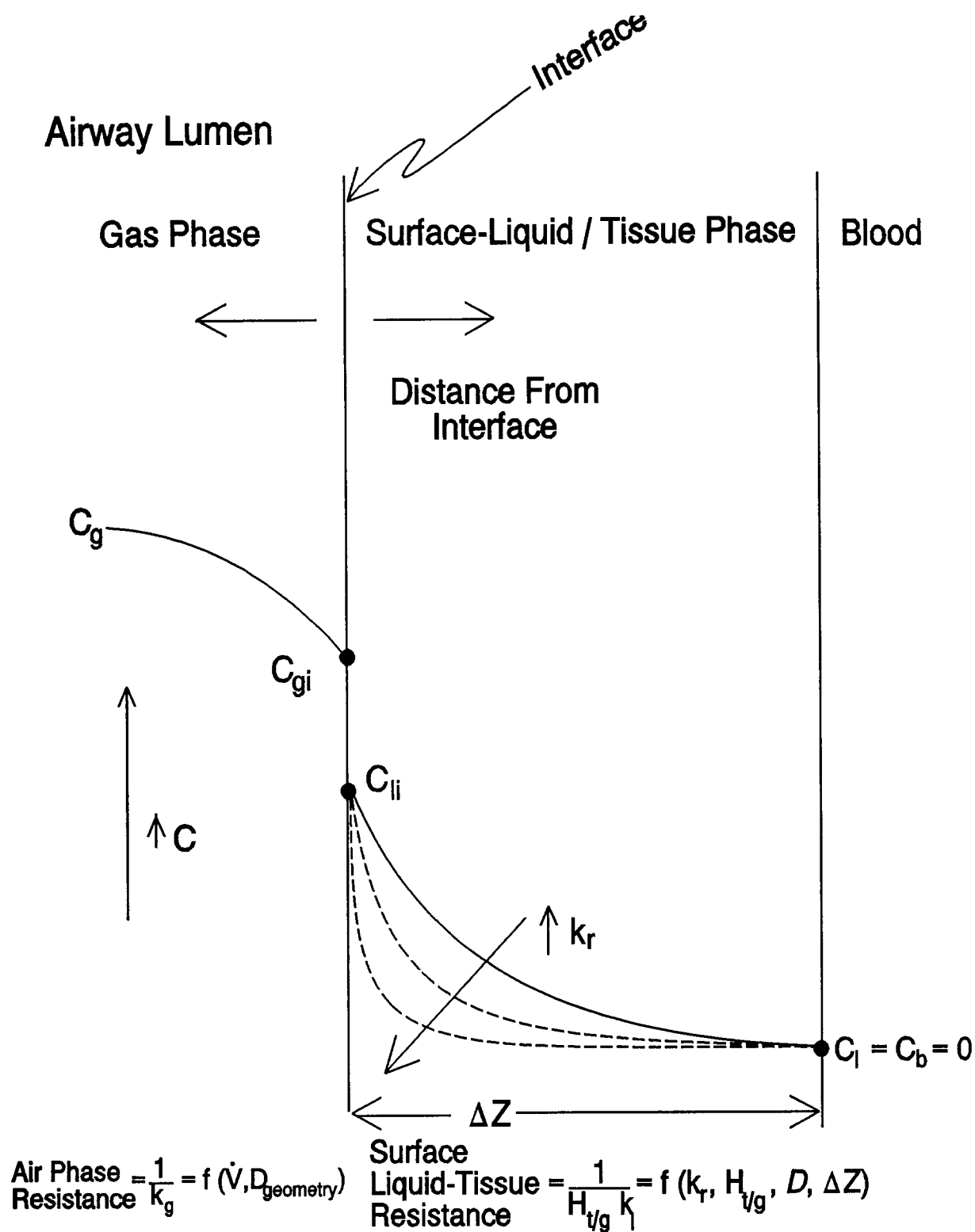


**Figure I-2. Schematic of two-phase mass transport resistance model. The definitions for the parameter symbols are provided in Table I-1.**

(Perry and Chilton, 1973), such that  $C_{l/g}$  is equal to the ratio of the surface-liquid/tissue concentration,  $C_l$ , to the gas partition coefficient,  $H_{l/g}$ .

The overall mass transport coefficient may be determined from the transport coefficients of each individual phase. It is obtained by considering the flux through each phase (Perry and Chilton, 1973) such that

$$N_g = k_g(C_g - C_{gi}) \quad (I-2)$$

where  $N_g$  is the flux through the air phase,  $k_g$  is the transport coefficient in the gas phase, and  $C_{gi}$  is the gas-phase concentration at the interface of the gas phase and the surface-liquid tissue phase, and

$$N_l = k_l(C_{li} - C_l) \quad (I-3)$$

where  $N_l$  is the flux through the surface liquid-tissue phase,  $k_l$  is the transport coefficient in the surface-liquid/tissue phase, and  $C_{li}$  is the surface-liquid/tissue concentration at the interface of the gas phase and the surface-liquid/tissue phase.

Steady state (or quasi-steady state as occurs in the respiratory tract during inhalation or exhalation) requires the following condition:

$$N = N_g = N_l, \quad (I-4)$$

or

$$N = K_g(C_g - C_{l/g}) = k_g(C_g - C_{gi}) = k_l(C_{li} - C_l). \quad (I-5)$$

In the two-phase resistance approach defined by Equation I-5 above, the overall mass transport resistance is defined by the reciprocal of the mass transport coefficient,  $1/K_g$ , and is composed of the resistance to lateral movement of the absorbing gas through the air and

through the liquid and tissue as shown in Figure I-2. The resistance in series can be derived from Equation I-5 as

$$\frac{1}{K_g} = \frac{1}{k_g} + \frac{1}{H_{t/g}k_l}. \quad (\text{I-6})$$

In the case where the surface liquid and tissue cannot be assumed to be a single compartment, a separate partition coefficient and transport coefficient would need to be incorporated into Equation I-6.

The definition of the overall mass transport coefficient provided in Equation I-6 may be used to evaluate the conditions in which a single phase, either gas phase or surface-liquid/tissue phase, determines the overall mass transport coefficient. To demonstrate predominance of a single phase, it is further assumed that blood flow does not contribute to the overall mass transport coefficient (i.e., that there is no accumulation in blood). In the case of a reactive gas and/or a gas relatively soluble in both the tissue and blood, the transport resistance through the gas phase,  $1/k_g$ , may be greater than the transport resistance in the other phases (i.e.,  $k_g \ll H_{t/g}k_l$ ) such that

$$1/K_g \approx 1/k_g. \quad (\text{I-7})$$

The gas phase term,  $k_g$ , is dependent on flow rate, flow geometry, and the gas phase diffusivity. In cross-species comparisons, the flow geometry differences of the species are likely to predominately determine  $k_g$ . Additionally, recent data found that  $k_g$  differed significantly between living subject geometry and cadaver geometry so that it is reasonable to expect geometry to affect interspecies differences (Lou, 1993).

Liquid phase controlled absorption (i.e.,  $H_{t/g}k_l \ll k_g$ ) is typically identified by a gas of moderate to low water solubility and low reactivity. In the case of a nonreactive gas,  $H_{t/g}k_l$  may be approximated by the surface-liquid/tissue:gas partition coefficient, the liquid diffusivity ( $D_l$ ), and the thickness of the liquid-tissue layer ( $\Delta y$ ), such that

$$H_{t/g}k_1 \approx \frac{D_1}{\Delta y}H_{t/g}. \quad (I-8)$$

For reactive gases,  $k_1$  would need to be evaluated to include the transformation rate (Bird et al., 1960; Perry and Chilton, 1973; Ultman, 1988). However, as the reactivity increases, it is less likely that the absorption rate will remain liquid phase controlled due to the increasing influence of the gas phase. In the case of a liquid-controlled absorption process,  $H_{t/g}k_1$  may be substituted for  $k_g$  in Equation I-7.

As discussed, each of the transport coefficients is dependent on the transport properties of the gas within the respective phase that alter the concentration gradient indicated in Figure I-1. Thus, in the case of the gas phase mass transport coefficient,  $k_g$ , the mass transport is affected by the flow rate (ventilation rate), the gas phase diffusivity, and the local (regional) airway geometry. The dependence of  $k_g$  on these parameters is discussed in greater detail by Hanna et al. (1989) and Lou (1993). The surface-liquid/tissue phase transport coefficient is determined by the phase thickness ( $\Delta z$ ), the liquid phase diffusivity, and the reactivity (e.g., ionic dissociation and metabolism) in the surface-liquid/tissue. The dependence of  $k_1$  on these parameters is discussed in greater detail by Ultman (1988).

The penetration fraction model may be used to empirically determine the overall mass transport coefficient (Section I.2.1), provided the fractional penetration,  $fp$ , is measured. Because  $fp$  is both gas and species specific, the  $K_g$  value will similarly be gas and species specific. However, data for  $fp$  and  $K_g$  specific to a gas or gases may be used in a predictive fashion by scaling to the physicochemical properties of solubility, diffusivity, and reactivity.

Using values of  $K_g$  obtained in a single species,  $K_g$  can be scaled within the species for a different gas by decomposing  $K_g$  to the individual transport resistances (i.e., the gas phase and surface-liquid/tissue phase mass transport coefficient). In humans, empirical measures of  $k_g$  have been obtained in casts of the human nasal cavity (Nuckols, 1981; Hanna and Scherer, 1986; Lou, 1993) and can be used to decompose  $K_g$ . Although  $k_g$  is species specific, it may be scaled to other gases by scaling to the gas diffusivity (Hanna et al., 1989). Therefore, for a gas in which  $k_g \ll H_{t/g}k_1$ , this scaling may be sufficient to predict  $fp$  and dose. Similar scaling using the diffusivity and reactivity of a gas for which  $fp$  is unknown may be performed for the surface-liquid/tissue phase transport coefficient,  $k_1$ . For gases in which the

prediction of  $K_g$ , and therefore  $f_p$ , depends on the surface-liquid/tissue phase, the solubility and reactivity of the gas must also be used in the scaling (Equation I-6).

A difficulty arises due to the lack of  $k_g$  values in airways of laboratory animals. Decomposition of an empirically determined  $K_g$  to the individual components must therefore be made based on a data base in which  $H_{t/g}k_l$  may be determined. An approach is under development to obtain data from several gases to decompose  $K_g$  into each component and perform an evaluation of  $k_g$  for gases in each category to obtain a measure of consistency within a species. This effort is underway and will be published as a technical support document to this publication.

Absorption within the respiratory tract cannot always be assumed to be modeled by a two-phase transport resistance model ignoring the blood concentration. In cases where the absorption in the blood contributes to overall absorption, additional mass transport resistances must be considered. Accumulation in the bloodstream may reduce the concentration driving force (and thereby reduce the absorption rate) as well as contribute to the development of a back pressure, which may result in desorption during exhalation due to the reversal in the concentration gradient between the air and tissue. Gases that are likely to exhibit these characteristics are Category 2 gases that are water soluble and rapidly reversibly reactive or those that are moderately to slowly irreversibly metabolized in the respiratory tract, previously referred to as "transition gases" (Dahl, 1990). The contribution of the blood to both the overall mass transport resistance and to the potential for desorption during exhalation was considered in the categorization of gases based on their physicochemical properties. The categorization of gases with respiratory effects is used as the basis for defining the model structure and, in particular, the overall mass transport coefficient.

## **I.2 MODEL FOR CATEGORY 1 GASES**

Category 1 gases are defined as gases that are highly water soluble and/or that may react rapidly and irreversibly in the surface liquid and tissue of the respiratory tract. Due to these physicochemical characteristics, these gases are distinguished by the property that a significant back pressure from the surface-liquid/tissue phase during exhalation does not develop. A back pressure resulting from the reversal in the concentration gradient between

the gas and the surface-liquid/tissue phase may cause significant desorption during exhalation which would require an adjustment to the dose as is considered in the model for Category 2 gases. Category 1 gases are further distinguished by the property that the gas does not significantly accumulate in the blood, which would reduce the concentration driving force and hence reduce the absorption rate. Examples of gases classified as Category 1 are hydrogen fluoride, chlorine, formaldehyde, and the volatile organic acids and esters.

In the following, the two empirical models discussed above are synthesized to allow the doses of gases of differing physicochemical properties to be scaled across species. The penetration fraction model will be utilized to determine the fraction absorbed in the ET region, the concentration entering and dose to the TB region, and the remaining concentration entering the PU region. The ventilation-perfusion model is used to evaluate dose to the PU region by substituting the concentration of the air exiting the TB region in place of the ambient concentration. The overall schematic for the approach is shown in Figure I-3. The definitions for the parameter symbols are provided in Table I-1.

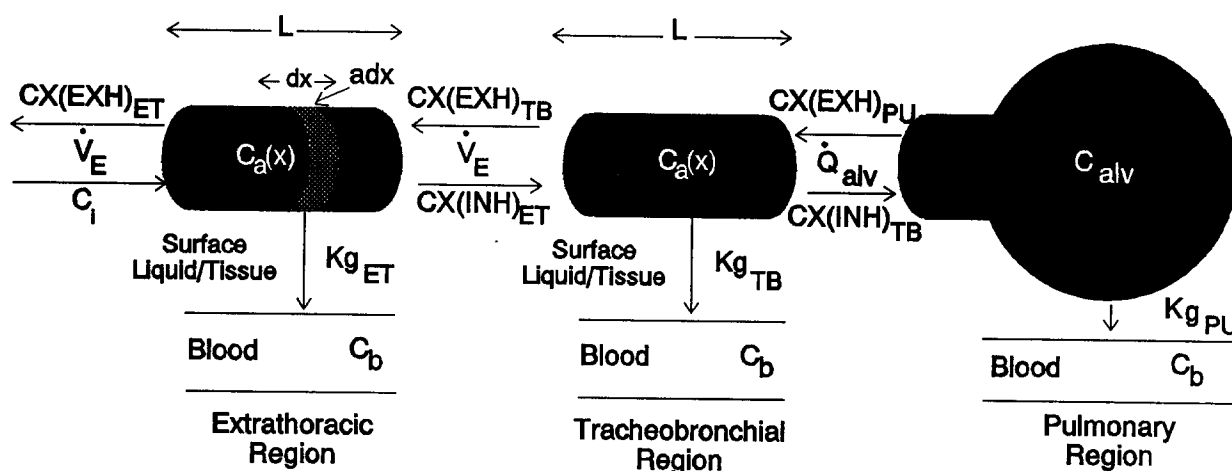


**Figure I-3.** Schematic of modeling approach to estimate regional respiratory tract dose of gases. The definitions for the parameter symbols are provided in Table I-1.

### I.2.1 Extrathoracic Region: The Penetration Fraction Model

The penetration fraction model, designed to evaluate the upper airway scrubbing efficiency, is based on a mass-balance approach. The change in mass traversing the gas phase of the extrathoracic region is balanced by the mass absorbed at the gas-liquid interface of the airway. This balance is written as

$$\dot{V} \frac{dC_g}{dx} = -K_{gET} a(C_i - C_{b/g}) \quad (I-9)$$

where  $\dot{V}$  is the volumetric flow rate;  $dC_g/dx$  is the rate of change of the airstream concentration (gas phase) as a function of distance into the airway,  $x$ ;  $K_{gET}$  is the overall mass transport coefficient between the airstream and the blood in the ET region;  $a$  is the local airway perimeter;  $C_i$  is the inspired gas concentration; and  $C_{b/g}$  is the gas concentration that would be in equilibrium with the blood concentration.  $C_{b/g}$  is equal to the ratio of the blood concentration,  $C_b$ , to the blood:gas (air) partition coefficient,  $H_{b/g}$ .

To evaluate the change in concentration over the length of the ET region, Equation I-9 is integrated resulting in the following relationship:

$$\frac{(CX(INH)_{ET} - C_{b/g})}{(C_i - C_{b/g})} = e^{\left(\frac{-K_{gET} aL}{\dot{V}}\right)}, \quad (I-10)$$

where  $CX(INH)_{ET}$  is the gas concentration exiting the ET region and  $L$  is the length of the airway such that the product of  $a$  and  $L$  is the surface area of the ET region,  $SA_{ET}$ .

Equation I-10 indicates that  $CX(INH)_{ET}$  will equal  $C_i$  at an infinite volumetric flow rate.

In the case of Category 1 gases/vapors,  $CX(INH)_{ET}$  and  $C_i$  are much greater than  $C_{b/g}$ , so that Equation I-10 can be further reduced to

$$f_{PET} = \frac{CX(INH)_{ET}}{C_i} = e^{\left(\frac{-K_{gET} SA_{ET}}{\dot{V}}\right)} \quad (I-11)$$

where  $fp_{ET}$  is the penetration fraction through the ET region and is given as the ratio of the gas concentration exiting the region,  $CX(INH)_{ET}$ , to the gas concentration entering the airway,  $C_i$ . The relationship shown in Equation I-11 suggests that the product of the overall mass transport coefficient and the surface area may be obtained by plotting  $fp_{ET}$  as a function of volumetric flow rate. Indeed, many investigators have used this method to present empirical results (Aharonson et al., 1974; Kleinman, 1984; Morris and Blanchard, 1992). As an example, provided that  $SA_{ET}$  is known, Equation I-11 may be used to evaluate  $K_{gET}$ , in the form of

$$\ln fp_{ET} = - K_{gET} SA_{ET} \left[ \frac{1}{\dot{V}} \right], \quad (I-12)$$

where  $K_{gET} SA_{ET}$  is the slope if the relationship between  $\ln fp_{ET}$  and  $1/\dot{V}$  is linear.

Equation I-12 is similar to the relationship developed by Morris and Blanchard (1992). Morris and Blanchard chose to fit  $D/fp_{ET}$  to  $1/\dot{V}$ , where  $D$  is the deposited fraction,  $1-fp_{ET}$ . Using Equation I-12 in conjunction with a power series expansion of the exponential term of Equation I-11 results in

$$\frac{D}{fp_{ET}} = \frac{K_{gET} SA_{ET}}{\dot{V}}. \quad (I-13)$$

It should be noted, however, that plotting either  $\ln fp_{ET}$  or  $D/fp_{ET}$  against  $1/\dot{V}$  may not be linear. The nonlinearity was first reported by Aharonson et al. (1974). Both Ultman (1988) and Hanna et al. (1989) attribute the nonlinearity to the contribution of the gas phase mass transport coefficient,  $k_g$ , to the overall transport rate. Thus,  $K_g$  is a function of  $\dot{V}$  when affected by  $k_g$ , thereby producing the nonlinearity.

Equation I-6 may be used to evaluate  $K_{gET}$  if sufficient information is available to calculate the individual mass transport coefficient for each phase. Empirical determinations of  $K_{gET}$  may also be obtained from Equation I-12. Furthermore, in the case of gas phase controlled absorption (i.e., in the case of Category 1 gases) where  $K_{gET} \approx k_{gET}$ , Equation I-12 can be used to evaluate the gas phase mass transport coefficient ( $k_g$ ) for each species.

To evaluate  $k_g$  for a single species, empirical measures of the fractional penetration of a gas in which the gas phase contributes to (or controls) the overall mass transport resistance must have been determined empirically. The fractional penetration obtained at several flow rates may be used to evaluate  $k_g$  from the following relationship, which is obtained by combining Equations I-12 and I-6 such that

$$-\ln fp_{ET} = \left( \frac{\dot{V}}{SA_{ET}} \right) \left( \frac{1}{k_g} + \frac{1}{H_{t/g}k_1} \right). \quad (I-14)$$

The value of  $k_g$  and its functional dependence on  $\dot{V}$  is determined by curve fitting the empirically determined  $fp_{ET}$  and  $\dot{V}$ , provided that  $H_{t/g}$  and  $k_1$  are known. In the case of a nonreactive gas,  $k_1$  may be simply estimated. Methods are also available to estimate  $k_1$  for reactive gases (Ultman, 1988). It should be noted that  $k_g$  will differ among gases and that  $k_g$  is a function of ventilation rate. Therefore,  $k_g$  must be scaled by the gas phase diffusivity. The ventilation dependence of  $k_g$  allows the two terms, gas phase and surface-liquid/tissue phase, to be separated. Thus,  $k_g$  may be evaluated from data of  $fp_{ET}$  of several gases to obtain a reasonable estimate of  $k_g$  in a single species, particularly for the rat, for which empirical data are most available. Values of  $k_g$  in other species may also be obtained from published uptake data (Morris and Smith, 1982; Stott and McKenna, 1984; Morris et al., 1986, 1991; Morris and Cavanagh, 1987; Morris, 1990; Dahl et al., 1991b; Bogdanffy et al., 1991; Morris and Blanchard, 1992; Bogdanffy and Taylor, 1993; Kuykendall et al., 1993).

By using the heat and mass transfer analogy, measures of change in inspired temperature may be used to obtain an independent estimate of  $k_g$  (Hanna et al., 1989). The mass transport coefficient,  $k_g$ , has also already been determined in human casts based on both mass transport studies (Hanna et al., 1989; Lou, 1993) and heat transport studies (Nuckols, 1981) from which  $k_g$  is directly calculated.

If the absorption is gas phase controlled (i.e., absorption is completely determined by transport through the gas phase), Equation I-12 may be used to determine the gas phase mass transport coefficient for a single species such that

$$k_g \approx \frac{-\dot{V} \ln fp_{ET}}{SA_{ET}}, \quad (I-15)$$

where  $k_g$  is substituted for  $K_g$ . Because  $k_g$  is a function of flow rate, a plot of  $\ln fp_{ET}$  against  $1/\dot{V}$  will be nonlinear. The nonlinearity determined from empirical data of a gas phase controlled absorption process can be used to evaluate the flow rate dependence of  $k_g$ . The flow rate dependence is of the form  $\dot{V}^n$  where  $n$  is typically between 0.5 to 0.8 (Hanna et al., 1989). Note also that  $k_g$  can not be determined if there is no penetration (i.e.,  $fp_{ET} = 0$ ) because  $\ln fp_{ET}$  is undefined. The value of  $k_g$  at a specific flow rate and in a single species should be relatively constant, changing only slightly as a function of the gas diffusivity. Using values for  $k_g$  determined in humans and in a laboratory animal species allows the scaling for dose in gas phase controlled absorption (i.e., where  $k_g \ll H_{t/g}k_l$ ).

In the case of surface-liquid/tissue phase controlled absorption, where  $K_g \approx H_{t/g}k_l$ , the value will be chemical-specific due to the dependence of  $H_{t/g}k_l$  on solubility and reactivity. Under these circumstances,  $H_{t/g}k_l$  would replace  $k_g$  in Equation I-14. The regression of  $\ln fp_x$  to  $1/\dot{V}$  would be linear provided that the reactivity is not saturable. Michaelis-Menton kinetics can be used to define  $k_l$  and incorporate saturation kinetics which may introduce a nonlinearity. However, saturation kinetics may be better described by the model for Category 2 gases in which there may be a significant accumulation in blood thereby reducing the absorption concentration gradient during inhalation, as well as a potential reversal of the concentration gradient, which would result in desorption during exhalation.

The rate of mass absorbed at the gas-surface interface of the airway in a region is simply the product of the absorbed fraction,  $1-fp_{ET}$ , and the total mass inhaled during a single breath,  $\dot{V}C_i$ . With this knowledge, a suitable metric of dose must now be chosen. If dose were to be defined on a mass per volume basis, it would implicitly assume that the outcome would be determined by concentration (i.e., mass/volume). This assumption would therefore argue that the most appropriate definition of dose should be one defined on the basis of surface area (i.e., the mass flux, or dose, defined as mass per surface area-time). The mass flux implies a concentration gradient in the tissue such that the localized concentration would be highest at the surface. The mass flux is thereby a more accurate predictor of the peak localized concentration and will be used to define dose for this application. The

regional gas dose (RGD), defined as the mass absorbed per surface area per minute ( $\text{mg}/\text{cm}^2\text{-min}$ ), to the extrathoracic region (ET) is given by

$$\text{RGD}_{\text{ET}} (\text{mass} / \text{cm}^2 - \text{min}) = (1 - f_{\text{pET}}) \frac{C_i \dot{V}}{\text{SA}_{\text{ET}}}. \quad (\text{I-16})$$

From Equation I-11, the regional gas dose to the ET may also be expressed as

$$\text{RGD}_{\text{ET}} = \frac{C_i \dot{V}}{\text{SA}_{\text{ET}}} \left( 1 - e^{-\frac{K_{\text{bET}} \text{SA}_{\text{ET}}}{\dot{V}_E}} \right). \quad (\text{I-17})$$

The dose expressed in Equation I-17 is applicable to any animal species provided the appropriate parameters of that species are used in the assessment. For example, because the purpose of this appendix is to address extrapolation of respiratory effects from experimental animal species to humans, the minute volume ( $\dot{V}_E$ ) is used as the default volumetric flow rate in the remainder of the derivations because it approximates the flow rate at which the animal was breathing during the experimental exposure. Further justification of the use of minute volume is the relatively little desorption that occurs during exhalation, a requirement by definition of Category 1 gases, suggesting that the dose should be averaged over the entire cycle. The default values for surface area and minute volume for the various species are provided in Chapter 4.

The regional gas dose ratio for the extrathoracic region ( $\text{RGDR}_{\text{ET}}$ ) of differing species used to calculate NOAEL(HEC) can also be developed using Equation I-17. A comparison between humans and an experimental test species would result in the following regional gas dose ratio (RDGR):

$$\text{RGDR}_{\text{ET}} = \frac{(\text{RGD}_{\text{ET}})_A}{(\text{RGD}_{\text{ET}})_H} = \frac{\left( \frac{C_i \dot{V}_E}{\text{SA}_{\text{ET}}} \right)_A \left( 1 - e^{-\frac{K_{\text{bET}} \text{SA}_{\text{ET}}}{\dot{V}_E}} \right)_A}{\left( \frac{C_i \dot{V}_E}{\text{SA}_{\text{ET}}} \right)_H \left( 1 - e^{-\frac{K_{\text{bET}} \text{SA}_{\text{ET}}}{\dot{V}_E}} \right)_H}, \quad (\text{I-18})$$

where the subscript A and H refer to values for laboratory animals and humans respectively. Because it is assumed that the laboratory animals and humans are exposed to the same concentration for purposes of extrapolating the observed toxicity,  $C_i$  can be deleted.

Equation I-18 represents the most general form of the ratio of ET regional dose between laboratory test species and humans for Category 1 gases. This equation will therefore serve as the basis for the default dosimetric adjustment. To evaluate the ratio, each term will need to be determined for the species of interest.

By definition, gases in Category 1 would be associated with large  $K_g$  values due to high  $k_g$  and low  $H_{t/g}k_1$  terms (Ultman, 1988). Thus, in these cases the exponent is greater than or equal to 1. Under these circumstances, the exponential term (the penetration fraction) approaches zero (less than 5% error when  $K_{gET} SA_{ET}/\dot{V}_{ET}$  is 3) and the  $RGDR_{ET}$  is simply<sup>1</sup>

$$RGDR_{ET} = \frac{(RGD_{ET})_A}{(RGD_{ET})_H} \approx \frac{\left(\frac{\dot{V}_E}{SA_{ET}}\right)_A}{\left(\frac{\dot{V}_E}{SA_{ET}}\right)_H}. \quad (I-19)$$

$RGDR_{ET}$  is determined by the ratio of ventilation rates and surface areas in each species. Assuming that the penetration fraction (i.e., the exponential term) reduces to zero is equivalent to assuming the gas is absorbed entirely in the ET region. Furthermore, based on Equation I-16, the absorption is assumed to be distributed equally. Studies currently in progress are anticipated to provide more localized measures of dose to the nasal cavity (Kimbell et al., 1993; Lou, 1993).

---

<sup>1</sup>Note that Equation I-19 may also be derived from Equation I-18 by determining the conditions whereby

$$\frac{(1 - \exp^{-K_{gET} \frac{SA_{ET}}{\dot{V}_E}})_A}{(1 - \exp^{-K_{gET} \frac{SA_{ET}}{\dot{V}_E}})_H} \approx 1.$$

These conditions will be a function of the default values for respiratory tract surface area and minute volume as well as the absolute value of the overall mass transport coefficient.

## I.2.2 Tracheobronchial Region: The Fractional Penetration Model

The penetration fraction model, and the analysis discussed in the previous section on the ET region, may also be used to describe absorption in the TB region. The major difference is that the concentration at the inlet of the TB region will be dependent on absorption in the ET region. Therefore, the penetration fraction through the TB region,  $fp_{TB}$ , may be described using Equation I-11 such that

$$fp_{TB} = \frac{CX(INH)_{TB}}{CX(INH)_{ET}} = e^{-\frac{K_{gTB} SA_{TB}}{\dot{V}_E}}, \quad (I-20)$$

where  $CX(INH)_{TB}$  is the concentration exiting the TB region;  $CX(INH)_{ET}$  is the concentration exiting the ET region and subsequently entering the TB region;  $SA_{TB}$  is the TB surface area;  $\dot{V}_E$  is the species-specific minute volume used in place of the volumetric flow rate, due to averaging between inhalation and exhalation; and  $K_{gTB}$  is the overall mass transport coefficient in the TB region. In the TB region,  $K_{gTB}$  and  $\dot{V}_E$  can be defined for each specific bronchial generation or as a value for the entire region as a whole using the trachea to characterize both parameters (Nuckols, 1981). Because measures of  $K_{gTB}$  are only available regionally, the value for  $K_{gTB}$  as used in the remaining discussion should be assumed to refer to a regional determination.

The regional gas dose to the TB region,  $RGD_{TB}$ , may be defined similar to the ET dose (Equation I-17) such that

$$RGD_{TB} = \frac{CX(INH)_{ET} \dot{V}_E}{SA_{TB}} \left( 1 - e^{-\frac{K_{gTB} SA_{TB}}{\dot{V}_E}} \right). \quad (I-21)$$

The dose ratio for the TB region ( $RGDR_{TB}$ ) between an experimental animal species and humans is therefore

$$\text{RGDR}_{\text{TB}} = \frac{(\text{RGD}_{\text{TB}})_{\text{A}}}{(\text{RGD}_{\text{TB}})_{\text{H}}} = \frac{\left[ \frac{\text{CX}(\text{INH})_{\text{ET}} \dot{V}_{\text{E}}}{\text{SA}_{\text{TB}}} \right]_{\text{A}}}{\left[ \frac{\text{CX}(\text{INH})_{\text{ET}} \dot{V}_{\text{E}}}{\text{SA}_{\text{TB}}} \right]_{\text{H}}} \frac{\left( 1 - e^{-\frac{-K_{\text{ETB}} \text{SA}_{\text{TB}}}{\dot{V}_{\text{E}}}} \right)_{\text{A}}}{\left( 1 - e^{-\frac{-K_{\text{ETB}} \text{SA}_{\text{TB}}}{\dot{V}_{\text{E}}}} \right)_{\text{H}}}, \quad (\text{I-22})$$

where A and H refer to laboratory animals and humans, respectively. Assuming the same inhaled concentration, the above dose ratio will be divided by  $C_i/C_i$  resulting in the concentration ratio  $(\text{CX}(\text{INH})_{\text{ET}}/C_i)$  in the numerator and denominator for both laboratory animal and human. This concentration ratio is  $fp_{\text{ET}}$ . The resultant gas dose ratio to the TB region is thereby

$$\text{RGDR}_{\text{TB}} = \frac{(\text{RGD}_{\text{TB}})_{\text{A}}}{(\text{RGD}_{\text{TB}})_{\text{H}}} = \frac{\left[ \frac{\dot{V}_{\text{E}}}{\text{SA}_{\text{TB}}} \right]_{\text{A}}}{\left[ \frac{\dot{V}_{\text{E}}}{\text{SA}_{\text{TB}}} \right]_{\text{H}}} \frac{(fp_{\text{ET}})_{\text{A}}}{(fp_{\text{ET}})_{\text{H}}} \frac{\left( 1 - e^{-\frac{-K_{\text{ETB}} \text{SA}_{\text{TB}}}{\dot{V}_{\text{E}}}} \right)_{\text{A}}}{\left( 1 - e^{-\frac{-K_{\text{ETB}} \text{SA}_{\text{TB}}}{\dot{V}_{\text{E}}}} \right)_{\text{H}}}. \quad (\text{I-23})$$

Thus, the results obtained from an evaluation of ET penetration are used to determine the dose to the TB region.

Similar to the ET region, Equation I-23 may be simplified when  $K_g$  is large (less than 5% error if  $K_{\text{ETB}} \text{SA}_{\text{TB}}/\dot{V}_{\text{ETB}}$  is greater than or equal to 3) such that Equation I-23 becomes<sup>2</sup>

---

<sup>2</sup>Note that Equation I-24 may also be derived from Equation I-23 by determining the conditions whereby

$$\frac{\left( 1 - \exp^{-\frac{-K_{\text{ETB}} \text{SA}_{\text{TB}}}{\dot{V}_{\text{E}}}} \right)_{\text{A}}}{\left( 1 - \exp^{-\frac{-K_{\text{ETB}} \text{SA}_{\text{TB}}}{\dot{V}_{\text{E}}}} \right)_{\text{H}}} \approx 1.$$

These conditions will be a function of the default values for respiratory tract surface area and minute volume as well as the absolute value of the overall mass transport coefficient.

$$\text{RGDR}_{\text{TB}} = \frac{(\text{RGD}_{\text{TB}})_A}{(\text{RGD}_{\text{TB}})_H} = \frac{\left[ \frac{\dot{V}_E}{\text{SA}_{\text{TB}}} \right]_A}{\left[ \frac{\dot{V}_E}{\text{SA}_{\text{TB}}} \right]_H} \frac{(\text{fp}_{\text{ET}})_A}{(\text{fp}_{\text{ET}})_H}. \quad (\text{I-24})$$

### I.2.3 Pulmonary Region: The Bohr Model

Ultman (1988) proposed a gas absorption model for the PU region by coupling the Bohr model to predict expired air concentration with a model descriptive of the progressive increase in the capillary blood concentration of the PU circulation. The steady-state model was developed by a mass balance approach in which the rate of uptake in a capillary segment,  $dy$ , is balanced by the differential increase in the total blood concentration, which includes both the reacted (transformed) and the unreacted form of the absorbing gas. The PU absorption model is given by

$$K_{g\text{PU}} \text{SA}_{\text{PU}} (C_{\text{alv}} - C_{\text{b/g}}) dy/L = \dot{Q}_T (dC_{\text{b}} + dC_{\text{b/r}}), \quad (\text{I-25})$$

where,  $K_{g\text{PU}}$  is the overall PU transport coefficient from the gas phase to the blood;  $\text{SA}_{\text{PU}}$  is the PU surface area;  $C_{\text{alv}}$  is the PU region gas concentration;  $C_{\text{b/g}}$  is the blood gas tension in equilibrium with the blood concentration,  $C_{\text{b}}$ ;  $\dot{Q}_T$  is the cardiac output; and  $C_{\text{b/r}}$  is the concentration of the gas in its chemically transformed state.

In the PU region, it is assumed that the absorption of the gas is not limited by absorption in the bloodstream. Therefore, perfusion-limited absorption processes are not considered in this appendix. As discussed earlier, perfusion-limited processes are more appropriate for PBPK models such as described in Appendix J.

Equation I-25 can be integrated such that

$$K_{g\text{PU}} \text{SA}_{\text{PU}} (C_{\text{alv}} - C_{\text{b/g}}) = \dot{Q}_T (C_{\text{T/V}} - C_{\text{T/A}}) \quad (\text{I-26})$$

where  $C_{T/V}$  and  $C_{T/A}$  are the concentration of the reacted and unreacted form of the absorbing gas in the venous (oxygenated) and arterial (unoxygenated—entering the PU region) blood, respectively. Consistent with the assumption that the blood concentration approaches zero (i.e., eliminating perfusion-limited absorption),  $C_{T/A}$  is assumed to be much greater than  $C_{T/V}$ . Under these circumstances, the right-hand side of Equation I-26 is simply  $(-\dot{Q}_T C_{T/A})$ .

The overall mass transport coefficient in the PU region,  $K_{gPU}$ , has been determined for carbon monoxide (CO) to be of the form (Ultman, 1988)

$$\frac{1}{K_{gPU} SA_{PU}} = \frac{1}{k_m SA_{PU}} + \frac{1}{H_{t/g} k_r V_b}, \quad (I-27)$$

where  $k_m$  is the alveolar membrane diffusion coefficient and  $k_m SA_{PU}$  is the alveolar membrane diffusing capacity,  $k_r$  is the reaction rate constant in blood, and  $V_b$  is the capillary blood volume. In the case of CO, the diffusion resistance ( $1/k_m SA_{PU}$ ) is three times greater than the blood reaction term and the mass transport in the PU region is therefore limited by the diffusion resistance. The PU diffusion capacity of CO may thereby serve as a reasonable estimate of the diffusion resistance of a nonreactive gas. In the case of a gas reactive in the PU tissue,  $K_{gPU}$  may be approximated by:

$$\frac{1}{K_{gPU} SA_{PU}} = \frac{1}{Ha (k_m SA_{PU})_{CO}} + \frac{1}{H_{t/g} k_r V_b} \quad (I-28)$$

where  $Ha$  is the Hatta number, a dimensionless parameter that depends on the ratio of the reaction to diffusion times. When the reaction is zero, the Hatta number is one and increases as the rate constant increases (Ultman, 1988). An increase in the Hatta number thus reduces the diffusion resistance and may increase the absorption rate.

The absorption rate to the bloodstream is also balanced by the change in airstream concentration. Using the Bohr model (Figure I-4), the mass balance of Equation I-26 is further expressed by:

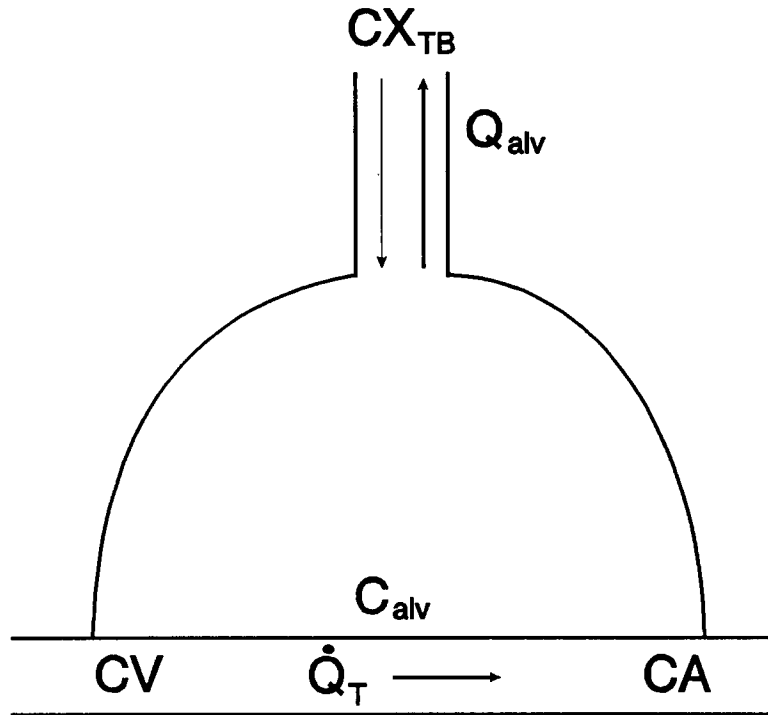


**Figure I-4. Bohr model of ventilation and uptake. The definitions for the parameter symbols are provided in Table I-1.**

$$\dot{Q}_{\text{alv}} (CX(\text{EXH})_{\text{TB}} - C_{\text{alv}}) = K_{\text{gPU}} SA_{\text{PU}} (C_{\text{alv}} - C_{\text{b/g}}) = -\dot{Q}_{\text{T}} C_{\text{T/A}}, \quad (\text{I-29})$$

where  $\dot{Q}_{\text{alv}}$  is the alveolar ventilation rate.

The first two terms in Equation I-29 are used to develop the ratio of the expired concentration to inspired concentration, which will be used as a penetration fraction of the PU region,  $f_{\text{pPU}}$ , defined as the ratio of  $C_{\text{alv}}$  to  $CX(\text{INH})_{\text{TB}}$  such that

$$\frac{C_{\text{alv}}}{CX(\text{INH})_{\text{TB}}} = \frac{\dot{Q}_{\text{alv}}}{K_{\text{gPU}} SA_{\text{PU}} (1 - C_{\text{b/g}} / C_{\text{alv}}) + \dot{Q}_{\text{alv}}}. \quad (\text{I-30})$$

However, for the case of diffusion-limited absorption,  $C_{\text{b/g}}$  is much less than  $C_{\text{alv}}$  such that the denominator on the right hand side of the Equation I-30 is simply  $(K_{\text{gPU}} SA_{\text{PU}} + \dot{Q}_{\text{alv}})$ .

The regional gas dose (RGD) to the pulmonary region (PU) is

$$\text{RGD}_{\text{PU}} = (1 - f_{\text{pPU}}) \frac{\dot{Q}_{\text{alv}}}{\text{SA}_{\text{PU}}} \text{CX}(\text{INH})_{\text{TB}}. \quad (\text{I-31})$$

Combining Equation I-30 and I-31 results in the following relationship:

$$\text{RGD}_{\text{PU}} = \left(1 - \frac{\dot{Q}_{\text{alv}}}{K_{\text{gPU}} \text{SA}_{\text{PU}} + \dot{Q}_{\text{alv}}}\right) \frac{\dot{Q}_{\text{alv}}}{\text{SA}_{\text{PU}}} \text{CX}(\text{INH})_{\text{TB}}, \quad (\text{I-32})$$

where the regional gas dose ratio to the pulmonary region ( $\text{RGDR}_{\text{PU}}$ ) between laboratory animal and humans is given by

$$\text{RGDR}_{\text{PU}} = \frac{(\text{RGD}_{\text{PU}})_{\text{A}}}{(\text{RGD}_{\text{PU}})_{\text{H}}} = \frac{\left(1 - \frac{\dot{Q}_{\text{alv}}}{K_{\text{gPU}} \text{SA}_{\text{PU}} + \dot{Q}_{\text{alv}}}\right)_{\text{A}}}{\left(1 - \frac{\dot{Q}_{\text{alv}}}{K_{\text{gPU}} \text{SA}_{\text{PU}} + \dot{Q}_{\text{alv}}}\right)_{\text{H}}} \frac{(\dot{Q}_{\text{alv}}/\text{SA}_{\text{PU}})_{\text{A}}}{(\dot{Q}_{\text{alv}}/\text{SA}_{\text{PU}})_{\text{H}}} \frac{(\text{CX}(\text{INH})_{\text{TB}})_{\text{A}}}{(\text{CX}(\text{INH})_{\text{TB}})_{\text{H}}}. \quad (\text{I-33})$$

Dividing both numerator and denominator by the inspired air concentration converts the last term to the product of the penetration fractions of the preceding regions such that

$$\text{RGDR}_{\text{PU}} = \frac{(\text{RGD}_{\text{PU}})_{\text{A}}}{(\text{RGD}_{\text{PU}})_{\text{H}}} = \frac{\left(1 - \frac{\dot{Q}_{\text{alv}}}{K_{\text{gPU}} \text{SA}_{\text{PU}} + \dot{Q}_{\text{alv}}}\right)_{\text{A}}}{\left(1 - \frac{\dot{Q}_{\text{alv}}}{K_{\text{gPU}} \text{SA}_{\text{PU}} + \dot{Q}_{\text{alv}}}\right)_{\text{H}}} \frac{(\dot{Q}_{\text{alv}}/\text{SA})_{\text{A}}}{(\dot{Q}_{\text{alv}}/\text{SA})_{\text{H}}} \frac{(f_{\text{pTB}})_{\text{A}}}{(f_{\text{pPU}})_{\text{H}}} \frac{(f_{\text{pET}})_{\text{A}}}{(f_{\text{pET}})_{\text{H}}}, \quad (\text{I-34})$$

where the ratios  $(f_{\text{pTB}})_{\text{A}}/(f_{\text{pTB}})_{\text{H}}$  and  $(f_{\text{pET}})_{\text{A}}/(f_{\text{pET}})_{\text{H}}$  must be determined from the penetration fraction model for the TB and ET regions, respectively. Equation I-34 may be further reduced to

$$\text{RGDR}_{\text{PU}} = \frac{(\text{RGD}_{\text{PU}})_{\text{A}}}{(\text{RGD}_{\text{PU}})_{\text{H}}} = \frac{\left(\frac{K_{\text{gPU}} \text{SA}_{\text{PU}}}{K_{\text{gPU}} \text{SA}_{\text{PU}} + \dot{Q}_{\text{alv}}}\right)_{\text{A}} \left(\frac{\dot{Q}_{\text{alv}}}{\text{SA}_{\text{PU}}}\right)_{\text{A}} (f_{\text{PTB}})_{\text{A}} (f_{\text{PET}})_{\text{A}}}{\left(\frac{K_{\text{gPU}} \text{SA}_{\text{PU}}}{K_{\text{gPU}} \text{SA}_{\text{PU}} + \dot{Q}_{\text{alv}}}\right)_{\text{H}} \left(\frac{\dot{Q}_{\text{alv}}}{\text{SA}_{\text{PU}}}\right)_{\text{H}} (f_{\text{PTB}})_{\text{H}} (f_{\text{PET}})_{\text{H}}}, \quad (\text{I-35})$$

from which the limiting values for the dose ratio may be obtained. At large values of  $K_{\text{gPU}}$ , as would be the case for Category 1 gases, Equation I-35 reduces to:

$$\text{RGDR}_{\text{PU}} = \frac{(\text{RGD}_{\text{PU}})_{\text{A}}}{(\text{RGD}_{\text{PU}})_{\text{H}}} = \frac{\left(\frac{\dot{Q}_{\text{alv}}}{\text{SA}_{\text{PU}}}\right)_{\text{A}} (f_{\text{PTB}})_{\text{A}} (f_{\text{PET}})_{\text{A}}}{\left(\frac{\dot{Q}_{\text{alv}}}{\text{SA}_{\text{PU}}}\right)_{\text{H}} (f_{\text{PTB}})_{\text{H}} (f_{\text{PET}})_{\text{H}}}. \quad (\text{I-36})$$

## I.2.4 DEFAULT APPROACH FOR CATEGORY 1 GASES

As mentioned earlier, more elaborate models such as those using a finite difference solution to the convective-diffusive equation have been developed and applied to specific gases for evaluation of local absorption rates (McJilton et al., 1972; Miller et al., 1985). The method in this appendix presents a reasonable alternative based on fewer parameters and one that is amenable to the types of uptake data routinely generated in some laboratories (Morris and Smith, 1982; Stott and McKenna, 1984; Morris and Cavanagh, 1986, 1987; Morris, 1990; Morris et al., 1986, 1991; Dahl et al., 1991b; Morris and Blanchard, 1992; Bogdanffy et al., 1991; Bogdanffy and Taylor, 1993; Kuykendall et al., 1993). It is hoped that this approach encourages development of these types of data for the various toxic air pollutants that the inhalation reference concentration RfC methods are intended to address.

Because uptake data on which to base  $K_{\text{g}}$  values are not available for many toxic chemicals, this section presents default approaches to those presented in the preceding Section I.2. The default approaches have been derived based on analyses of the limiting conditions described in that section. It is assumed that the values for  $\dot{V}_{\text{E}}$  and the SA values for the various respiratory tract regions will be constants within each species.

### I.2.4.1 Default Approach for Extrathoracic Region

By definition, Category 1 gases are associated with large  $K_g$  values, which simplifies the regional gas dose ratio in the extrathoracic region ( $RGDR_{ET}$ ) to

$$RGDR_{ET} = \frac{(RGD_{ET})_A}{(RGD_{ET})_H} \approx \frac{\left(\frac{\dot{V}_E}{SA_{ET}}\right)_A}{\left(\frac{\dot{V}_E}{SA_{ET}}\right)_H}. \quad (I-37)$$

The ratio is based on an averaged dose over the entire ET region because more localized dosimetry is not yet possible across all species. This default is appropriate when  $K_{gET} (SA_{ET}/\dot{V}_E)$  is greater than 3 or when

$$\frac{(1 - \exp^{-K_{gET} \frac{SA_{ET}}{\dot{V}_E}})_A}{(1 - \exp^{-K_{gET} \frac{SA_{ET}}{\dot{V}_E}})_H} \approx 1.$$

The objective of the dosimetric adjustment is to address interspecies extrapolation of gas doses associated with toxic respiratory effects. Because it has been established (Dahl, 1990; ICRP, 1993) that the types of compounds that are likely to cause respiratory tract toxicity have high reactivity (either ionic dissociation or metabolism) and solubility (i.e., have relatively high  $K_{gET}$ ), Equation I-37 is thus chosen as the default approach for dosimetric adjustment of gases with ET effects. The regional gas dose ratio ( $RGDR_{ET}$ ) calculated in Equation I-37 would be used as the  $DAF_r$  or the multiplier of the  $NOAEL^*(ADJ)$  as described in Chapter 4 (Equation 4-3).

### I.2.4.2 Default Approach for Tracheobronchial Region

As discussed above, the basis of the methods for Category 1 gases was the penetration fraction model to determine the fraction of inhaled dose penetrating the ET region and

thereby available for uptake in the TB region. Thus, the regional gas dose ratio for the tracheobronchial region ( $RGDR_{TB}$ ) is calculated as

$$RGDR_{TB} = \frac{(RGD_{TB})_A}{(RGD_{TB})_H} = \frac{\left(\frac{\dot{V}_E}{SA_{TB}}\right)_A}{\left(\frac{\dot{V}_E}{SA_{TB}}\right)_H} \frac{(fp_{ET})_A}{(fp_{ET})_H} \frac{(1 - e^{-\frac{K_{gTB} SA_{TB}}{\dot{V}_E}})_A}{(1 - e^{-\frac{K_{gTB} SA_{TB}}{\dot{V}_E}})_H} \quad (I-38)$$

If the penetration fraction is unknown due to the lack of data on  $K_{gTB}$ , it is reasonable to assume that  $K_g$  is large, which is consistent with the definition of Category 1 gases, such that the exponential term of Equation I-38 reduces to zero. The same result may be achieved by determining the conditions in which the third ratio of the right hand side of Equation I-38 reduces to 1. These conditions will be a function of the default values for respiratory tract surface area and minute volume as well as the absolute value of the overall mass transport coefficient. Using the definition of  $fp_{ET}$  results in the following dose ratio

$$RGDR_{TB} = \frac{(RGD_{TB})_A}{(RGD_{TB})_H} = \frac{\left(\frac{\dot{V}_E}{SA_{TB}}\right)_A}{\left(\frac{\dot{V}_E}{SA_{TB}}\right)_H} \frac{(e^{-K_{gET} \frac{SA_{ET}}{\dot{V}_E}})_A}{(e^{-K_{gET} \frac{SA_{ET}}{\dot{V}_E}})_H}, \quad (I-39)$$

which can be rearranged to

$$RGDR_{TB} = \frac{(RGD_{TB})_A}{(RGD_{TB})_H} = \frac{\left(\frac{\dot{V}_E}{SA_{TB}}\right)_A}{\left(\frac{\dot{V}_E}{SA_{TB}}\right)_H} \frac{\left(e^{-\frac{SA_{ET}}{\dot{V}_E}}\right)_A^{(K_{gET})_A}}{\left(e^{-\frac{SA_{ET}}{\dot{V}_E}}\right)_H^{(K_{gET})_H}} \quad (I-40)$$

If  $(K_{gET})_A$  can be assumed to be equal to  $(K_{gET})_H$ , then Equation I-40 can be further simplified to

$$RGDR_{TB} = \frac{(RGD_{TB})_A}{(RGD_{TB})_H} = \frac{\left(\frac{\dot{V}_E}{SA_{TB}}\right)_A}{\left(\frac{\dot{V}_E}{SA_{TB}}\right)_H} \frac{\left[e^{-\frac{SA_{ET}}{\dot{V}_E}}\right]_A}{\left[e^{-\frac{SA_{ET}}{\dot{V}_E}}\right]_H}^{K_{gET}} \quad (I-41)$$

If  $K_{gET}$  is further assumed to be one, Equation I-41 reduces further such that only minute volume and surface areas are needed to evaluate the dose ratio, such that:

$$RGDR_{TB} = \frac{(RGD_{TB})_A}{(RGD_{TB})_H} = \frac{\left(\frac{\dot{V}_E}{SA_{TB}}\right)_A}{\left(\frac{\dot{V}_E}{SA_{TB}}\right)_H} \frac{\left[e^{-\frac{SA_{ET}}{\dot{V}_E}}\right]_A}{\left[e^{-\frac{SA_{ET}}{\dot{V}_E}}\right]_H}. \quad (I-42)$$

If  $K_{gET}$  is available for each species, Equation I-39 would be the preferred default equation.

#### I.2.4.3 Default Approach for Pulmonary Region

As discussed in Section I.2.3, the regional gas dose ratio for the PU region ( $RGDR_{PU}$ ) is given by Equation I-35:

$$RGDR_{PU} = \frac{(RGD_{PU})_A}{(RGD_{PU})_H} = \frac{\left(\frac{K_{g_{PU}} SA_{PU}}{K_{g_{PU}} SA_{PU} + \dot{Q}_{alv}}\right)_A}{\left(\frac{K_{g_{PU}} SA_{PU}}{K_{g_{PU}} SA_{PU} + \dot{Q}_{alv}}\right)_H} \frac{\left(\frac{\dot{Q}_{alv}}{SA_{PU}}\right)_A}{\left(\frac{\dot{Q}_{alv}}{SA_{PU}}\right)_H} \frac{(fp_{TB})_A}{(fp_{TB})_H} \frac{(fp_{ET})_A}{(fp_{ET})_H}, \quad (I-35)$$

which at large  $K_{g_{PU}}$  values reduces to

$$\text{RGDR}_{\text{PU}} = \frac{(\text{RGD}_{\text{PU}})_{\text{A}}}{(\text{RGD}_{\text{PU}})_{\text{H}}} = \frac{\left(\frac{\dot{Q}_{\text{alv}}}{\text{SA}_{\text{PU}}}\right)_{\text{A}} (f_{\text{pTB}})_{\text{A}} (f_{\text{pET}})_{\text{A}}}{\left(\frac{\dot{Q}_{\text{alv}}}{\text{SA}_{\text{PU}}}\right)_{\text{H}} (f_{\text{pTB}})_{\text{H}} (f_{\text{pET}})_{\text{H}}}. \quad (\text{I-43})$$

If the penetration fractions to each of the preceding regions are unknown due to lack of data on  $K_{\text{gET}}$  and  $K_{\text{gTB}}$ , the approach to deriving a default equation for the PU region is described below.

Using the definition of  $f_{\text{pET}}$  and  $f_{\text{pTB}}$  results in the following gas dose ratio for the PU region:

$$\text{RGDR}_{\text{PU}} = \frac{(\text{RGD}_{\text{PU}})_{\text{A}}}{(\text{RGD}_{\text{PU}})_{\text{H}}} = \frac{\left(\frac{\dot{Q}_{\text{alv}}}{\text{SA}_{\text{PU}}}\right)_{\text{A}} \left(e^{-K_{\text{gTB}} \frac{\text{SA}_{\text{TB}}}{\dot{V}_{\text{E}}}}\right)_{\text{A}} \left(e^{-K_{\text{gET}} \frac{\text{SA}_{\text{ET}}}{\dot{V}_{\text{E}}}}\right)_{\text{A}}}{\left(\frac{\dot{Q}_{\text{alv}}}{\text{SA}_{\text{PU}}}\right)_{\text{H}} \left(e^{-K_{\text{gTB}} \frac{\text{SA}_{\text{TB}}}{\dot{V}_{\text{E}}}}\right)_{\text{H}} \left(e^{-K_{\text{gET}} \frac{\text{SA}_{\text{ET}}}{\dot{V}_{\text{E}}}}\right)_{\text{H}}}, \quad (\text{I-44})$$

which can be rearranged to

$$\text{RGDR}_{\text{PU}} = \frac{(\text{RGD}_{\text{PU}})_{\text{A}}}{(\text{RGD}_{\text{PU}})_{\text{H}}} = \frac{\left(\frac{\dot{Q}_{\text{alv}}}{\text{SA}_{\text{PU}}}\right)_{\text{A}} \left[e^{\frac{-\text{SA}_{\text{TB}}}{\dot{V}_{\text{E}}}(K_{\text{gTB}})_{\text{A}}}\right]_{\text{A}} \left[e^{\frac{-\text{SA}_{\text{ET}}}{\dot{V}_{\text{E}}}(K_{\text{gET}})_{\text{A}}}\right]_{\text{A}}}{\left(\frac{\dot{Q}_{\text{alv}}}{\text{SA}_{\text{PU}}}\right)_{\text{H}} \left[e^{\frac{\text{SA}_{\text{TB}}}{\dot{V}_{\text{E}}}(K_{\text{gTB}})_{\text{H}}}\right]_{\text{H}} \left[e^{\frac{-\text{SA}_{\text{ET}}}{\dot{V}_{\text{E}}}(K_{\text{gET}})_{\text{H}}}\right]_{\text{H}}}. \quad (\text{I-45})$$

If  $(K_{\text{gET}})_{\text{A}}$  and  $(K_{\text{gTB}})_{\text{A}}$  are assumed to be equal to  $(K_{\text{gET}})_{\text{H}}$  and  $(K_{\text{gTB}})_{\text{H}}$ , respectively, then Equation I-45 can be further simplified to

$$\text{RGDR}_{\text{PU}} = \frac{(\text{RGD}_{\text{PU}})_{\text{A}}}{(\text{RGD}_{\text{PU}})_{\text{H}}} = \frac{\left( \frac{\dot{Q}_{\text{alv}}}{\text{SA}_{\text{PU}}} \right)_{\text{A}}}{\left( \frac{\dot{Q}_{\text{alv}}}{\text{SA}_{\text{PU}}} \right)_{\text{H}}} \left[ \frac{\left( e^{-\frac{\text{SA}_{\text{TB}}}{\dot{V}_{\text{E}}}} \right)_{\text{A}}}{\left( e^{-\frac{\text{SA}_{\text{TB}}}{\dot{V}_{\text{E}}}} \right)_{\text{H}}} \right]^{K_{\text{gTB}}} \left[ \frac{\left( e^{-\frac{\text{SA}_{\text{ET}}}{\dot{V}_{\text{E}}}} \right)_{\text{A}}}{\left( e^{-\frac{\text{SA}_{\text{ET}}}{\dot{V}_{\text{E}}}} \right)_{\text{H}}} \right]^{K_{\text{gET}}} \quad (1-46)$$

If it is further assumed that the value of  $K_{\text{g}}$  is equal to 1 for each region, the resulting default equation reduces to an equation requiring only surface area and minute ventilation parameters. It should be noted that as comparative transport studies become available, Equation I-45 would be preferable because it includes the differences in mass transport in each region for each species.

### I.3 Model for Category 2 Gases

The Category 2 or "transitional" gases are those that have physicochemical properties that are likely to result in the gas significantly accumulating in blood. Accumulation in the blood will reduce the concentration driving force during inspiration and thereby reduce the absorption rate or dose upon inhalation. In addition, these gases are distinguished from Category 1 gases in that there exists the potential for significant desorption during exhalation. A back pressure (i.e., reversal of the concentration gradient at the air-liquid interface) may occur during expiration when the exhaled air concentration is less than the concentration of the surface liquid established during inspiration. Category 2 gases include those which are moderately water soluble. These gases may also either react rapidly and reversibly with the surface liquid or they may be moderately to slowly metabolized irreversibly in the respiratory tract.

A PBPK modeling approach as shown schematically in Figure I-5 is proposed to describe the determinants of absorption for this category of gas. A similar model with a more detailed description of blood flow has been proposed by Overton and Graham (1994). The PBPK approach is used to evaluate the steady-state blood concentration that is necessary to calculate both the absorption flux on inhalation and the desorption flux during exhalation.

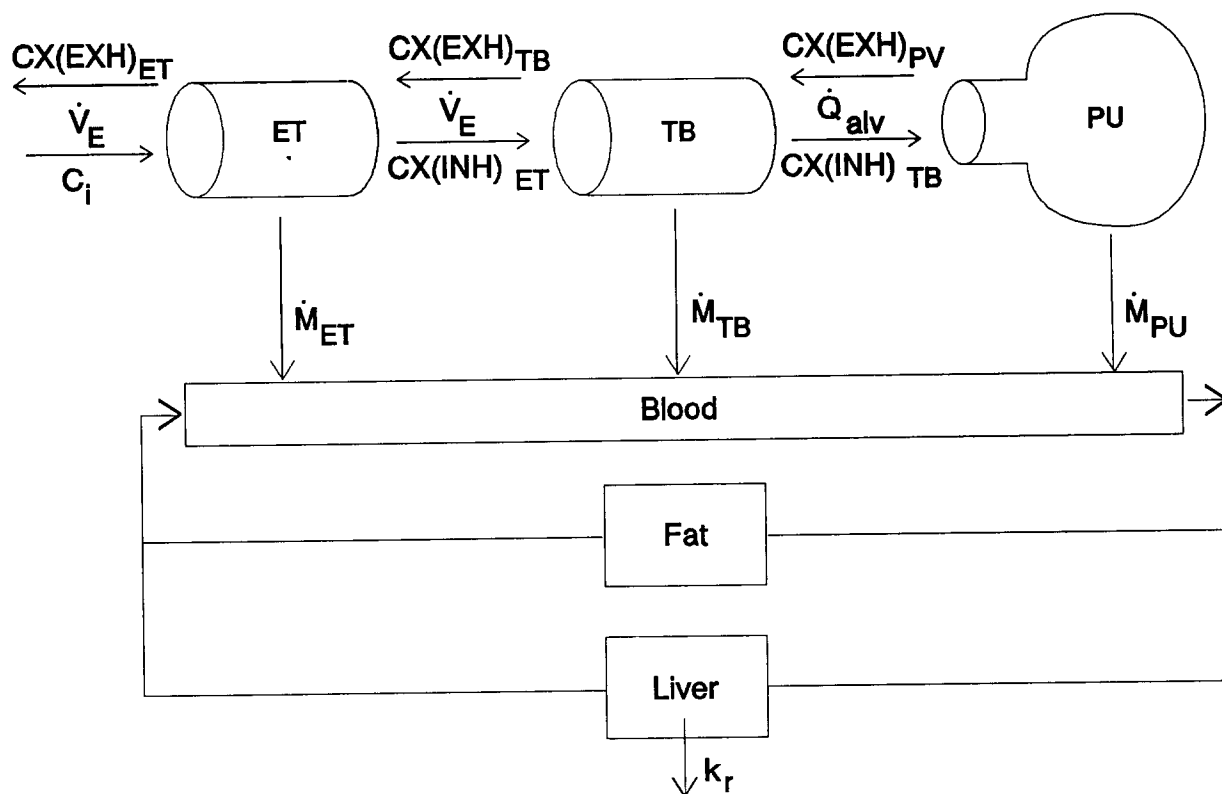


**Figure I-5. Schematic of physiologically based pharmacokinetic modeling approach to estimate respiratory tract dose of gases in Category 2. The definitions for the parameter symbols are provided in Table I-1.**

The derivation of the dose to the three respiratory tract regions will be developed in a similar fashion as that for Category 1 gases (Section I.2). Each region will be considered individually. Following the general description of the modeling approach for each region, a mass balance approach using a PBPK analysis will be developed to determine the blood concentration. A summary of the results and equations will be provided at the end of this section along with the default formulation.

### **I.3.1 Model for Category 2 Gases: Extrathoracic Region**

As with the Category 1 gases, the change in concentration in the ET region (Section I.2.1) can be described by Equation I-9. If it is assumed that sufficient time has passed to allow a steady-state blood concentration to be developed, Equation I-9 can be integrated, resulting in Equation I-10. In the case of Category 1, the blood concentration was

assumed to be much less than the airstream or interfacial concentrations. For Category 2, however, the blood concentration must be retained. Thus, the fraction of gas that penetrates to the TB region is given by rearranging Equation I-10 such that:

$$fp_{ET} = e^{-K_{bET} \frac{SA_{ET}}{\dot{V}_E}} + \frac{C_{b/g}}{C_i} \left[ 1 - e^{-K_{bET} \frac{SA_{ET}}{\dot{V}_E}} \right]. \quad (I-47)$$

As defined in Equation I-16, the dose on inhalation to the ET region,  $RGD(INH)_{ET}$ , may be obtained by substituting Equation I-47 into Equation I-16 and rearranging to obtain

$$RGD(INH)_{ET} = \left[ 1 - \frac{C_{b/g}}{C_i} \right] (1 - e^{-K_{bET} \frac{SA_{ET}}{\dot{V}_E}}) \frac{C_i \dot{V}_E}{SA_{ET}}. \quad (I-48)$$

The form of the overall mass transport coefficient in Equation I-48 differs from that to describe Category 1 gases because a term to describe the disposition of the gas in blood is required. Approaches to include this term are reviewed by Ultman (1988). In the case where there is either no reaction or the reversible nature of the reaction can be handled by adjusting  $H_{t/g}$  to be in equilibrium with the dissociated form of the gas, the mass transport coefficient for Category 2 gases may be determined from:

$$\frac{1}{K_{gET}} = \frac{1}{k_g} + \frac{1}{H_{t/g}k_l} + \frac{S_p}{H_{b/g}\dot{Q}_b}, \quad (I-49)$$

where  $S_p$  is the blood perfusion surface area,  $H_b$  is the blood:air partition coefficient, and  $Q_b$  is the local blood flow rate. The mass transport coefficient for gases, which are moderately to slowly metabolized in the tissue phase is given by

$$\frac{1}{K_{gET}} = \frac{1}{k_g} + \frac{1}{H_{t/g}k_l} + \frac{F}{H_{b/g}k_r V_{LG}}, \quad (I-50)$$

where  $F$  is the flux fraction reaching the blood, and  $V_{LG}$  is the volume of lung tissue. The flux fraction,  $F$ , is less than one if the absorbing gas reacts with constituents in the surface liquid and tissue phases.

Equation I-48 addresses the dose upon inhalation only. To evaluate the total dose, including events occurring during exhalation, the potential for desorption and the desorption flux must be evaluated. Desorption will reduce the total dose over a respiratory cycle; the dose associated with an observed effect is therefore less than that if only the dose on inhalation was considered. In the following section, the desorption term is developed by first considering the tissue depth in which desorption may influence tissue concentration and, by analogy, tissue dose.

### **I.3.1.1 Theoretical Considerations for Modeling Desorption**

Empirical data has indicated that desorption can be important to estimating the respiratory tract dose (Gerde and Dahl, 1991; Dahl et al., 1991b). Unless the tissue concentration is greater than the exhalation airstream concentration, there will be no desorption during exhalation and, in fact, there is actually the potential for additional absorption. To evaluate the potential desorption, it is assumed that the blood concentration attains a relatively constant concentration independent of the respiratory flow cycle. Because it is assumed that the potential desorption will not impact the blood concentration, desorption will only impact the concentration profile in the tissue. The tissue concentration profile during exhalation is a function of the duration of exhalation. If desorption occurs, the surface-liquid/tissue concentration will decrease during exhalation, as will the concentration gradient between the air (gas phase) and blood. An example of the change in the tissue concentration profile that may occur during desorption is shown in Figure I-6.

In Figure I-6, the change in tissue concentration is shown to penetrate the entire surface-liquid/tissue phase as a result of the change in airstream concentration between inhalation and exhalation,  $C(\text{INH})$  and  $C(\text{EXH})$ , respectively. The extent to which the tissue concentration profile changes is as yet unknown and must be evaluated to formulate the desorption term. To estimate the depth in the tissue that may be influenced by the change in flow direction and hence airstream concentration, an analytic solution is employed to evaluate the time course of the concentration profile in the tissue when the surface is exposed

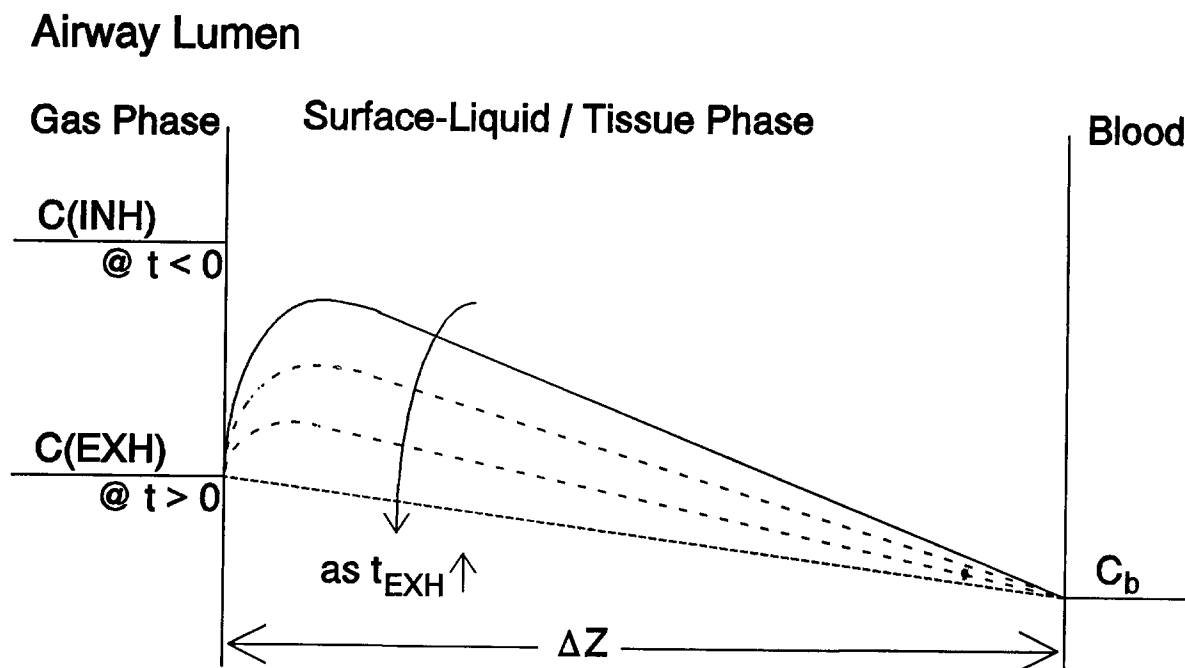


**Figure I-6. Schematic of surface-liquid/tissue phase concentration during exhalation.**

to a step change in concentration associated with the flow reversal. To avoid assumptions about the tissue thickness, it is assumed that the tissue is infinitely thick.

In Figure I-7, the initial conditions prior to imposing the step change is shown in which the tissue concentration is  $C_0$  throughout. At time zero ( $t=0$ ), the step change in the airstream concentration is imposed and the change in tissue concentration with distance and time is illustrated. Given the conditions described above and further assuming no reaction in the surface liquid-tissue layer, the solution is given in the form

$$\frac{(C_S - C_z)}{(C_S - C_0)} = \operatorname{erf} \left[ \frac{z}{2\sqrt{Dt}} \right], \quad (\text{I-51})$$

where  $C_S$  is the imposed concentration;  $C_z$  is the concentration in the surface liquid/tissue, which is a function of time ( $t$ ) and distance into the layer ( $z$ );  $C_0$  is the initial concentration;

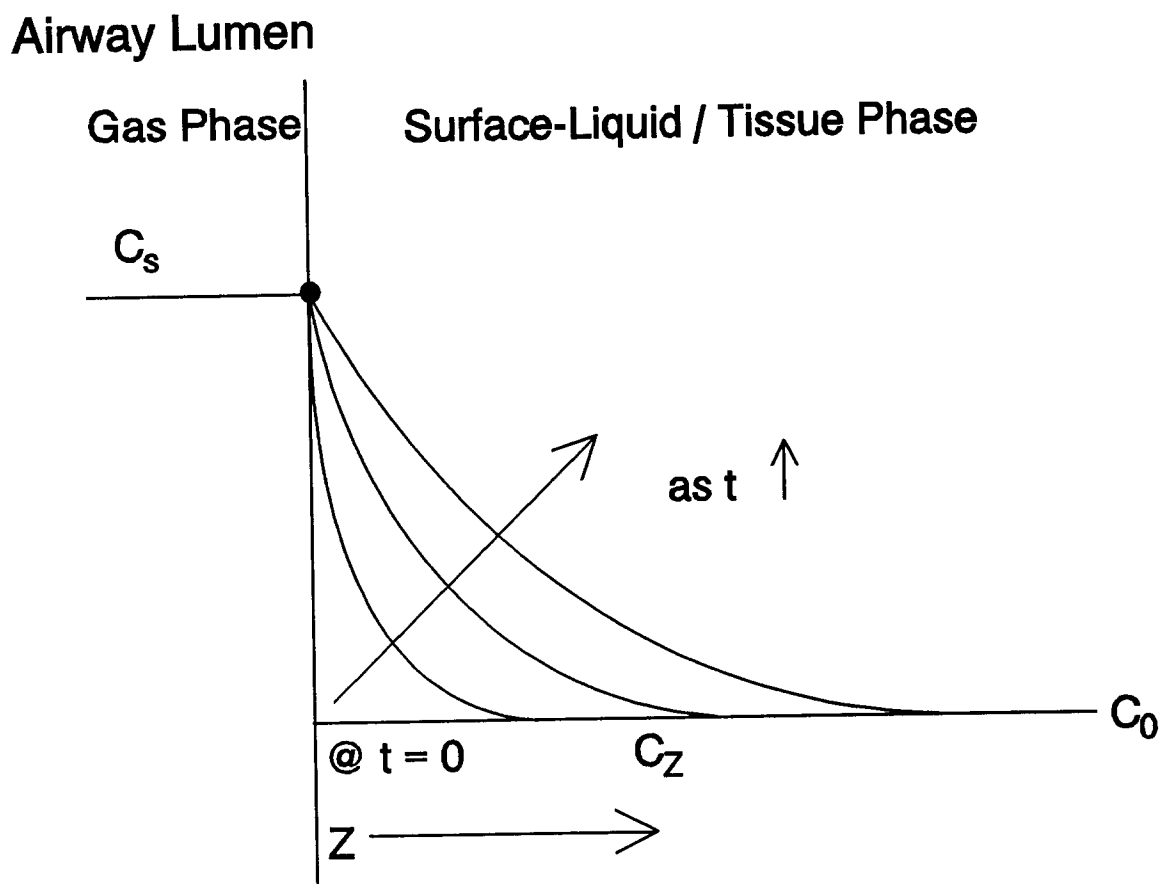


**Figure I-7. Schematic of change in surface-liquid/tissue phase concentration with distance ( $z$ ) and time.**

and erf is the error function. The term on the left hand side of the equation is the nondimensional concentration such that, when  $C_z$  is in equilibrium with the gas phase concentration  $C_s$ , the nondimensional concentration is zero whereas when  $C_z$  is equal to  $C_0$ , the nondimensional concentration is one.

To determine the depth to which the change in the surface concentration impacts the tissue concentration, the time for exhalation in humans is estimated to be approximately 3 s during rest. The time would decrease at increased ventilation rates. Using the above equation, the distance in which the nondimensional concentration attains 0.5 (i.e., the distance in which the local concentration is one-half the concentration difference) is determined to be approximately 70  $\mu\text{m}$ . This distance represents significant penetration into the surface-liquid/tissue phase.

### 1.3.1.2 Formulation of the Desorption Term

The above estimate indicates that an imposed step change in air (gas phase) concentration as occurs during exhalation results in the tissue concentration at  $70 \mu\text{m}$  attaining 50% of the equilibrium value within 3 s. Because this distance is of the order of the distance between the air-surface liquid/tissue interface and blood (Miller et al., 1985), it will be assumed in the derivation of the desorption term that the entire depth of the surface liquid-tissue phase between its interface with the gas phase and the blood may be impacted by desorption. Thus, a conservative assumption would be to assume that the gradient of an absorbing, nonreactive gas achieves a linear profile quickly during both inhalation and exhalation and that the gas phase transport resistance does not affect desorption. Therefore, the desorbed mass due to the flow reversal may be obtained by evaluating the change in mass necessary to effectively reduce the tissue gradient from the inhalation gradient to the exhalation gradient as indicated in Figure I-8.

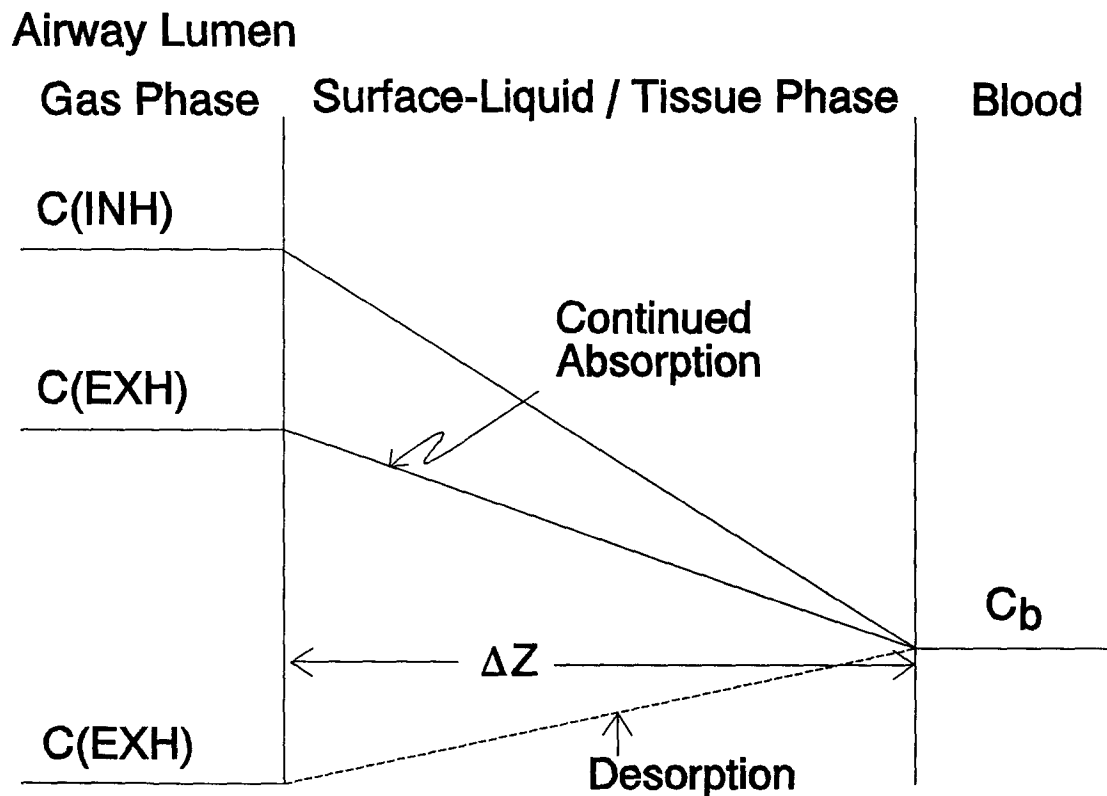


Figure I-8. Schematic of change in mass during breathing cycle.

In Figure I-8, two cases are noted with respect to the exhalation tissue concentration profile. In the first case, the exhalation airstream concentration,  $C(\text{EXH})$ , is greater than the concentration in equilibrium with the blood concentration. Consequently, the gradient is still directed inward such that absorption would continue during exhalation. However, there would be an initial loss of mass associated with the change in the concentration profile as shown in Figure I-6. The second case shown in Figure I-8 is that in which the  $C(\text{EXH})$  is less than  $C_b$ , such that the gradient is directed outward. In this case, desorption occurs due to the step change in concentration associated with the flow reversal as well as a reversal in the concentration gradient between the air and blood. It is assumed, however, that the mass transferred during exhalation is associated primarily with achieving the exhalation tissue profile.

The desorbed mass ( $M_d$ ) due to the step change in airstream concentration is therefore assumed to be determined by subtracting the average concentration represented by the tissue gradients between inspiration and expiration, such that

$$M_{d_{\text{ET}}} = \left( \frac{CX(\text{INH})_{\text{ET}} - CX(\text{EXH})_{\text{TB}}}{2} \right) \Delta Z_{\text{ET}} SA_{\text{ET}}, \quad (\text{I-52})$$

where  $\Delta Z_{\text{ET}}$  is the surface-liquid/tissue phase thickness of the ET region. Because the blood concentration is assumed to be the same during inhalation and exhalation, it does not appear in the above equation.

In the case of a reactive gas, Equation I-52 will overestimate the desorbed mass because the concentration gradient is likely to be curvilinear and a decrease in the concentration profile would also be achieved by reaction and not through desorption. It is also possible that the reaction could be sufficient to effectively result in further absorption during exhalation due to the reduced tissue concentrations (similar to Case 2 described for Figure I-8). As an estimate of the desorbed mass of a reactive gas, an exponential decay term is added to Equation I-52 to account for the tissue reactivity, such that

$$M_{d_{ET}} = \left[ \frac{CX(INH)_{ET} - CX(EXH)_{TB}}{2} \right] \Delta Z_{ET} SA_{ET} e^{-k_i(t_{EXH})}, \quad (I-53)$$

where  $t_{EXH}$  is the time of exhalation.

The regional desorbed dose (mass/cm<sup>2</sup> -time) during exhalation is therefore  $M_d$  divided by the product of the surface area and the exhalation time, such that

$$RGD(EXH)_{ET} = \frac{M_{d_{ET}}}{SA_{ET} t_{EXH}}. \quad (I-54)$$

The total dose in the ET region, accounting for both absorption during inhalation and desorption during exhalation, is therefore:

$$RGD(TOTAL)_{ET} = \frac{C_i \dot{V}_E}{SA_{ET}} \left[ 1 - \frac{C_{b/g}}{C_i} \right] (1 - e^{-K_{sET} \frac{SA_{ET}}{\dot{V}_E}}) - \frac{M_{d_{ET}}}{SA_{ET} t_{EXH}}. \quad (I-55)$$

### I.3.2 Model for Category 2 Gases: Tracheobronchial Region

The model developed for the analysis of total dose to the ET region for gases in Category 2 is directly applicable to the determination of the total dose to the TB region, such that

$$RGD(TOTAL)_{TB} = \frac{CX(INH)_{ET} \dot{V}_E}{SA_{TB}} \left[ 1 - \frac{C_{b/g}}{CX(INH)_{ET}} \right] (1 - e^{-K_{sTB} \frac{SA_{TB}}{\dot{V}_E}}) - \frac{M_{d_{TB}}}{SA_{TB} t_{EXH}}, \quad (I-56)$$

where the desorbed mass is similarly defined as above. Thus, for gases that do not react irreversibly,  $M_d$  is given by:

$$M_{d_{TB}} = \left[ \frac{CX(INH)_{TB} - CX(EXH)_{PU}}{2} \right] \Delta Z_{TB} SA_{TB}, \quad (I-57)$$

and for those gases that do react irreversibly  $M_d$  is given by

$$M_{d_{TB}} = \left[ \frac{CX(INH)_{TB} - CX(EXH)_{PU}}{2} \right] \Delta Z_{TB} SA_{TB} e^{-k_r(t_{EXH})}. \quad (I-58)$$

where  $\Delta Z_{TB}$  is surface-liquid/tissue phase thickness of the TB region.

Substituting for  $CX(INH)_{ET}$  using Equation I-47 and the definition of  $f_{PET}$ , Equation I-56 becomes

$$RGD(TOTAL)_{TB} = \frac{C_i \dot{V}_E}{SA_{TB}} e^{-\frac{K_{gET} SA_{ET}}{\dot{V}_E}} \left[ 1 - \frac{C_{b/g}}{C_i} \right] \left( 1 - e^{-\frac{K_{gTB} SA_{TB}}{\dot{V}_E}} \right) - \frac{M_{d_{TB}}}{SA_{TB} t_{EXH}}. \quad (I-59)$$

### I.3.3 Model for Category 2 Gases: Pulmonary Region

The dose to the PU region for the Category 2 gases may be derived on the basis of equations provided previously (Section I.2.3). From Equation I-30 the ratio of the expired concentration to the inspired concentration of this region (i.e., the penetration fraction of the PU region) is defined as

$$\frac{CX(EXH)_{PU}}{CX(INH)_{TB}} = \frac{\dot{Q}_{alv}}{K_{gPU} SA_{PU} \left[ 1 - \frac{C_{b/g}}{CX(EXH)_{PU}} \right] + \dot{Q}_{alv}}, \quad (I-60)$$

where  $CX(EXH)_{PU}$  is the concentration exiting the PU region and therefore includes the desorption term.

In the previous section describing PU dose (Section I.2.3),  $K_{gPU}$  is defined only for a reactive gas (Equation I-28). However, for gases that are nonreactive or reversibly reactive, a more appropriate form would be (Ultman, 1988)

$$\frac{1}{K_{g_{PU}}} = \frac{1}{H_{t/g} k_l SA_{PU}} + \frac{S_p}{H_{b/g} Q_b}. \quad (I-61)$$

The PU dose as defined for Category 1 gases was based on the assumption that  $C_{b/g}$  was less than  $C_{alv}$ . This assumption is not applicable to the transitional gases of Category 2 because of the potential for elevated blood concentrations. Consequently, the total dose to the PU region for these gases is defined as

$$RGD(TOTAL)_{PU} = \left[ 1 - \frac{\dot{Q}_{alv}}{[K_{g_{PU}} SA_{PU} \left( 1 - \frac{C_{b/g}}{CX(EXH)_{PU}} \right) + \dot{Q}_{alv}]} \right] \frac{\dot{Q}_{alv}}{SA_{PU}} CX(INH)_{TB} \quad (I-62)$$

Equation I-62, although the most general form of the PU dose, can also be formulated more simply by assuming

$$C_{alv} = CX(EXH)_{PU} = C_{b/g} \quad (I-63)$$

because Category 2 gases are moderately water soluble and likely to reach equilibrium between alveolar air concentration and the blood. Under these conditions, the PU dose is simply the difference between the inhaled concentration,  $CX(INH)_{TB}$ , and the exhaled concentration,  $CX(EXH)_{PU}$ , such that

$$RGD(TOTAL)_{PU} = \frac{CX(INH)_{TB} - CX(EXH)_{PU}}{SA_{PU}} \dot{Q}_{alv}, \quad (I-64)$$

which by substitution for  $CX(INH)_{TB}$  and  $CX(EXH)_{PU}$  rearranges to

$$\text{RGD(TOTAL)}_{\text{PU}} = C_i \frac{\dot{Q}_{\text{alv}}}{\text{SA}_{\text{PU}}} \left[ \left( 1 - \frac{C_{\text{b/g}}}{C_i} \right) \left( e^{-\frac{K_{\text{ET}} \text{SA}_{\text{ET}}}{\dot{V}_E}} \right) \left( e^{-\frac{K_{\text{TB}} \text{SA}_{\text{TB}}}{\dot{V}_E}} \right) \right] \quad (\text{I-65})$$

Equation I-65 represents the most generalized equation resulting from the simplifying assumption that the PU dose is proportional to the difference between the inhaled and exhaled concentrations.

### I.3.4 Modeling the Blood Compartment for Category 2 Gases

As defined, Category 2 gases will accumulate in the blood. Thus, an explicit derivation to determine concentration of the gas in the blood is required to solve for the dose into each region. In particular, the term that must be evaluated is  $(1 - C_{\text{b/g}}/C_i)$ , which appears in each of the equations necessary to solve the regional dose. This term includes the blood concentration because  $C_{\text{b/g}}$  is the concentration in the gas phase which would be in equilibrium with the blood (i.e.,  $C_{\text{b/g}} = C_{\text{b}}/H_{\text{b/g}}$ ).

The blood concentration is derived by a mass balance approach. It is assumed that the systemic blood compartment is well mixed so that the change in concentration is due to the input mass delivered through the respiratory tract, loss due to metabolism in the lung tissue, redistribution of the gas in the systemic compartments (including the fat compartment) during intermittent exposures, and loss due to systemic metabolism (modeled in the liver compartment), such that

$$V_{\text{b}} \frac{dC_{\text{b}}}{dt} = \Sigma(\text{RGD(TOT)}_{\text{RT}} \text{SA(TOT)}_{\text{RT}}) - C_{\text{art}}(\text{CL}_{\text{sys}} + \text{CL}_{\text{fat}}) - V_{\text{LG}} \dot{E}_{\text{LG}} \quad (\text{I-66})$$

where  $V_{\text{b}}$  and  $V_{\text{LG}}$  are the volumes of the blood and lung compartments, respectively,  $C_{\text{b}}$  is the average blood concentration;  $\Sigma(\text{RGD(TOT)}_{\text{RT}} \text{SA(TOT)}_{\text{RT}})$  is the summed product of the dose and surface area of each region in the respiratory tract;  $C_{\text{art}}$  is the arterial blood concentration;  $\text{CL}_{\text{sys}}$  and  $\text{CL}_{\text{fat}}$  are the clearance from the systemic (i.e., assumed to be dominated by the liver compartment) and the fat compartments, respectively; and  $\dot{E}_{\text{LG}}$  is the elimination rate in the lung compartment due to metabolism. The total mass transport rate to

the respiratory tract (mass/time) is given in the above equation as the summed product of the dose and surface area of each region in the respiratory tract. However, the total dose to the respiratory tract may also be obtained by the difference in inhalation and exhalation concentrations, such that

$$\Sigma (\text{RGD}(\text{TOT})_{\text{RT}} \text{SA}(\text{TOT})_{\text{RT}}) = \dot{V}_E (C_i - \text{CX}(\text{EXH})_{\text{ET}}). \quad (\text{I-67})$$

The term that implicitly includes the blood concentration and is necessary to solve regional dose is obtained from Equation I-67. Ignoring further absorption or desorption that may occur during expiration,  $\text{CX}(\text{EXH})_{\text{ET}}$  may be approximated by  $\text{CX}(\text{EXH})_{\text{PU}}$ , which is equivalent to  $C_{\text{alv}}$ , the alveolar concentration, which is in equilibrium with the blood (Equation I-63). Thus

$$\dot{V}_E (C_i - \text{CX}(\text{EXH})_{\text{ET}}) = \dot{V}_E C_i \left(1 - \frac{C_{\text{b/g}}}{C_i}\right). \quad (\text{I-68})$$

To determine the respiratory tract dose during the exposure, it will be assumed that the system is in quasi-steady state such that the change in the average blood concentration ( $dC_b/dt$ ) is zero (Equation I-66). Under these conditions, the mass delivery rate to the respiratory tract surface (defined in Equation I-67) is equal to the loss due to clearance from the liver and fat as well as metabolism in the respiratory tract tissue. Combining Equations I-66 through I-68 under steady state conditions results in

$$\dot{V}_E (C_i - C_{\text{alv}}) = C_{\text{art}}(\text{CL}_{\text{sys}} + \text{CL}_{\text{fat}}) + V_{\text{LG}} \dot{E}_{\text{LG}}. \quad (\text{I-69})$$

This relationship, however, can be further reduced for Category 2 gases.

In the case of gases that are relatively insoluble in water (Category 3, Appendix J), the fat compartment plays an important role in the distribution of the gas. The fat compartment may absorb mass at the start of and/or during an intermittent exposure and therefore

represents an additional loss from the arterial blood concentration. At the end of the exposure, leaching from the fat compartment may be an additional input to the blood. Because the initial dose of gases with respiratory toxicity accounts for the dose that may be leached subsequently from the fat, no additional dose following the end of exposure needs to be accounted for. Furthermore, the contribution of the fat compartment is reduced for Category 2 gases because the gas will not partition significantly to the fat because of its lower fat to blood partition coefficient. In addition, the concentrations in the systemic compartments are in equilibrium with the blood during steady state. Thus, the uptake by the fat will be assumed zero, consistent with the definition Category 2 gases because of their partition coefficient. The assumption of a steady state is conservative because it will underestimate the dose to the respiratory tract compartments that are the objective of the derivation in this appendix. The assumptions of steady state and of equilibrium between tissue and blood compartments results in the elimination of  $CL_{fat}$  from Equation I-69.

Rearranging Equation I-69 to solve for systemic elimination results in

$$CL_{sys} = \dot{V}_E \frac{(C_i - C_{alv})}{C_{art}} - \frac{V_{LG}\dot{E}_{LG}}{C_{art}}, \quad (I-70)$$

where  $CL_{fat}$  is zero as described above. However, the ratio of the exhaled concentration,  $C_{alv}$ , to  $C_{art}$  is approximated by  $H_{b/g}$ . Equation I-70 may therefore be rewritten as

$$CL_{sys} = \dot{V}_E \left( \frac{1}{H_{EFF}} - \frac{1}{H_{b/g}} \right) - \frac{V_{LG}\dot{E}_{LG}}{C_{art}}, \quad (I-71)$$

where  $H_{EFF}$  is the steady state blood to inhaled gas concentration ratio observed in an experimental situation (Andersen, 1981), which is referred to here as an effective partition coefficient.

It is now necessary to more specifically incorporate the loss terms for systemic clearance and respiratory tract metabolism. It will be assumed that systemic clearance is

predominately due to metabolism in the liver and is given by (Andersen, 1981; Pang and Rowland, 1977)

$$CL_{\text{sys}} \approx CL_{\text{LIV}} = \dot{Q}_T E_T, \quad (\text{I-72})$$

where  $CL_{\text{LIV}}$  is the clearance from the liver compartment;  $\dot{Q}_T$  is the cardiac output; and  $E_T$  is the liver extraction efficiency. The elimination rate from the lung compartment,  $\dot{E}_{\text{LG}}$ , is defined according to Michaelis-Menton kinetics:

$$\dot{E}_{\text{LG}} = \frac{C_{\text{LG}} V_{\text{MAX}}}{(K_M + C_{\text{LG}})} = k_{\text{LG}} C_{\text{LG}}, \quad (\text{I-73})$$

where  $V_{\text{MAX}}$  is the maximum velocity of saturable (Michaelis-Menton) metabolism path; where  $C_{\text{LG}}$  is the lung tissue concentration;  $K_M$  is the Michaelis constant; and  $k_{\text{LG}}$  is the elimination rate from the lung compartment.

Combining Equations I-71 to I-73 provides the loss terms in relation to  $H_{\text{EFF}}$ :

$$\dot{Q}_T E_T = \dot{V}_E \left( \frac{1}{H_{\text{EFF}}} - \frac{1}{H_{\text{b/g}}} \right) - V_{\text{LG}} k_{\text{LG}} \frac{C_{\text{LG}}}{C_{\text{art}}}. \quad (\text{I-74})$$

Assuming the respiratory tract tissue concentration,  $C_{\text{LG}}$ , is in equilibrium with the blood, the ratio  $C_{\text{LG}}/C_{\text{art}}$  is equivalent to the tissue:blood partition coefficient,  $H_{\text{t/b}}$ . Solving for  $H_{\text{EFF}}$  yields

$$H_{\text{EFF}} = \frac{\dot{V}_E}{\dot{Q}_T E_T + V_{\text{LG}} k_{\text{LG}} H_{\text{t/b}} + \frac{\dot{V}_E}{H_{\text{b/g}}}}. \quad (\text{I-75})$$

Combining Equation I-68 with the definition of  $H_{\text{b/g}}$  and  $H_{\text{EFF}}$  results in

$$\dot{V}_E C_i \left(1 - \frac{C_{b/g}}{C_i}\right) = \dot{V}_E (C_i - C_{alv}) = \dot{V}_E C_i \left(\frac{H_{b/g} - H_{EFF}}{H_{b/g}}\right). \quad (I-76)$$

Upon substitution of I-75 into I-76, the term necessary to solve the dose ratio in Equations I-55, I-59, and I-65 is obtained:

$$\left(1 - \frac{C_{b/g}}{C_i}\right) = \frac{\dot{Q}_T E_T H_{b/g} + V_{LG} k_{LG} H_{t/b} H_{b/g}}{\dot{Q}_T E_T H_{b/g} + V_{LG} k_{LG} H_{t/b} H_{b/g} + \dot{V}_E}, \quad (I-77)$$

where  $H_{t/g}$  is equal to the product of  $H_{t/b}$  and  $H_{b/g}$ . Equation I-77 may be simplified by considering the range of partition coefficients, extraction efficiency and the respiratory tract tissue concentration.

At large values of  $H_{t/g}$  (and consequently  $H_{b/g}$  since  $H_{b/t} \times H_{t/g} = H_{b/g}$ ), the term on the right hand side of Equation I-77 approximates one. Therefore,  $C_{b/g} \ll C_i$  which is the definition of Category 1 gases (i.e., those gases that are highly soluble and/or rapidly irreversibly reactive) for which the approach presented in Section I.2.4 applies. This case is consistent with a greater extraction efficiency of the respiratory tract relative to the systemic clearance as well as absorption proximal to the PU region. Conversely, at low values of  $H_{t/g}$ , absorption proximal to the PU region is negligible and the relative efficiency of systemic clearance is greater than that of the respiratory tract extraction (as well as uptake). The approach for category 3 gases presented in Appendix J applies in this case.

The remaining gases are those which are moderately water soluble (intermediate value of  $H_{t/g}$ ) and are therefore the Category 2 gases. For Category 2 gases, Equation I-77 reduces to

$$\left(1 - \frac{C_{b/g}}{C_i}\right) = \frac{\dot{Q}_T}{\dot{V}_E} E_T H_{b/g} \left(1 + \frac{V_{LG} k_{LG} H_{t/b}}{\dot{Q}_T E_T}\right). \quad (I-78)$$

since  $\dot{V}_E / \dot{Q}_T H_{b/g} \gg E_T + (V_{LG} k_{LG} / \dot{Q}_T) H_{t/b}$ .

Equation I-78 can be further reduced since  $\dot{Q}_T$  approximates  $\dot{V}_E$ . The magnitude of the blood concentration is determined by the relative significance of the metabolism which occurs in the respiratory tract versus systemic elimination (as shown in the ratio  $V_{LG}k_{LG}H_{t/b}/\dot{Q}_TE_T$ ). If systemic elimination is much larger, Equation I-78 reduces to

$$\left(1 - \frac{C_{b/g}}{C_i}\right) = E_T H_{b/g} \cdot \quad (I-79)$$

At the maximum, it will be assumed that the respiratory tract elimination would be equal to that of the systemic elimination under which circumstances

$$\left(1 - \frac{C_{b/g}}{C_i}\right) = 2E_T H_{b/g} \cdot \quad (I-80)$$

It will be further assumed that the systemic elimination term is defined for maximum elimination, i.e. assuming liver saturation kinetics, such that  $E_T$  is defined by  $E_{MAX}$ , the maximum extraction efficiency. The maximum extraction efficiency is approximately  $0.25\dot{Q}_T$  due to the flow limitation to the liver (Andersen, 1981). Thus, Category 2 gases can be defined based on systemic elimination and the relative significance of respiratory tract metabolism to systemic elimination.

### I.3.5 Default Approach for Category 2 Gases

The default approach is developed by ignoring the desorption associated with exhalation. This assumption may be valid in as much as the mass in the tissue that is desorbed during exhalation is replaced on inhalation. Whether, in general, this assumption results in an overestimate or underestimate of the dose is not clear because ignoring the desorbed mass may not significantly impact the concentration driving force (i.e., the concentration of the gas at the surface-liquid/tissue interface and the concentration in the blood may be proportionately affected).

In comparing cyclic absorption-desorption and unidirectional absorption, the concentration at the interface between the air and surface liquid is likely to be lower in the

case of desorption and the driving force would therefore be lower than in the case of unidirectional absorption if the blood concentration were equal in both cases. The net effect would suggest that ignoring desorption would overestimate the absorbed mass or dose. However, by overestimating the absorbed mass in the case of unidirectional absorption, the blood concentration will be elevated over the absorption-desorption case. The elevated blood concentration will also reduce the concentration driving force. Therefore, although ignoring desorption will increase the surface liquid concentrations, the blood concentration will similarly be overestimated, so that the concentration driving force may not be dissimilar than with desorption described.

The dose to each region, ignoring desorption, is therefore obtained by combining Equation I-79 or I-80 (depending on the significance of respiratory tract metabolism) with each of the individual dosimetry calculations in Equations I-55, I-59, and I-65 for the ET, TB, and PU regions, respectively.

### I.3.5.1 Default Approach for Extrathoracic Region

From Equation I-54, the regional gas dose ratio (ignoring desorption) for the ET region ( $RGDR_{ET}$ ) is given by

$$RGDR_{ET} = \frac{(RGD_{ET})_A}{(RGD_{ET})_H} = \frac{\left(\frac{C_i \dot{V}_E}{SA_{ET}}\right)_A \left(1 - \frac{C_{b/g}}{C_i}\right)_A \left(1 - e^{-K_{gET} \frac{SA_{ET}}{\dot{V}_E}}\right)_A}{\left(\frac{C_i \dot{V}_E}{SA_{ET}}\right)_H \left(1 - \frac{C_{b/g}}{C_i}\right)_H \left(1 - e^{-K_{gET} \frac{SA_{ET}}{\dot{V}_E}}\right)_H} \quad (I-81)$$

However,  $K_{gET}$  for Category 2 gases is by definition less than 1. Assuming  $K_{gET}$  is equal to or less than 0.5, a power series expansion of the exponential term results in the following relationship:

$$\text{RGDR}_{\text{ET}} = \frac{(\text{RGD}_{\text{ET}})_{\text{A}}}{(\text{RGD}_{\text{ET}})_{\text{H}}} = \frac{\left(\text{C}_i \frac{\dot{V}_{\text{E}}}{\text{SA}_{\text{ET}}}\right)_{\text{A}} \left(1 - \frac{\text{C}_{\text{b/g}}}{\text{C}_i}\right)_{\text{A}} \left(-\text{K}_{\text{g}_{\text{ET}}}\frac{\text{SA}_{\text{ET}}}{\dot{V}_{\text{E}}}\right)_{\text{A}}}{\left(\text{C}_i \frac{\dot{V}_{\text{E}}}{\text{SA}_{\text{ET}}}\right)_{\text{H}} \left(1 - \frac{\text{C}_{\text{b/g}}}{\text{C}_i}\right)_{\text{H}} \left(-\text{K}_{\text{g}_{\text{ET}}}\frac{\text{SA}_{\text{ET}}}{\dot{V}_{\text{E}}}\right)_{\text{H}}}. \quad (\text{I-82})$$

Assuming the same inspired concentration, simplifies the  $\text{RGDR}_{\text{ET}}$  to

$$\text{RGDR}_{\text{ET}} = \frac{(\text{RGD}_{\text{ET}})_{\text{A}}}{(\text{RGD}_{\text{ET}})_{\text{H}}} = \frac{\text{K}_{\text{g}_{\text{ETA}}}}{\text{K}_{\text{g}_{\text{ETH}}}} \frac{\left(1 - \frac{\text{C}_{\text{b/g}}}{\text{C}_i}\right)_{\text{A}}}{\left(1 - \frac{\text{C}_{\text{b/g}}}{\text{C}_i}\right)_{\text{H}}}. \quad (\text{I-83})$$

If the overall mass transport coefficients ( $\text{K}_{\text{g}_{\text{ET}}}$ ) are assumed equal as in the case of Category 1 gases, the regional gas dose ratio is reduced to the ratio of  $(1 - \text{C}_{\text{b/g}}/\text{C}_i)$ .

Two cases were developed for the derivation of the blood term as expressed in Equations I-79 and I-80. The first case in which systemic elimination is assumed to be much greater than respiratory tract metabolism such that

$$\text{RGDR}_{\text{ET}} = \frac{(\text{RGD}_{\text{ET}})_{\text{A}}}{(\text{RGD}_{\text{ET}})_{\text{H}}} = \frac{\text{K}_{\text{g}_{\text{ETA}}}}{\text{K}_{\text{g}_{\text{ETH}}}} \frac{(0.25 \dot{Q}_{\text{T}}\text{H}_{\text{b/g}})_{\text{A}}}{(0.25 \dot{Q}_{\text{T}}\text{H}_{\text{b/g}})_{\text{H}}}, \quad (\text{I-84})$$

and the second case in which respiratory tract metabolism is assumed to be of equal significance with systemic elimination such that

$$\text{RGDR}_{\text{ET}} = \frac{(\text{RGD}_{\text{ET}})_{\text{A}}}{(\text{RGD}_{\text{ET}})_{\text{H}}} = \frac{\text{K}_{\text{g}_{\text{ETA}}}}{\text{K}_{\text{g}_{\text{ETH}}}} \frac{(0.5 \dot{Q}_{\text{T}}\text{H}_{\text{b/g}})_{\text{A}}}{(0.5 \dot{Q}_{\text{T}}\text{H}_{\text{b/g}})_{\text{H}}}, \quad (\text{I-85})$$

where  $E_{MAX}$  is equal to  $0.25 \dot{Q}_T$ . Because the constants are equal in the numerator and denominator, Equations I-84 and I-85 reduce to the same equation:

$$RGDR_{ET} = \frac{(RGD_{ET})_A}{(RGD_{ET})_H} = \frac{K_{g_{ETA}}}{K_{g_{ETH}}} \frac{(\dot{Q}_T H_{b/g})_A}{(\dot{Q}_T H_{b/g})_H}, \quad (I-86)$$

which can be further reduced if the overall mass transport coefficients ( $K_{g_{ET}}$ ) are assumed to be equal.

### I.3.5.2 Default Approach for Tracheobronchial Region

From Equation I-58, the regional gas dose ratio (ignoring desorption) for the tracheobronchial region ( $RGDR_{TB}$ ) is given by

$$RGDR_{TB} = \frac{(RGD_{TB})_A}{(RGD_{TB})_H} = \frac{(C_i \frac{\dot{V}_E}{SA_{TB}})_A}{(C_i \frac{\dot{V}_E}{SA_{TB}})_H} \frac{(e^{-K_{g_{ET}} \frac{SA_{ET}}{\dot{V}_E}})_A}{(e^{-K_{g_{ET}} \frac{SA_{ET}}{\dot{V}_E}})_H} \frac{(1 - \frac{C_{b/a}}{C_i})_A}{(1 - \frac{C_{b/a}}{C_i})_H} \frac{(1 - e^{-K_{g_{TB}} \frac{SA_{TB}}{\dot{V}_E}})_A}{(1 - e^{-K_{g_{TB}} \frac{SA_{TB}}{\dot{V}_E}})_H}. \quad (I-87)$$

As in the ET region,  $K_{g_{TB}}$  for Category 2 gases is by definition less than 1 and a power series expansion of the exponential term for the TB region similarly reduces the last term to the ratio of the  $K_{g_{TB}}$ . The exponential term for the ET term in Equation I-86 is reduced by assuming  $K_{g_{ET}}$  is the same for each species as was assumed for Category 1 gases. At values of  $K_{g_{ET}}$  less than or equal 0.5, the ET exponential term approaches one. Thus, assuming the same inspired concentrations, Equation I-86 becomes

$$RGDR_{TB} = \frac{(RGD_{TB})_A}{(RGD_{TB})_H} = \frac{K_{g_{TBA}}}{K_{g_{TBH}}} \frac{(1 - \frac{C_{b/a}}{C_i})_A}{(1 - \frac{C_{b/a}}{C_i})_H}. \quad (I-88)$$

As above, Equation I-88 is further reduced by substituting Equation I-79 for the case in which systemic elimination predominates:

$$\text{RGDR}_{\text{TB}} = \frac{(\text{RGD}_{\text{TB}})_{\text{A}}}{(\text{RGD}_{\text{TB}})_{\text{H}}} = \frac{K_{g_{\text{TB A}}}}{K_{g_{\text{TB H}}}} \frac{(0.25 \dot{Q}_{\text{T}} H_{\text{b/a}})_{\text{A}}}{(0.25 \dot{Q}_{\text{T}} H_{\text{b/a}})_{\text{H}}} . \quad (\text{I-89})$$

By substituting Equation I-80 for the case in which respiratory tract metabolism and systemic elimination are of equal significance, Equation I-88 becomes:

$$\text{RGDR}_{\text{TB}} = \frac{(\text{RGD}_{\text{TB}})_{\text{A}}}{(\text{RGD}_{\text{TB}})_{\text{H}}} = \frac{K_{g_{\text{TB A}}}}{K_{g_{\text{TB H}}}} \frac{(0.5 \dot{Q}_{\text{T}} H_{\text{b/a}})_{\text{A}}}{(0.5 \dot{Q}_{\text{T}} H_{\text{b/a}})_{\text{H}}} , \quad (\text{I-90})$$

where  $E_{\text{MAX}}$  is equal to  $0.25 \dot{Q}_{\text{T}}$ . Because the constants are equal in the numerator and denominator, Equations I-89 and I-90 reduce to the same equation:

$$\text{RGDR}_{\text{TB}} = \frac{(\text{RGD}_{\text{TB}})_{\text{A}}}{(\text{RGD}_{\text{TB}})_{\text{H}}} = \frac{K_{g_{\text{TB A}}}}{K_{g_{\text{TB H}}}} \frac{(\dot{Q}_{\text{T}} H_{\text{b/a}})_{\text{A}}}{(\dot{Q}_{\text{T}} H_{\text{b/a}})_{\text{H}}} , \quad (\text{I-91})$$

which can be further reduced if the overall mass transport coefficients ( $K_{g_{\text{TB}}}$ ) are assumed to be equal.

### I.3.5.3 Default Approach for Pulmonary Region

From Equation I-64, the regional gas dose ratio (ignoring desorption) for the PU region ( $\text{RGDR}_{\text{PU}}$ ) is given by

$$\text{RGDR}_{\text{PU}} = \frac{(\text{RGD}_{\text{PU}})_{\text{A}}}{(\text{RGD}_{\text{PU}})_{\text{H}}} = \frac{(C_i \frac{\dot{Q}_{\text{alv}}}{SA_{\text{PU}}})_{\text{A}}}{(C_i \frac{\dot{Q}_{\text{alv}}}{SA_{\text{PU}}})_{\text{H}}} \frac{(e^{-K_{\text{ET}} \frac{SA_{\text{ET}}}{\dot{V}_E}})_{\text{A}}}{(e^{-K_{\text{ET}} \frac{SA_{\text{ET}}}{\dot{V}_E}})_{\text{H}}} \frac{(e^{-K_{\text{ETB}} \frac{SA_{\text{TB}}}{\dot{V}_E}})_{\text{A}}}{(e^{-K_{\text{ETB}} \frac{SA_{\text{TB}}}{\dot{V}_E}})_{\text{H}}} \frac{(1 - \frac{C_{\text{b/a}}}{C_i})_{\text{A}}}{(1 - \frac{C_{\text{b/a}}}{C_i})_{\text{H}}} . \quad (\text{I-92})$$

The default ratio is obtained by assuming the mass transport coefficients for the ET and the TB region are the same in each species. The exponential term for both the ET and TB term in Equation I-90 thereby reduces to one. Thus, assuming the same inspired concentrations, Equation I-90 becomes

$$\text{RGDR}_{\text{PU}} = \frac{(\text{RGD}_{\text{PU}})_{\text{A}}}{(\text{RGD}_{\text{PU}})_{\text{H}}} = \frac{\left(\frac{\dot{Q}_{\text{alv}}}{\text{SA}_{\text{PU}}}\right)_{\text{A}} \left(1 - \frac{C_{\text{b/a}}}{C_{\text{i}}}\right)_{\text{A}}}{\left(\frac{\dot{Q}_{\text{alv}}}{\text{SA}_{\text{PU}}}\right)_{\text{H}} \left(1 - \frac{C_{\text{b/a}}}{C_{\text{i}}}\right)_{\text{H}}} \quad (\text{I-93})$$

The  $\text{RGDR}_{\text{PU}}$  must be evaluated for each case described in section I.3.4. In the case where systemic elimination determines the blood term, the PU regional gas dose ratio is given by

$$\text{RGDR}_{\text{PU}} = \frac{(\text{RGD}_{\text{PU}})_{\text{A}} \left(\frac{\dot{Q}_{\text{alv}}}{\text{SA}_{\text{PU}}}\right)_{\text{A}} (0.25 \dot{Q}_{\text{T}} H_{\text{b/g}})_{\text{A}}}{(\text{RGD}_{\text{PU}})_{\text{H}} \left(\frac{\dot{Q}_{\text{alv}}}{\text{SA}_{\text{PU}}}\right)_{\text{H}} (0.25 \dot{Q}_{\text{T}} H_{\text{b/g}})_{\text{H}}} \quad (\text{I-94})$$

where  $E_{\text{MAX}}$  is equal to  $0.25 \dot{Q}_{\text{T}}$ .

In the case where respiratory tract metabolism and systemic elimination are equally important, the PU regional gas dose ratio is given by

$$\text{RGDR}_{\text{PU}} = \frac{(\text{RGD}_{\text{PU}})_{\text{A}} \left(\frac{\dot{Q}_{\text{alv}}}{\text{SA}_{\text{PU}}}\right)_{\text{A}} (0.5 \dot{Q}_{\text{T}} H_{\text{b/g}})_{\text{A}}}{(\text{RGD}_{\text{PU}})_{\text{H}} \left(\frac{\dot{Q}_{\text{alv}}}{\text{SA}_{\text{PU}}}\right)_{\text{H}} (0.5 \dot{Q}_{\text{T}} H_{\text{b/g}})_{\text{H}}} \quad (\text{I-95})$$

where  $E_{\text{MAX}}$  is equal to  $0.25 \dot{Q}_{\text{T}}$ . Because the constants are equal in the numerator and denominator, Equations I-94 and I-95 reduce to the same equation:

$$\text{RGDR}_{\text{PU}} = \frac{(\text{RGD}_{\text{PU}})_{\text{A}}}{(\text{RGD}_{\text{PU}})_{\text{H}}} = \frac{\left(\frac{\dot{Q}_{\text{alv}}}{\text{SA}_{\text{PU}}}\right)_{\text{A}} (\dot{Q}_{\text{T}}\text{H}_{\text{b/g}})_{\text{A}}}{\left(\frac{\dot{Q}_{\text{alv}}}{\text{SA}_{\text{PU}}}\right)_{\text{H}} (\dot{Q}_{\text{T}}\text{H}_{\text{b/g}})_{\text{H}}} . \quad (\text{I-96})$$

### I.3.6 Model for Category 2 Gases: Total Respiratory Tract

In the event that remote (extrarespiratory) toxicity is associated with a gas in Category 2, the dose to the respiratory tract, and therefore to the blood, is necessary to establish the dose ratio. However, in this case, the surface area of the respiratory tract is irrelevant, only the overall absorption rate in mass/time ( $\text{RGD}_{\text{RT}}$ ) is important which is given by

$$\text{RGD}_{\text{RT}} = \dot{V}_{\text{E}}(C_{\text{i}} - \text{CX}(\text{EXH})_{\text{ET}}) = \dot{V}_{\text{E}}C_{\text{i}}\left(1 - \frac{C_{\text{b/a}}}{C_{\text{i}}}\right) , \quad (\text{I-97})$$

such that the dose ratio (assuming the same inspiratory concentration) is

$$\frac{(\text{RGD}_{\text{RT}})_{\text{A}}}{(\text{RGD}_{\text{RT}})_{\text{H}}} = \frac{(\dot{V}_{\text{E}})_{\text{A}}}{(\dot{V}_{\text{E}})_{\text{H}}} \frac{\left(1 - \frac{C_{\text{b/a}}}{C_{\text{i}}}\right)_{\text{A}}}{\left(1 - \frac{C_{\text{b/a}}}{C_{\text{i}}}\right)_{\text{H}}} , \quad (\text{I-98})$$

to be evaluated for each of the cases described in Section I.3.4. In the case where systemic elimination determines the blood term, the regional gas dose ratio for remote (extrarespiratory) effects of Category 2 gases is given by where  $E_{\text{MAX}}$  is equal to  $0.25 \dot{Q}_{\text{T}}$ .

In the case where respiratory tract metabolism and systemic elimination are equally important, the regional gas dose ratio for remote (extrarespiratory) effects of Category 2 gases is given by

$$\text{RGDR}_{\text{ER}} = \frac{(\text{RGD}_{\text{RT}})_{\text{A}}}{(\text{RGD}_{\text{RT}})_{\text{H}}} = \frac{(\dot{V}_{\text{E}})_{\text{A}}}{(\dot{V}_{\text{E}})_{\text{H}}} \frac{(0.25 \dot{Q}_{\text{T}} \text{H}_{\text{b/g}})_{\text{A}}}{(0.25 \dot{Q}_{\text{T}} \text{H}_{\text{b/g}})_{\text{H}}}, \quad (\text{I-99})$$

$$\text{RGDR}_{\text{ER}} = \frac{(\text{RGD}_{\text{RT}})_{\text{A}}}{(\text{RGD}_{\text{RT}})_{\text{H}}} = \frac{(\dot{V}_{\text{E}})_{\text{A}}}{(\dot{V}_{\text{E}})_{\text{H}}} \frac{(0.5 \dot{Q}_{\text{T}} \text{H}_{\text{b/g}})_{\text{A}}}{(0.5 \dot{Q}_{\text{T}} \text{H}_{\text{b/g}})_{\text{H}}}, \quad (\text{I-100})$$

where  $E_{\text{MAX}}$  is equal to  $0.25 \dot{Q}_{\text{T}}$ . Because the constants are equal in the numerator and denominator, Equations I-99 and I-100 reduce to the same equation:

$$\text{RGDR}_{\text{ER}} = \frac{(\text{RGD}_{\text{RT}})_{\text{A}}}{(\text{RGD}_{\text{RT}})_{\text{H}}} = \frac{(\dot{V}_{\text{E}})_{\text{A}}}{(\dot{V}_{\text{E}})_{\text{H}}} \frac{(\dot{Q}_{\text{T}} \text{H}_{\text{b/g}})_{\text{A}}}{(\dot{Q}_{\text{T}} \text{H}_{\text{b/g}})_{\text{H}}}. \quad (\text{I-101})$$

## **APPENDIX J. DERIVATION OF AN APPROACH TO DETERMINE HUMAN EQUIVALENT CONCENTRATIONS FOR EXTRARESPIRATORY EFFECTS OF CATEGORY 3 GAS EXPOSURES BASED ON A PHYSIOLOGICALLY BASED PHARMACOKINETIC MODEL USING SELECTED PARAMETER VALUES**

This appendix describes in detail the derivation of the procedure used in Chapter 4 to estimate no-observed-adverse-effect level human equivalent concentrations ( $\text{NOAEL}_{[\text{HEC}]}$ s) for extrarepiratory effects of gases (or vapors) in Category 3. The derivation is mathematical in nature in that the equations of state that describe the disposition of inhaled compounds in a generalized physiologically based pharmacokinetic (PBPK) model are manipulated so as to obtain a conservative estimate (with respect to the model assumptions) of  $\text{NOAEL}_{[\text{HEC}]}$ s as a function of the average animal exposure concentrations ( $\text{NOAEL}_{[\text{ADJ}]}$ ). A PBPK model is used because of the success of this type of model. For example, PBPK models that describe the body as five compartments (gas exchange and the fat, poorly perfused, richly perfused, and liver/metabolizing tissue groups) have been applied successfully to estimating the internal concentrations of chemicals (e.g., styrene, methanol, and ethylene dichloride) for the purpose of risk assessment. Although PBPK modeling is the choice procedure in risk assessment for dose extrapolation, this approach is not possible without the values of physiological and biochemical parameters used in the modeling process, nor without a thorough understanding of the agent's mechanism of action. These data generally are not available for most compounds.

The proposed method is based on a PBPK model in which all of any number of compartments are in parallel and in which for any compartment there can be any number of paths of removal by linear and saturable processes. Selected relevant parameter values are replaced by qualitative assumptions about species similarity and the response of internal concentrations to exposure scenarios. In order to obtain a  $\text{NOAEL}_{[\text{HEC}]}$ , the assumption is made that the effective dose for dose-response purposes is the arterial blood concentration of

the gas or its concentration multiplied by time ( $C \times T$ ). (These assumptions are specified in detail in the METHODS section.) This latter assumption is consistent with our current understanding of systemic toxicity for a majority of chemicals, because the toxicity of most environmental chemicals is more directly related to the concentration of the parent compound at the target site over a period of time than to the exposure concentration over an equivalent time period.

In addition to deriving conservative  $\text{NOAEL}_{[\text{HEC}]}$  estimates based on arterial blood concentrations, the method also predicts that the average blood concentration of an inhaled compound in any human tissue compartment does not exceed the average blood concentration in the corresponding animal compartment.

## **J.1 METHODS**

### **J.1.1 Assumption Imposed by the Inhalation Reference Concentration Methodology**

*Assumption I.* Noncancer toxic effects observed in chronic animal bioassays are the basis for the determination of NOAELs and the operational derivation of inhalation reference concentrations (RfCs) for human exposures, as described in Chapter 4. The animal exposure scenario is experiment-dependent and usually intermittent (e.g., 6 h/day, 5 days/week for many weeks) and is assumed periodic. Human exposure concentration is continuous and constant for 70 years. The "lifetime" chronic animal exposure scenario is equivalent to the human chronic exposure scenario for the purpose of extrapolating the NOAEL.

### **J.1.2 Additional Assumptions for the Proposed Method**

*Assumption II.* All the concentrations of the inhaled gas within the animal's body are periodic with respect to time (i.e., periodic steady state—the concentration versus time profile is the same for every week). Figure 4-9 illustrates the time course to achieve periodicity for a chemical with blood:air and fat:blood partition coefficients of 1,000 and 100, respectively. Periodicity is achieved for this chemical after approximately 5 weeks. As discussed in Chapter 4 (Section 4.3.6.2), it is practical to require that these experimental periodic conditions should be met during "most" of the experiment duration in order for this model

application to result in an accurate estimate for use in the dose-response analysis. For example, if the condition is met for nine-tenths of the time (e.g., periodic during the last 90 weeks of a 100-week experiment), then estimates of average concentrations will be in error by less than 10%. Thus, the requirement for application of this model is that periodicity is achieved for 90% of the exposure period. If this is likely not to have occurred, additional uncertainty in the extrapolation is imparted and should be addressed by an uncertainty factor (Section 4.3.6.2). During most of the time humans are exposed, given Assumption I of continuous exposure, their internal concentrations are constant and in dynamic equilibrium with their exposure concentration.

**Assumption III.** A PBPK model describes the uptake and disposition of inhaled compounds in animals and humans. The model is diagramed in Figure J-1, and the equations of state are given by Equations J-1 through J-6. Table J-1 defines the variables and constants in the equations.

$$dM_p/dt = \dot{Q}_{alv} \times (CE - C_p + \dot{Q}_T \times (CV - CA) - r_p(CA) \quad (J-1)$$

$$dM_j/dt = Q_j \times (CA - C_j) - r_j(C_j); j = 1,2,3,\dots,n \quad (J-2)$$

$$r_p(CA) = \left[ \sum_i VKF_{pi} \right] \times CA + \sum_i \left[ VMAX_{pi} \times CA / (KM_{pi} + CA) \right] \quad (J-3a)$$

$$r_j(C_j) = \left[ \sum_i VKF_{ji} \right] \times C_j + \sum_i \left[ VMAX_{ji} \times C_j / (KM_{ji} + C_j) \right]; j = 1 \text{ to } n \quad (J-3b)$$

$$\dot{Q}_T \times CV = \left[ \sum_j Q_j \times C_j \right] \quad (J-4)$$

$$\dot{Q}_T = \sum_j Q_j \quad (J-5)$$

$$CA = H_{b/g} \times C_p \quad (J-6)$$

The equations describe a model with the following properties: (1) in the respiratory tract compartment, the air, tissue and capillary blood concentrations are in equilibrium with

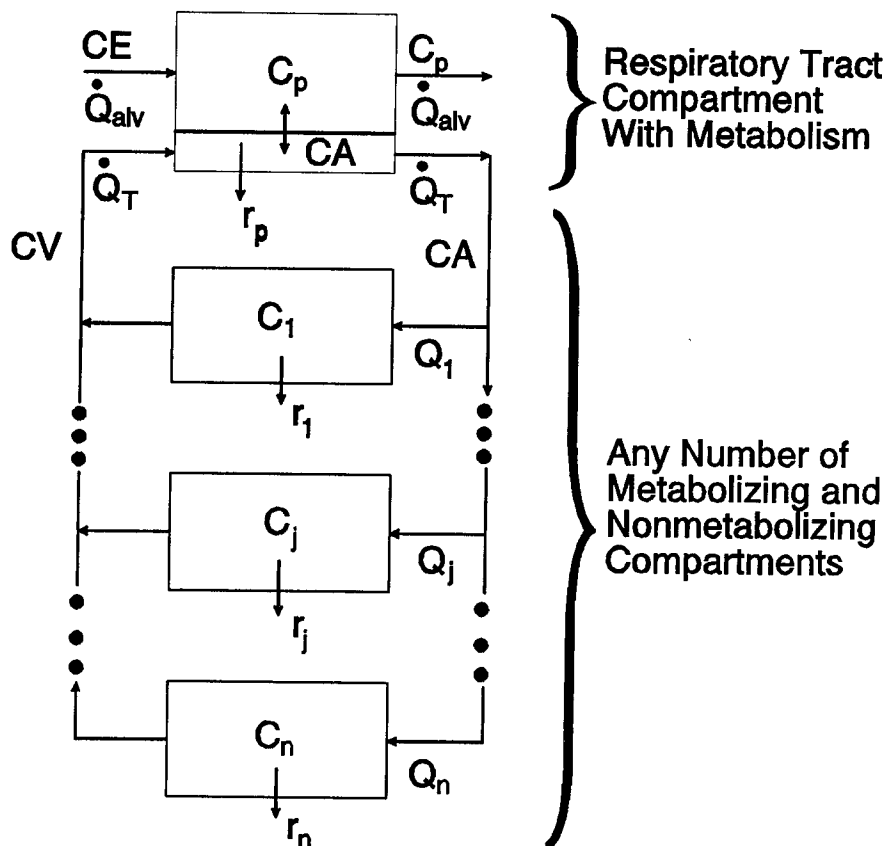


**Figure J-1. Schematic of the physiologically based pharmacokinetic model assumed to describe the uptake and distribution of inhaled compounds.**

respect to each other; (2) in each extrarespiratory (systemic) compartment, the blood and tissue concentrations are in equilibrium with respect to each other; (3) the metabolism and other loss mechanisms are taken into account in the tissue of the respiratory tract compartment and in the extrarespiratory (systemic) compartments; and (4) both first-order and saturable loss rates are represented and are defined in terms of blood concentrations regardless of whether or not they occur in tissue or blood.

Equations J-1, J-2, J-4, and J-5 are the dynamical equations of state or mass-balance equations for the model. Equations J-3a and 3b define the possible loss rates in each compartment in terms of linear rates (e.g.,  $VKF_{ji} \times C_j$ ) and rates of the Michaelis-Menton type (e.g.,  $VMAX_{pi} \times CA/[KM_{pi} + CA]$ ). In each compartment, the model allows for

TABLE J-1. DEFINITION OF SYMBOLS

## General

V	Compartment volume
n	The number of extrarrespiratory compartments
$M_p$	Mass of inhaled compound in gas-exchange compartment
M	Mass in compartment other than gas exchange
×	Multiplication symbol
—	Overbar indicates average
$H_{b/g}$	Blood to air partition coefficient
P	Period of periodic exposure concentration
L	Liters
h	Hours

## Subscripts

i	i-th path of loss of primary compound
p	Gas-exchange compartment
j	j-th extrarrespiratory compartment
A	Animal
H	Human
HEC	Human equivalent concentration

## Flow Rates (L/h)

$\dot{Q}_{alv}$	Alveolar ventilation
$\dot{Q}_T$	Cardiac output
Q	Extrarrespiratory (systemic) compartment perfusion rate

## Concentrations (mg/L)

C	In venous blood within and leaving extrarrespiratory (systemic) compartment
CE	Exposure
$C_p$	In air of pulmonary region
CA	In arterial (unoxygenated) blood
CV	In venous (oxygenated) blood entering gas-exchange region

## Biochemical

r	Removal rate due to metabolism, reactions, excretion, etc. (mg/h); when denoted as r(c) this indicates dependence on given concentration
VMAX	Maximum velocity of saturable (Michaelis-Menton) metabolism path (mg/h)
KM	Michaelis constant (mg/L)
KF	First-order rate constant ( $h^{-1}$ )
VKF	Equals to $V \times KF$ (L/h)

more than one path of elimination or metabolism or for no losses (i.e., set both of a compartment's kinetic parameters, VKF and VMAX, to zero). Equation J-6 gives the assumed relationship between the arterial blood concentration and the concentration in the air of the pulmonary region.

According to Assumption I, the exposure concentration is periodic for laboratory animals and constant for humans; in both cases, concentration of exposure (CE) can be written as

$$CE = f(t) \times \overline{CE}, \quad (J-7)$$

where:

$\overline{CE}$  = the average exposure concentration, and

$f$  = a periodic function of time (t) such that

$$f(t + P) = f(t) \quad (J-8a)$$

$$\int_t^{t+P} f(t) \times dt = 1; \quad (J-8b)$$

and P is the period of the periodic exposure concentration.

**Assumption IV.** Because the toxicologically effective dose to a given target tissue depends on the animal species and chemical compound, its specification is typically not available so that definition of a surrogate dose must be somewhat arbitrary. However, the toxic effects of some compounds are expected to be directly related to the inhaled parent compound in the blood. Furthermore, the use of the average blood concentration is an internal dose "closer" to the target than a dose based on exposure concentration. Basing the effective dose extrapolation on another surrogate (e.g., metabolite) would require knowledge of the mechanisms of action and additional information about human and animal physiological parameters. Thus, for animal to human exposure extrapolation, the human equivalent

exposure concentration ( $CE_{[HEC]}$ ) is defined in terms of the average arterial blood concentration of the inhaled parent compound by requiring that the human equilibrium concentration of arterial blood be less than or equal to the time-averaged arterial blood concentration of the animal; that is,  $CA_H \leq \overline{CA}_A$ . Note that the time average concentrations are the area under the curve over a period divided by the length (time) of a period (e.g., average concentration over 1 week). The equality condition defines the upper limit on an acceptable human arterial blood concentration; thus, for mathematical simplicity this assumption is formulated as:

$$CA_H = \overline{CA}_A. \quad (J-9)$$

Because of this requirement,  $CA_H$  is a function of  $\overline{CE}_A$ , because  $\overline{CA}_A$  depends on  $\overline{CE}_A$ .

**Assumption V.** Similarity of species is assumed in that KM and the ratios  $Q/\dot{Q}_{alv}$ ,  $VKF/\dot{Q}_{alv}$ , and  $VMAX/\dot{Q}_{alv}$  are defined as species independent for each removal process (see Table J-1 for definitions). The invariance of the first ratio is based on the assumption that the percent of blood flow to any compartment is independent of species and that cardiac output ( $\dot{Q}_T = \text{sum of all } Q_j$ ) scales, with respect to body weight, in the same way as the ventilation rate ( $\dot{Q}_{alv}$ ); (i.e., the ratio of  $\dot{Q}_T$  to  $\dot{Q}_{alv}$  is species-independent). The metabolic constants VMAX and VKF are assumed to scale in the same way as  $\dot{Q}_{alv}$ . Justification for this assumption about rates is based on the observation that for many species, rates scale in the same way with respect to body weight (e.g., in proportion to basal metabolism, body surface area, or body weight to some power) (Dedrick, 1973; Weiß, 1977; Dedrick and Bischoff, 1980; Boxenbaum, 1982; Rowland, 1985; Travis and White, 1988; Travis et al., 1990; Federal Register, 1992b). The invariance of the ratios  $VKF/\dot{Q}_{alv}$  and  $VMAX/\dot{Q}_{alv}$  follows.

Most of the above assumptions are well supported by data on comparative anatomy and physiology, as detailed in the cited and other allometry references (Federal Register, 1992b). Collectively, they embody the concept of a basically similar mammalian physiological and anatomical plan that varies primarily in scale from one species to another. The most

problematic issue is the scaling of rates of individual metabolic transformation reactions as  $BW^{3/4}$ . Not only are there few data on such scaling, but some individual metabolic enzyme systems have been shown to vary across species (Federal Register, 1992b). However, several points should be made. First, there are data that support the proposition of  $BW^{3/4}$  in specific cases (Federal Register, 1992b). For example, these same scaling assumptions have been used in successful PBPK modeling across species (Ramsey and Andersen, 1984; Andersen et al., 1987a; Ward et al., 1988; Allen and Fisher, 1993; Fisher and Allen, 1993). Second, overall metabolic rate (oxygen consumption, resting metabolic rate) clearly scales as  $BW^{3/4}$ . Indeed, this is the issue around which physiological allometry was developed. Scaling an individual metabolic step in this way corresponds to keeping it in proportion to general metabolism, which seems the best default (Federal Register, 1992b). Third, daily intake of natural toxins (the usual targets of toxicant-metabolizing enzymes) depend on intake of air, water, and food which all scale as  $BW^{3/4}$ . That is, scaling detoxification processes in proportion to their anticipated load also predicts  $BW^{3/4}$ . Variation around scaling as  $BW^{3/4}$  does not invalidate the general scaling argument, nor does it provide evidence for any different scaling factor. Rather, the variation simply illustrates that any single conception of interspecies scaling can accommodate only the general trends, not the diversity of particular instances (Federal Register, 1992b). Clearly, as proposed in Section 3.2.2, when data or more sophisticated models are available for interspecies extrapolation, they should be used in preference to the default method presented herein.

Subject to the Assumptions, Equations J-1 to J-9 must be manipulated to determine  $CE_{HEC}$  as a function of the average animal exposure concentration,  $\overline{CE}_A$ . Because the concentrations and masses of a parent compound within a compartment are assumed to be periodic, the integral of the left-hand side (LHS) of Equations J-1 and J-2 over a time length of the period is zero; for example

$$\int_t^{t+P} (dM/dt') \times dt' = M(t + P) - M(t) = 0. \quad (J-10)$$

Also note that for equilibrium or steady state, as in the human case, the LHS of each of these equations (J-1 and J-2) is zero by definition. Performing the period average of both sides of Equations J-1 to J-6, the following are obtained:

$$0 = \dot{Q}_{\text{alv}} \times (\overline{\text{CE}} - \overline{\text{C}}_p) + \dot{Q}_T \times (\overline{\text{CV}} - \overline{\text{CA}}) - \bar{r}_p \quad (\text{J-11})$$

$$0 = Q_j \times (\overline{\text{CA}} - \overline{\text{C}}_j) - \bar{r}_j; j = 1, 2, 3, \dots, n \quad (\text{J-12})$$

$$\bar{r}_p = \left[ \sum_i \text{VKF}_{pi} \right] \times \overline{\text{CA}} + \sum_i \left[ \text{VMAX}_{pi} \times \left[ \frac{\overline{\text{CA}}}{(\text{KM}_{pi} + \overline{\text{CA}})} \right] \right] \quad (\text{J-13a})$$

$$\bar{r}_j = \left[ \sum_i \text{VKF}_{ji} \right] \times \overline{\text{C}}_j + \sum_i \left[ \text{VMAX}_{ji} \times \left[ \frac{\overline{\text{C}}_j}{(\text{KM}_{ji} + \overline{\text{C}}_j)} \right] \right]; j = 1 \text{ to } n \quad (\text{J-13b})$$

$$\dot{Q}_T \times \overline{\text{CV}} = \left[ \sum_j Q_j \times \overline{\text{C}}_j \right] \quad (\text{J-14})$$

$$\dot{Q}_T = \sum_j Q_j \quad (\text{J-15})$$

$$\overline{\text{CA}} = H_{b/g} \times \overline{\text{C}}_p \quad (\text{J-16})$$

The steady-state equations for humans are obtained from Equations J-1 and J-2 by setting the LHS of these equations to zero (the equilibrium or steady-state condition). The complete set of equations of state for humans can be obtained from Equations J-11 through J-16 by redefining the average concentrations or terms as equilibrium values (i.e., remove the overbars).

The above equations are simplified by combining Equations J-11 and J-16 to give

$$(\dot{Q}_{\text{alv}}/H_{b/g} + \dot{Q}_T) \times \overline{\text{CA}} = (\dot{Q}_{\text{alv}} \times \overline{\text{CE}}) + (\dot{Q}_T \times \overline{\text{CV}}) - \bar{r}_p, \quad (\text{J-17})$$

and Equation J-12 is expressed as

$$Q_j \times \overline{\text{CA}} = Q_j \times \overline{\text{C}}_j + \bar{r}_j; j = 1 \text{ to } n. \quad (\text{J-18})$$

Both sides of Equations J-17 and J-18 are divided by  $\dot{Q}_{alv}$  and  $Q_j$ , respectively, to give

$$u \times \overline{CA} = \overline{CE} + w \times \overline{CV} - \bar{r}_p/\dot{Q}_{alv}, \text{ and} \quad (\text{J-19a})$$

$$\overline{CA} = \overline{C}_j + \bar{r}_j/Q_j; j = 1 \text{ to } n, \quad (\text{J-19b})$$

where:

$$w = \dot{Q}_T/\dot{Q}_{alv}, \text{ and}$$

$$u = (H_{b/g}^{-1} + \dot{Q}_T/\dot{Q}_{alv}).$$

According to Assumption V,  $w$  is species independent. The parameter  $u$  is species-dependent (via  $H_{b/g}$ ) and will be identified as such with subscripts A and H for laboratory animal and human, respectively. For simplicity and unless otherwise noted, averaged concentrations (indicated by overbar) will be those of animals and nonaveraged (no overbar) concentrations will be those of humans.

Applied to humans, Equations J-19a and J-19b are written as

$$u_H \times CA = CE + w \times CV - r_{pH}(CA)/\dot{Q}_{alv_H}, \text{ and}$$

$$CA = C_j + r_{jH}(C_j)/Q_{jH}; j = 1 \text{ to } n.$$

For laboratory animals, Equations J-19a and J-19b are written as

$$u_A \times \overline{CA} = \overline{CE} + w \times \overline{CV} - \bar{r}_{pA}/\dot{Q}_{alv_A}, \text{ and} \quad (\text{J-20c})$$

$$\overline{CA} = \overline{C}_j + \bar{r}_{jA}/Q_{jA}; j = 1 \text{ to } n. \quad (\text{J-20d})$$

The loss terms in Equations J-3,  $r_p(CA)$  and the  $r_j(C_j)$ 's, are concave functions with the property that their second derivatives with respect to  $CA$  and  $C_j$ , respectively, are less than or

and also,

$$u_A - u_H = H_{b/g_A}^{-1} - H_{b/g_H}^{-1}.$$

Thus, Equation J-24 can be written as

$$(H_{b/g_A}^{-1} - H_{b/g_H}^{-1}) \times \overline{CA} \geq \overline{CE} - CE + w \times (\overline{CV} - CV), \text{ or} \quad (\text{J-26a})$$

$$CE \geq \overline{CE} + w \times (\overline{CV} - CV) + (H_{b/g_H}^{-1} - H_{b/g_A}^{-1}) \times \overline{CA}. \quad (\text{J-26b})$$

Comparing Equations J-22b and J-23b, and using J-25b one sees that the blood concentration of the inhaled compound in any human compartment is less than or equal to the average blood concentration in the corresponding animal compartment; that is

$$C_j \leq \overline{C}_j. \quad (\text{J-27})$$

Because of Assumption V, ( $Q_{jA}/\dot{Q}_{TA} = Q_{jH}/\dot{Q}_{TH}$ ), it follows from Equation J-14 applied to both humans and animals, and from Equation J-27, that

$$CV \leq \overline{CV}. \quad (\text{J-28})$$

Thus, the term  $w \times (\overline{CV} - CV) \geq 0$  can be dropped from Equation J-26b without affecting the inequality.

$$CE \geq \overline{CE} + (H_{b/g_H}^{-1} - H_{b/g_A}^{-1}) \times \overline{CA} \quad (\text{J-29})$$

Note that CE is the constant inhaled human concentration that would give rise to a human constant blood level that is no greater than  $\overline{CA}$ . If we choose the actual human exposure concentration to be less than or equal to this CE, as defined by  $CA = \overline{CA}$ , then the actual human arterial blood concentration will be less than or equal to  $\overline{CA}$ .

equal to zero. As a consequence, the average of each of these functions is less than or equal to the function evaluated at the average concentration. Suppressing the subscripts, this property is expressed as

$$\bar{r} \leq r(\bar{C}). \quad (\text{J-21})$$

Considering Equations J-21, J-20c, and J-20d, the following is noted:

$$u_A \times \bar{CA} \geq \bar{CE} + w \times \bar{CV} - r_{pA}(\bar{CA})/\dot{Q}_{alv_A}, \text{ and} \quad (\text{J-22a})$$

$$\bar{CA} \leq \bar{C}_j + r_{jA}(\bar{C}_j)/Q_{jA}; j = 1 \text{ to } n. \quad (\text{J-22b})$$

Using Equation J-9, Assumption IV (in the presentation notation,  $CA = \bar{CA}$ ), Equations J-20a and J-20b for human are written in terms of the animal arterial blood concentration by replacing CA with  $\bar{CA}$  as follows:

$$u_H \times \bar{CA} = CE + w \times CV - r_{pH}(\bar{CA})/\dot{Q}_{alv_H} \quad (\text{J-23a})$$

$$\bar{CA} = C_j + r_{jH}(C_j)/Q_{jH}; j = 1 \text{ to } n. \quad (\text{J-23b})$$

Subtract the LHS and the right hand side (RHS) of Equation J-23a from the LHS and RHS of Equation J-22a, respectively, to obtain

$$(u_A - u_H) \times \bar{CA} \geq \bar{CE} - CE + (w \times \bar{CV} - w \times CV) - (r_{pA}(\bar{CA})/\dot{Q}_{alv_A} - r_{pH}(\bar{CA})/\dot{Q}_{alv_H}). \quad (\text{J-24})$$

Because of Assumption V, for any concentration value, C,

$$r_{pA}(C)/\dot{Q}_{alv_A} = r_{pH}(C)/\dot{Q}_{alv_H}, \text{ and}$$

$$r_{jA}(C)/Q_{jA} = r_{jH}(C)/Q_{jH};$$

The following two cases are now considered with respect to the partition coefficient.

$$\text{Case I: } H_{b/g_A} \geq H_{b/g_H}$$

The second term on the RHS of Equation J-29 is greater than or equal to zero; thus, the term can be dropped from the RHS without affecting the inequality. Obviously, with respect to model assumptions, a conservative human exposure concentration is  $\overline{CE}$ . Therefore, in terms of the variables in Chapter 4, an estimated conservative  $\text{NOAEL}^*_{[\text{HEC}]}$  is given by

$$\text{NOAEL}^*_{[\text{HEC}]} = \overline{CE} = \text{NOAEL}^*_{[\text{ADJ}]}, \quad (\text{J-30})$$

where:

$\text{NOAEL}^*_{[\text{ADJ}]}$  = the observed NOAEL or analogous effect level concentration obtained with an alternate approach as described in Appendix A, adjusted for exposure duration (Equation 4-2).

$$\text{Case II: } H_{b/g_A} < H_{b/g_H}$$

The second term on the RHS of Equation J-29 is negative in this instance. The inhaled concentration must be greater than or equal to the exhaled concentration; this requires that  $\overline{CE} \geq \overline{C_p}$  or  $\overline{CA} \leq H_{b/g_A} \times \overline{CE}$ . In Equation J-29,  $\overline{CA}$  can be replaced by the larger value,  $H_{b/g_A} \times \overline{CE}$ , and still preserve the inequality, hence

$$\overline{CE} \geq \overline{CE} + (H_{b/g_H}^{-1} - H_{b/g_A}^{-1}) \times H_{b/g_A} \times \overline{CE}, \text{ or} \quad (\text{J-31a})$$

$$\overline{CE} \geq \overline{CE} \times (H_{b/g_A}/H_{b/g_H}). \quad (\text{J-31b})$$

In this case, an estimated conservative  $\text{NOAEL}^*_{[\text{HEC}]}$  is given by

$$\text{NOAEL}^*_{[\text{HEC}]} = (\text{H}_{\text{b/g}_A} / \text{H}_{\text{b/g}_H}) \times \overline{\text{CE}} = (\text{H}_{\text{b/g}_A} / \text{H}_{\text{b/g}_H}) \times \text{NOAEL}_{[\text{ADJ}]}, \quad (\text{J-32})$$

where:

$\text{NOAEL}^*_{[\text{ADJ}]}$  = the observed NOAEL or analogous effect level concentration obtained with an alternate approach as described in Appendix A, adjusted for exposure duration (Equation 4-2).

## J.2 AN EXAMPLE OF THE RELATIONSHIP BETWEEN THE PROPOSED AND OTHER METHODS

A perspective on the proposed method can be attained by examination of Figures J-2 and J-3, plots of  $\text{NOAEL}^*_{[\text{HEC}]}$  versus  $\text{NOAEL}^*_{[A]}$  for the rat and mouse, respectively. These plots were created by choosing the equivalent exposure concentration that resulted in the human arterial blood concentration being equal to the average arterial blood concentration of the animal, using several methods, for the representative volatile organic compound dichloromethane (DCM).

In Figures J-2 and J-3, the "previous" method refers to the method of using the ratio of the ventilation rate divided by body weight in the laboratory animal to the ventilation rate divided by body weight in the human ratio for calculating  $\text{NOAEL}^*_{[\text{HEC}]}$  estimates (Federal Register, 1980), with the modification that alveolar ventilation rates are used (U.S. Environmental Protection Agency, 1988a). The  $\text{NOAEL}^*_{[\text{ADJ}]}$  of the laboratory animal (Equation 4-2) is multiplied by the ratio to calculate the  $\text{NOAEL}^*_{[\text{HEC}]}$  estimate using this method. "Optimal" method refers to the use of a specific PBPK model with an extensive set of experimentally determined physiological parameters for the three species (Andersen et al., 1987a). The same model and human parameters were used for the "similar" method, but the animal parameters were determined by scaling from the human values, as defined in Assumption V. The "proposed" results are based on the methods proposed in this document and derived in this appendix.

In keeping with the results of the derivation that is the subject of this appendix, the "proposed"  $\text{NOAEL}^*_{[\text{HEC}]}$  estimates are less than the "similar" method estimates. With

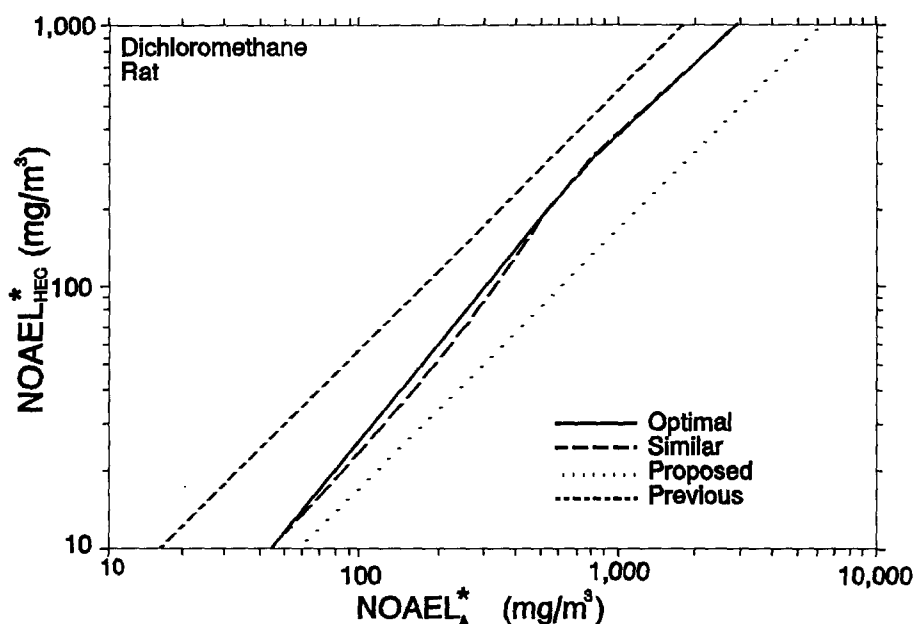


**Figure J-2.** Plot of  $\text{NOAEL}^*_{[\text{HEC}]}$  versus  $\text{NOAEL}^*_{[\text{A}]}$  for the rat for four possible methods (proposed, previous, similar, and optimal) of determining  $\text{NOAEL}_{[\text{HEC}]}$  estimates as defined in the text. For any given observed  $\text{NOAEL}^*_{[\text{A}]}$ , the corresponding HEC estimate is found by going up to the method(s) line and over to the y axis. The inhaled compound is dichloromethane. NOTE:  $\text{NOAEL}^*_{[\text{A}]} = \text{animal NOAEL}^*_{[\text{ADJ}]}$ .

Source: Overton and Jarabek (1989a,b).

respect to the relationship of the proposed predictions to the other methods of calculation, the following observations are noted.

The "proposed" method lines are parallel to the "previous" lines and result in 3.4 and 6.9 times smaller, or more conservative,  $\text{NOAEL}^*_{[\text{HEC}]}$  estimates than the "previous" method for the rat and mouse, respectively. The "proposed" rat  $\text{NOAEL}^*_{[\text{HEC}]}$  estimates also fall below (i.e., are more conservative than) those of the "optimal" method by a range of 1.4 to 2.4. Except at high exposure concentrations (above approximately  $1,600 \text{ mg/m}^3$ ), where the estimates are smaller by about 1.3, the "proposed" mouse  $\text{NOAEL}^*_{[\text{HEC}]}$  estimates are up to 1.5 times greater than the "optimal"  $\text{NOAEL}^*_{[\text{HEC}]}$  estimates. This supports current evidence that the mouse is not "similar" to humans in some cases (Reitz et al., 1988). However, for this species, the "proposed" method estimates more closely approximate the

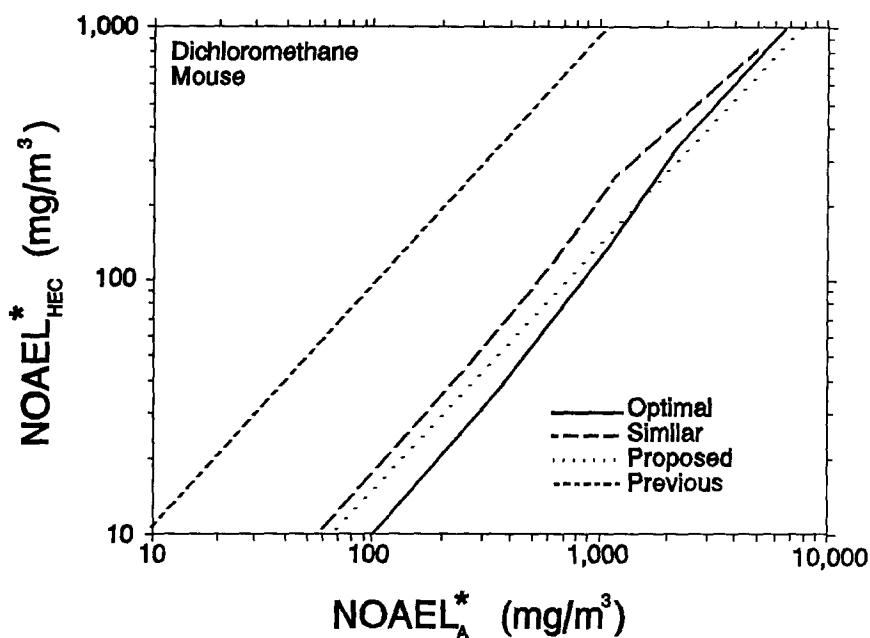


Figure J-3. Plot of  $\text{NOAEL}^*_{\text{HEC}}$  versus  $\text{NOAEL}^*_{\text{A}}$  for the mouse for four possible methods (proposed, previous, similar, and optimal) of determining  $\text{NOAEL}^*_{\text{HEC}}$  estimates as defined in the text. For any given observed  $\text{NOAEL}^*_{\text{A}}$ , the corresponding HEC estimate is found by going up to the method(s) line and over to the y axis. The inhaled compound is dichloromethane. NOTE:  $\text{NOAEL}^*_{\text{A}} = \text{animal NOAEL}^*_{\text{ADJ}}$ .

Source: Overton and Jarabek (1989a,b).

"optimal" method estimates than do the "previous" estimates and the "proposed" method is conservative (estimates all fall below) the "similar" method. It also should be noted that the "optimal", "similar", and "proposed" methods result in smaller  $\text{NOAEL}^*_{\text{HEC}}$  estimates for the mouse relative to the rat for the same exposure concentration, whereas the previous methodology results in the opposite relationship of estimates between the two species.

### J.2.1 Discussion

Considering the "optimal" method estimates to represent the best possible dose extrapolation based on internal blood concentrations, then the "proposed" method is more realistic than the "previous" method. Because the blood:air partition coefficients are more

readily available than are complete physiological parameter data, the proposed method represents a simple default approach when extensive PBPK modeling is not feasible.

### **J.2.2 Research and Development**

The approach presented in this appendix has resulted from modeling research focused on determining the key parameters of gas uptake, distribution, and target tissue accumulation. Future efforts will incorporate the anatomic and some aspects of the clearance data being compiled for research to support the particle model described in Appendix G. Model evaluation plans include comparing the efficiency of various dose surrogates and an approach to address the apparent nonsimilarity of the mouse. Application of the model to address mixtures of gases and of dose partitioning between gas and particles is also envisioned.